### Title

Dynamic upregulation of the rate-limiting enzyme for valerolactam biosynthesis in Corynebacterium glutamicum




### Authors

Zhao, Xixi
Wu, Yanling
Feng, Tingye
et al.



### Publication Date

2023-05-01

### DOI

10.1016/j.ymben.2023.02.005

# Dynamic upregulation of the rate-limiting enzyme for valerolactam biosynthesis in *Corynebacterium glutamicum*

Xixi Zhao[a,b,1], Yanling Wu[a,b,c,1], Tingye Feng[a,b], Junfeng Shen[a,b], Huan Lu[a,b], Yunfeng Zhang[a,b], Howard H. Chou[a,b,c,d], Xiaozhou Luo[a,b,c,d]*, Jay D. Keasling[a,e,f,g,h,i]

[a]Center for Synthetic Biochemistry, Shenzhen Institute of Synthetic Biology, Shenzhen Institutes of Advanced Technology, Chinese Academy of Sciences, Shenzhen 518055, China.

[b]CAS Key Laboratory of Quantitative Engineering Biology, Shenzhen Institute of Synthetic Biology, Shenzhen Institutes of Advanced Technology, Chinese Academy of Sciences, Shenzhen 518055, China.

[c]University of Chinese Academy of Sciences, Beijing 100049, China

[d]Shenzhen Key Laboratory for the Intelligent Microbial Manufacturing of Medicines, Shenzhen Institutes of Advanced Technology, Chinese Academy of Sciences, Shenzhen 518055, China.

[e]Joint BioEnergy Institute, Lawrence Berkeley National Laboratory, Emeryville, CA 94608, USA.

[f]Biological Systems and Engineering Division, Lawrence Berkeley National Laboratory, Berkeley, CA 94720, USA.

[g]QB3 Institute, University of California, Berkeley, Berkeley, CA 94720, USA.

[h]Department of Chemical and Biomolecular Engineering and Department of Bioengineering, University of California, Berkeley, Berkeley, CA 94720, USA.

[i]The Novo Nordisk Foundation Center for Biosustainability, Technical University Denmark, Kemitorvet, Building 220, Kongens Lyngby 2800, Denmark.

[1]These authors contributed equally to this work.

*Corresponding author: xz.luo@siat.ac.cn

## Highlights

- Design of a dynamic upregulation system (ChnR/Pb, valerolactam biosensor) for the rate-limiting enzymes in the valerolactam biosynthetic pathway.
- Laboratory evolution to engineer ChnR/Pb to have higher sensitivity and a higher dynamic output range.
- The highest titer of Valerolactam reached 12.33 g/L in a 1.2 L fermenter.

**Abstract**

Valerolactam is a monomer used to manufacture high-value nylon-5 and nylon-6,5. However, the biological production of valerolactam has been limited by the inadequate efficiency of enzymes to cyclize 5-aminovaleric acid to produce valerolactam. In this study, we engineered *Corynebacterium glutamicum* with a valerolactam biosynthetic pathway consisting of DavAB from *Pseudomonas putida* to convert L-lysine to 5-aminovaleric acid and β-alanine CoA transferase (Act) from *Clostridium propionicum* to produce valerolactam from 5-aminovaleric acid. Most of the L-lysine was converted into 5-aminovaleric acid, but promoter optimization and increasing the copy number of Act were insufficient to significantly improve the titer of valerolactam. To eliminate the bottleneck at Act, we designed a dynamic upregulation system (a positive feedback loop based on the valerolactam biosensor ChnR/Pb). We used laboratory evolution to engineer ChnR/Pb to have higher sensitivity and a higher dynamic output range, and the engineered ChnR-B1/Pb-E1 system was used to overexpress the rate-limiting enzymes (Act/ORF26/CaiC) that cyclize 5-aminovaleric acid into valerolactam. In glucose fed-batch culture, we obtained 12.33 g/L valerolactam from the dynamic upregulation of Act, 11.88 g/L using ORF26, and 12.15 g/L using CaiC. Our engineered biosensor (ChnR-B1/Pb-E1 system) was also sensitive to 0.01-100 mM caprolactam, which suggests that this dynamic upregulation system can be used to enhance caprolactam biosynthesis in the future.

**Keywords**: Dynamic regulation, valerolactam, biosensor engineering, *Corynebacterium glutamicum*.

## 1. Introduction

Lactams are used as monomers for the synthesis of industrial polyamides (nylon-4, nylon-5, nylon-6, nylon-6,5, etc.) (Yeom et al., 2018)(Chae et al., 2017)(Zhang et al., 2017b). Nylons are widely used in automobile parts, carpets, and packaging due to their high tensile strength, good elasticity, and excellent abrasion resistance. The global market for nylon-6 (with caprolactam as the monomer) was estimated at USD 15 billion in 2019, and the market is growing, propelled, in part, by an increasing demand for lightweight vehicles (Gordillo Sierra and Alper, 2020). Nylon-6,5 can be synthesized using valerolactam and caprolactam as monomers and has different properties than nylon-6 due to the addition of valerolactam (Park et al., 2014). Valerolactam and caprolactam are currently produced by petrochemical processes that require high temperatures and harsh acidic conditions, are energy intensive, and produce large amounts of waste. Biosynthesis of these lactams will alleviate many of these issues (Gordillo Sierra and Alper, 2020).

The biosynthetic pathway to produce valerolactam from lysine has three enzymes, DavB (L-lysine monooxygenase) and DavA (5-aminovaleramide amidohydrolase) from *Pseudomonas putida* and an enzyme for the cyclization step of 5-aminovaleric acid (5-AVA) to valerolactam (Chae et al., 2017)(Zhang et al., 2017b). Recently, *Corynebacterium glutamicum* was engineered to produce 48.3 g/L 5-AVA by balancing the expression of heterologous *davAB*

genes from *P. putida*, reducing the formation of the byproduct glutarate, increasing 5-AVA export and reducing 5-AVA reimport (Rohles et al., 2022). Additionally, *Escherichia coli* WL3110 was engineered with the same pathway to produce 90.59 g/L 5-AVA from 120 g/L L-lysine (Park et al., 2014). While 5-AVA has been produced in high titer, there has been less progress in producing valerolactam. When Act (β-alanine CoA transferase) was used for the cyclization step, 1.18 g/L valerolactam was synthesized from glucose in *Escherichia coli* (Chae et al., 2017), and 705 mg/L valerolactam was synthesized from 10 g/L L-lysine when DavB, DavA, and ORF26 (acyl-CoA ligase) were co-expressed in *E. coli* (Zhang et al., 2017b). The limited titer of the biosynthesized valerolactam is due to the inefficiency of the cyclization of 5-AVA to valerolactam (Zhang et al., 2017b)(Gordillo Sierra and Alper, 2020).

In traditional metabolic engineering strategies, heterologously expressed pathway genes are modulated by increasing the DNA copy number, optimizing promoter and ribosome binding strength, and engineering pathway enzymes to maximize the production of the target chemicals (Brockman and Prather, 2015). These strategies can effectively improve titer, rate, and yield of the desired final product. Additionally, dynamic regulation systems have been effective for increasing the titer of products through the upregulation or downregulation of pathway genes by internally sensing metabolite levels in real time (Zhang et al., 2012)(Dahl et al., 2013)(Jones et al., 2015)(Yang et al., 2018). For example, the transcription factor CatR has been designed for the dynamic upregulation

of salicylate biosynthesis in the muconic acid biosynthetic pathway, and this strategy successfully increased the muconic acid titer by 5.87-fold compared with static control (Yang et al., 2018). Another strategy for dynamic regulation has been designed based on a positive feedback loop, in which the gene product enhances its own production directly or indirectly by amplifying the expression level of enzymes for its production. In *Neurospora crassa*, the transcription factor CLR-2 was placed under the control of *Pcbh-1*, which is a target of CLR-2. The expression level of CLR-2 was significantly increased using this positive feedback loop and hence amplified the expression of approximately 50% of 78 lignocellulosic degradation-related genes, which revealed a previously unappreciated role of CLR-2 in the lignocellulosic degradation gene network (Matsu-Ura et al., 2018). Finally, a LuxR-based positive feedback loop was designed as a genetic signal amplifier, and the maximum expression level of the output signal was substantially increased in the strains with a positive feedback loop compared to those without (Nistala et al., 2010). In light of the previously reported biosensors for various lactams (ChnR/Pb system), we reasoned that it should be possible to increase the titer of valerolactam by dynamically upregulating the rate-limiting cyclization step.

*C. glutamicum* was chosen as the host to produce valerolactam because it is known to produce high levels of lysine and 5-AVA (Fig. 1A)(Becker et al., 2011)(Shin et al., 2016) (Chae et al., 2017)(Zhang et al., 2017b)(Rohles et al., 2022). We engineered wild-type *C. glutamicum* with *davAB* and *act* by

traditional metabolic engineering to increase its production of valerolactam. The lactam biosensor was then optimized and used to control the expression of the cyclization enzyme, leading to a 10-fold improvement in valerolactam production during fed-batch fermentation (Chae et al., 2017).

## 2. Materials and Methods

### 2.1 Experimental materials

All bacterial strains and plasmids used in this study are listed in Table 1 and Table S1 respectively. All primers were synthesized at GENEWIZ (Suzhou, China) and are listed in Table S2. The valerolactam biosynthetic pathway genes *davB* and *davA* from *Pseudomonas putida* KT2440, *act* from *Clostridium propionicum*, *orf26* from *Streptomyces aizunensis*, and *caiC* from *Escherichia coli* were codon optimized for all *C. glutamicum* and synthesized at GENEWIZ (Suzhou, China) (the sequences of the *C. glutamicum*-codon optimized versions of *davB* and *davA* from *P. putida* were the same as those described by (Shin et al., 2016)). The sequences of the *C. glutamicum* codon-optimized genes are listed in Table S3.

**Table 1** Bacterial strains used in this study.

| Strain | Description | Source |
|---|---|---|
| *E. coli* DH5α | General cloning purpose. Genotype: F⁻ φ80*lac*ZΔM15 Δ(*lac*ZYA-*arg*F) | Lab stock |

| | | |
|---|---|---|
| | U169 *rec*A1 *end*A1 *hsd*R17($r_K^-$, $m_K^+$) *pho*A *sup*E44 *thi*-1 *gyr*A96 *rel*A1 $\lambda^-$ | |
| *E. coli* DH10B | $F^-$*mcr*A Δ(*mrr-hsd*RMS-*mcr*BC) φ80*lac*ZΔM15 Δ*lac*X74 *rec*A1 *end*A1 *ara*D139 Δ(*ara-leu*)7697 *gal*U *gal*K $\lambda^-$*rps*L($Str^R$) *nup*G | Lab stock |
| *C. glutamicum* ATCC 13032 | Wilt type | Lab stock |
| *C. glutamicum* XT1 | *C. glutamicum* ATCC 13032 derivate, *lysC* (C932T) | This study |
| *C. glutamicum* Val-1 | *C. glutamicum* XT1 harboring pCES208-H1davAB | This study |
| *C. glutamicum* Val-2 | *C. glutamicum* XT1 harboring pCES208-H1davAB-act | This study |
| *C. glutamicum* Val-3 | *C. glutamicum* XT1 harboring pHCP-H1davAB-act | This study |
| *C. glutamicum* Val-4 | *C. glutamicum* XT1 harboring pHCP-H1davAB-H1act | This study |
| *C. glutamicum* Val-5 | *C. glutamicum* XT1 harboring pHCP-H1davAB-Pb-act-chnR | This study |
| *C. glutamicum* Val-6 | *C. glutamicum* XT1 harboring pHCP-H1davAB-E1-act | This study |
| *C. glutamicum* Val-7 | *C. glutamicum* XT1 harboring pHCP-H1davAB-E1-act-chnR | This study |
| *C. glutamicum* | *C. glutamicum* XT1 harboring pHCP- | This |

| | | |
|---|---|---|
| Val-8 | H1davAB-Pb-act-B1 | study |
| *C. glutamicum* Val-9 | *C. glutamicum* XT1 harboring pHCP-H1davAB-E1-act-B1 | This study |
| *C. glutamicum* Val-10 | *C. glutamicum* XT1 harboring pHCP-H1davAB-orf26 | This study |
| *C. glutamicum* Val-11 | *C. glutamicum* XT1 harboring pHCP-H1davAB-E1-orf26-B1 | This study |
| *C. glutamicum* Val-12 | *C. glutamicum* XT1 harboring pHCP-H1davAB-caiC | This study |
| *C. glutamicum* Val-13 | *C. glutamicum* XT1 harboring pHCP-H1davAB-E1-caiC-B1 | This study |

Luria-Bertani (LB) broth or plates (1.5%, w/v, agar) containing appropriate antibiotics were used for *E. coli* inoculation, plasmid propagation, and transformation. Kanamycin (50 μg/mL) and chloramphenicol (25 μg/mL) were added to the medium when necessary. *E. coli* DH5α was used for general cloning purposes, and *E. coli* DH10B was used for biosensor characterization and mutant library construction and sorting.

*Corynebacterium glutamicum* ATCC13032 was used as the base strain for the construction of the L-lysine-producing and valerolactam-producing chassis strains. LBHIS (tryptone 5 g/L, yeast extract 2.5 g/L, NaCl 5 g/L, BHI 18.5 g/L, sorbitol 91 g/L, pH=7.2) broth or plates with 25 μg/mL kanamycin were used for

148 the cultivation or transformation of *C. glutamicum*.

149

150 **2.2 Genetic manipulation**

151 All DNA manipulation was performed according to standard protocols (Green
152 and Sambrook, 2012). Phanta DNA polymerase (Vazyme, Biotech, Co., Ltd.,
153 China) was used for DNA fragment amplification by polymerase chain reaction
154 (PCR, ThermoFisher ProFlex PCR system). The kits for DNA fragment
155 purification and gel extraction were purchased from Omega Bio-Tek Inc.
156 (Norcross, GA, USA). The plasmid miniprep kit was purchased from TIANGEN
157 Biotech (Beijing, China), and the Gibson assembly reaction kit was purchased
158 from New England Biolabs (NEB, Ipswich, MA, USA).

159 The plasmid pK18mobsacB was used for point mutation of the *lysC* gene in the
160 *C. glutamicum* ATCC13032 genome. The primers P1 and P2 were used to
161 amplify the pK18 backbone from pK18mobsacB, primers P3 and P4 with a point
162 mutation (C932T, red font) were used to amplify part of *lysC* from the *C.*
163 *glutamicum* ATCC13032 genome, and primers P5 with a point mutation (C932T,
164 red font) and P6 were used to amplify the other part of *lysC* and 588 bp of the
165 *lysC* downstream fragment from the *C. glutamicum* ATCC13032 genome; the
166 **pK18-lysC** plasmid was obtained by Gibson assembly of the above three
167 fragments. Then, pK18-lysC was transformed into *C. glutamicum* ATCC13032.
168 After double crossover homologous recombination driven by sucrose selection
169 based on the function of *sacB* (Schäfer et al., 1994), we obtained the ***C.***

170 ***glutamicum* XT1** (*lysC*: C932T) strain with sequence confirmation.

171 For promoter strength analysis in *C. glutamicum* XT1, primers P7 (containing
172 part of the H1 sequence) and P8 were used to amplify the H1-mCherry fragment
173 from pBbSlactam, primers P9 and P10 (containing part of the H1 sequence)
174 were used to amplify the pEC backbone from pEC-XK99E, and then Gibson
175 assembly of the above two fragments was performed to obtain **pH1-mCherry**.
176 Primers P11 (containing part of the H2 sequence) and P8 were used to amplify
177 the H2-mCherry fragment from pBbSlactam, primers P12 (containing part of the
178 H2 sequence) and P9 were used to amplify the pEC backbone from pEC-
179 XK99E, and Gibson assembly of the above two fragments was used to obtain
180 **pH2-mCherry**. Primers P13 (containing part of the H9 sequence) and P8 were
181 used to amplify the H9-mCherry fragment from pBbSlactam, primers P14
182 (containing part of the H9 sequence) and P9 were used to amplify the pEC
183 backbone from pEC-XK99E, and Gibson assembly of the above two fragments
184 was performed to obtain **pH9-mCherry**. Primers P15 (containing part of the
185 H10 sequence) and P8 were used to amplify the H10-mCherry fragment from
186 pBbSlactam, primers P16 (containing part of the H9 sequence) and P9 were
187 used to amplify the pEC backbone from pEC-XK99E, and Gibson assembly of
188 the above two fragments was performed to obtain **pH10-mCherry**.

189 To construct the high copy number plasmids derived from pCES208 (a kind gift
190 from Prof. Sang Yup Lee's Lab, (Park et al., 2008)), it was necessary to

191 introduce a nonsense mutation in the *parB* locus (Choi et al., 2018). Primers
192 P17 (with point mutation of *parB*, red font) and P18 (with point mutation of *parB*,
193 red font) were used to insert the point mutation into *parB*. Then, Gibson
194 assembly of this single PCR fragment was performed to obtain the **pHCP**
195 plasmid, and pCES208 and pHCP were used as backbones to construct the
196 valerolactam biosynthetic pathway. Primers P19 (containing part of the H1
197 sequence) and P20 (containing part of the RBS for *davB* and the RBS sequence
198 is from (Shin et al., 2016)) were used to amplify H1-*davA* from the synthesized
199 codon-optimized *davA* plasmid. Primers P21 (containing the RBS for *davB*) and
200 P22 (containing the RBS (Rohles et al., 2016) for *act*/*orf26*/*caiC*) were used to
201 amplify the *davB* fragment from the synthesized codon-optimized *davB* plasmid.
202 Primers P23 and P24 were used to amplify the *act* fragment from the
203 synthesized codon-optimized *act* plasmid, and then primers P19 and P24 were
204 used for fusion PCR of the H1-*davA*, *davB* and *act* fragments to obtain the H1-
205 davAB-act fragment. Primers P25 and P26 were used to amplify the pHCP
206 backbone from the pHCP plasmid, and then Gibson assembly of the pHCP
207 backbone and H1-davAB-act was performed to obtain the **pHCP-H1davAB-act**
208 plasmid. For pCES208-H1davAB-act plasmid construction, primers P25 and
209 P26 were used to amplify the pCES208 backbone from the pCES208 plasmid,
210 and then Gibson assembly of the pCES208 backbone with the H1-davAB-act
211 fragment was performed to obtain the plasmid. For pCES208-H1davAB plasmid
212 construction, primer P19 and primer P27 were used to amplify the H1davAB

fragment from H1davAB-act, and then Gibson assembly of pCES208 with H1davAB was performed to obtain the plasmid.

For pHCP-H1davAB-H1act plasmid construction, primers P21 and P28 were used to amplify *davB*-H1 from the synthesized codon-optimized *davB* plasmid. Primer P19 and primer P24 were used to amplify the H1-*act* fragment from the synthesized codon-optimized *act* plasmid, and then primers P19 and P24 were used for fusion PCR of the H1-*davA*, *davB*-H1 and H1-*act* fragments to obtain the H1-davAB-H1-act fragment. Gibson assembly of the H1-davAB-H1-act fragment with the pHCP backbone was used to obtain the plasmid.

For pHCP-H1davAB-Pb-act-chnR plasmid construction, primers P21 and P29 were used to amplify *davB*-Pb from the synthesized codon-optimized *davB* plasmid. Primers P30 and P31 were used to amplify the Pb fragment from pBbSlactam, primers P32 and P33 were used to amplify the Pb-*act* fragment from the synthesized codon-optimized *act* plasmid, primers P34 and P35 were used to amplify the *chnR* fragment from pBbSlactam, primers P19 and P29 were used for fusion PCR of H1-*davA* and *davB*-Pb to obtain the H1-davAB-Pb fragment, primers P30 and P35 were used for fusion PCR of Pb, Pb-*act* and *chnR* to obtain the Pb-*act*-chnR fragment, and then Gibson assembly of the H1-davAB-Pb, Pb-*act*-chnR and pHCP backbone was used to obtain the plasmid.

For construction of the other valerolactam biosynthetic pathway, many of the same primers were used to amplify the mutants from the different templates.

For example, for pHCP-H1davAB-E1act construction, primers P30 and P31 were used to amplify Pb-E1 from the pBbS-E1 plasmid, primers P32 and P24 were used to amplify *act* from the synthesized codon-optimized *act* plasmid, and primers P30 and P24 were used for fusion PCR of Pb-E1 and *act* fragments to obtain the E1-act fragment. Gibson assembly of H1-*davA*, *davB*, and E1-act was carried out to obtain **pHCP-H1davAB-E1act**.

For construction of dynamic regulation of *act* by ChnR/Pb-E1 system. Primers P30 and P35 were used for fusion PCR of Pb-E1, Pb-*act* and *chnR* to obtain the E1-*act*-chnR fragment, and then Gibson assembly of the H1-davAB-Pb, E1-*act*-chnR and pHCP backbone was performed to obtain **pHCP-H1davAB-E1-act-chnR**.

For construction of dynamic regulation of *act* by ChnR-B1/Pb system. Primers P34 and P35 were used to amplify the *chnR*-B1 fragment from pBbS-E1B1, then primers P30 and P35 were used for fusion PCR of Pb, Pb-*act* and *chnR*-B1 to obtain the Pb-*act*-B1 fragment. Next, Gibson assembly of the H1-davAB-Pb, Pb-*act*-B1 and pHCP backbone was performed to obtain **pHCP-H1davAB-Pb-act-B1**.

For construction of dynamic regulation of *act* by ChnR-B1/Pb-E1 system. Primers P30 and P35 were used for fusion PCR of Pb-E1, Pb-*act* and *chnR*-B1 to obtain the E1-*act*-B1 fragment, and then Gibson assembly of the H1-davAB-Pb, E1-*act*-B1 and pHCP backbone was performed to obtain **pHCP-H1davAB-**

**E1-act-B1**.

For construction of ORF26 as the catalysts for the cyclization step of valerolactam biosynthesis. Primers P36 and P37 were used to amplify the *orf26* fragment from the synthesized codon-optimized orf26 plasmid, then primers P19 and P37 were used for fusion PCR of the H1-*davA*, *davB* and *orf26* fragments to obtain the H1-davAB-orf26 fragment. Next, Gibson assembly of the pHCP backbone and H1-davAB-orf26 was used to obtain the **pHCP-H1davAB-orf26** plasmid.

For construction of dynamic regulation of *orf26* by ChnR-B1/Pb-E1 system. Primers P36 and P38 were used to amplify Pb-orf26 from the synthesized codon-optimized orf26 plasmid, and primers P30 and P35 were used for fusion PCR of Pb-E1, Pb-*orf26* and *chnR*-B1 to obtain the E1-orf26-B1 fragment. Then, Gibson assembly of the H1-davAB-Pb, E1-*orf26*-B1 and pHCP backbone was performed to obtain the **pHCP-H1davAB-E1-orf26-B1** plasmid.

For construction of CaiC as the catalysts for the cyclization step of valerolactam biosynthesis Primers P39 and P40 were used to amplify the *caiC* fragment from the synthesized codon-optimized *caiC* plasmid, then primers P19 and P40 were used for fusion PCR of the H1-*davA*, *davB* and *caiC* fragments to obtain the H1-davAB-caiC fragment. Next, Gibson assembly of the pHCP backbone and H1-davAB-caiC was used to obtain the **pHCP-H1davAB-caiC** plasmid.

For construction of dynamic regulation of *caiC* by ChnR-B1/Pb-E1 system.

Primers P39 and P41 were used to amplify Pb-*caiC* from the synthesized codon-optimized *caiC* plasmid, and primers P30 and P35 were used for fusion PCR of Pb-E1, Pb-*caiC* and *chnR*-B1 to obtain E1-*caiC*-B1. Then, Gibson assembly of the H1-davAB-Pb, E1-*caiC*-B1 and pHCP backbone was performed to obtain **pHCP-H1davAB-E1-caiC-B1**.

All the above Gibson assembly reactions were transformed into *E. coli* DH5α, and the plasmids were sequenced.

### 2.3 Promoter analysis

The constructed pH1-mCherry, pH2-mCherry, pH9-mCherry, and pH10-mCherry plasmids were transformed into *C. glutamicum* XT1 using electro transformation (Ruan et al., 2015). Three randomly selected colonies from each plate were inoculated into 3 mL of LBHIS with 25 μg/mL kanamycin and incubated at 30 °C and 200 rpm shaking for 16-18 hours. Then the cells were inoculated (1:100) into 96-deep well plates containing 1 mL of LBHIS and 25 μg/mL kanamycin. The cells in the 96-deep well plates were cultured in a high-speed shaker at 30 °C and 800 rpm. One hundred microliters of culture medium were removed at 12 h, 24 h, 36 h, and 48 h for mCherry fluorescence signal analysis ($\lambda_{ex}$=575 nm, $\lambda_{em}$=620 nm) with an Infinite 200 PRO (TECAN, San Jose, CA).

### 2.4 Mutant library construction and biosensor engineering

For valerolactam biosensor engineering, the primers P42 and P43 were used to amplify sfGFP from pMD19-sfGFP, which was a kind gift from Prof. Fu's laboratory (SIAT, Shenzhen, China). The primers P44 and P45 were used to amplify the backbone from pBbSlactam, and then Gibson assembly of the backbone and sfGFP was performed to obtain pBbS-sfGFP. Primers P46 and P47 (N in red font was indicated as the putative binding site of the transcription factor ChnR (Cheng et al., 2000), Table S2) were used to amplify the Pb site-saturated mutant library fragments followed by Gibson assembly and transformation into *E. coli* DH10B to obtain the Pb mutant library. Then, 20-30 colonies were randomly selected for sequencing to analyze the quality of the library. *E. coli* DH10B with the Pb mutant library was sorted with 1 mM valerolactam by fluorescence-activated cell sorting (FACS, BD Aria III, San Jose, USA) to obtain the colonies with the highest 1% sfGFP signal. These colonies were plated on LB agar with 25 μg/mL chloramphenicol. Approximately 500 colonies were randomly placed into 96-deep well plates with 1 mL of LB (including 25 μg/mL chloramphenicol and 1 mM valerolactam) and cultured for 12 hours at 37 °C and 800 rpm in a high-speed shaker. Samples (100 μL) were then placed into 96-well plates for sfGFP fluorescence analysis ($\lambda_{ex}$=488 nm, $\lambda_{em}$=520 nm). A mutant Pb-E1 (5'-3': TGTAGCCCACC) showed a much higher sfGFP signal in response to 1 mM valerolactam than the wild type (5'-3': ttgtttggatc). The plasmid with this mutation was named pBbS-E1.

Primers P48 and P49 were used for error-prone PCR (epPCR) of the *chnR*

gene to engineer the transcription factor ChnR to generate a mutant with a higher binding affinity for valerolactam. epPCR was performed according to the instruction manual of the GeneMorph II Random Mutagenesis Kit (Agilent Technologies, #200550). To obtain a library with both low and medium mutation frequencies of ChnR, 4 tubes (50 μL) were used for epPCR with 300 ng-500 ng of target DNA, which were conducted as follows: 95 °C for 2 min, 23× (95 °C for 30 s, 55 °C for 30 s, 72 °C for 1 min and 15 s), and 72 °C for 10 min. The epPCR products were subjected to gel extraction for library construction. Primers P50 and P51 were used to amplify the E1 backbone from pBbS-E1 followed by Gibson assembly of the *chnR* epPCR products and E1 backbone, and the Gibson reaction products were transformed into *E. coli* DH10B competent cells to obtain the ChnR random mutant library (~1*10^6 colonies were obtained). Approximately 40 colonies from the ChnR library were randomly selected for sequencing to assess the quality of the mutant library. The library was cultured with 1 mM valerolactam for 12 h, and the colonies with the top 1% sfGFP signal were sorted by FACS. These colonies were recultured with 1 mM valerolactam for a second round of FACS. Approximately 1000 colonies from the second round of FACS were randomly placed into 96-deep well plates with 1 mL of LB (including 25 μg/mL chloramphenicol and 1 mM valerolactam) and cultured for 12 hours at 37 °C and 800 rpm in a high-speed shaker. Then, 100 μL samples were placed in 96-well plates for sfGFP fluorescence analysis ($\lambda_{ex}$=488 nm, $\lambda_{em}$=520 nm), and a new mutant, ChnR-B1

(S63G, V121A) showed a much higher sfGFP signal to 1 mM valerolactam than the control pBbS-E1. The plasmid with this ChnR (S63G, V121A) mutation was named pBbS-E1B1.

### 2.5 Flask culture of the *C. glutamicum* strains to produce L-lysine and recombinant *C. glutamicum* XT1 to produce valerolactam

To compare the L-lysine production by *C. glutamicum* ATCC13032 and XT1, the strains from the glycerol stock were cultured on LBHIS agar for 24 hours, and then three randomly picked colonies were recultured on new LBHIS agar for 24 hours for the second round of activation. Three colonies each of *C. glutamicum* WT and XT1 from the second-round activation plates were cultured in LBHIS medium at 30 °C and 200 rpm shaking for 17-18 hours as the seed culture. For flask culture, the seed culture was added to a 250 mL flask containing 25 mL of growth medium (100 g/L glucose, 1 g/L $MgSO_4$, 1 g/L $K_2HPO_4$, 1 g/L $KH_2PO_4$, 1 g/L urea, 40 g/L $(NH_4)_2SO_4$, 10 g/L yeast extract, 100 μg/mL biotin, 10 mg/L β-alanine, 10 mg/L thiamine HCl, 10 mg/L nicotinic acid, 1.3 mg/L $(NH_4)_6MoO_{24}$, 40 mg/L $CaCl_2$, 10 mg/L $FeSO_4$, 10 mg/L $MnSO_4$, 5 mg/L $CuSO_4$, 10 mg/L $ZnSO_4$, and 5 mg/L $NiCl_2$) to have an initial $OD_{600}$=0.1, which was modified based on previous research (Shin et al., 2016). Each flask contained 0.75 g of $CaCO_3$ to maintain the pH at ~7.0 during cultivation, and the flasks were cultured at 30 °C with shaking at 220 rpm. Then, 500 μL samples were removed at 24 hours, 48 hours and 72 hours for quantitative analysis of L-lysine.

To examine whether increasing the expression of valerolactam biosynthetic pathway genes can improve valerolactam production, the plasmids pCES208-H1davAB, pCES208-H1davAB-act and pHCP-H1davAB-act were transformed into *C. glutamicum* XT1. To compare the strong constitutive promoter and the dynamically upregulated system of *act* for valerolactam biosynthesis, the pHCP-H1davAB-act, pHCP-H1davAB-H1act, and pHCP-H1davAB-Pb-act-chnR plasmids were transformed into *C. glutamicum* XT1. To compare the engineered biosensor system-assisted dynamic upregulation of *act* for valerolactam biosynthesis, the pHCP-H1davAB-E1-act, pHCP-H1davAB-E1-act-chnR, pHCP-H1davAB-Pb-act-B1, and pHCP-H1davAB-E1-act-B1 plasmids were transformed into *C. glutamicum* XT1. To determine whether the engineered biosensor system could assist in the dynamic upregulation of ORF26 and CaiC to produce more valerolactam than the strong consistent promoter, the plasmids pHCP-H1davAB-orf26 and pHCP-H1davAB-E1-orf26-B1, pHCP-H1davAB-caiC, and pHCP-H1davAB-E1-caiC-B1 were transformed into *C. glutamicum* XT1. Three randomly selected colonies from the above transformation plates were cultured in LBHIS medium with 25 μg/mL kanamycin at 30 °C and 200 rpm shaking for 17-18 hours as seed culture. For flask cultures, the seed culture was added to a 250 mL flask containing 25 mL of fermentation medium to have an initial $OD_{600}$=0.1, the fermentation medium was the same as the L-lysine production medium, plus 25 μg/mL kanamycin. Each flask contained 0.75 g of $CaCO_3$ to maintain the pH at ~7.0 during cultivation. The

386 culture conditions were 30 °C at 220 rpm for 48 hours, and 1 mL samples were
387 removed for measuring the $OD_{600}$ and quantitative analysis of L-lysine, 5-AVA
388 and valerolactam.
389
390 **2.6 Fed-batch fermentation to produce valerolactam**
391 The glycerol stocks of *C. glutamicum* XT1 pHCP-H1davAB-E1-act-B1, *C.*
392 *glutamicum* XT1 pHCP-H1davAB-E1-orf26-B1, and *C. glutamicum* XT1 pHCP-
393 H1davAB-E1-caiC-B1 were first cultured on LBHIS agar with 25 μg/mL
394 kanamycin, and after 24 hours, the activated colonies were transferred to a new
395 LBHIS plate with 25 μg/mL kanamycin for the second generation cultures. The
396 second generation cultures were collected and inoculated into a 250 mL flask
397 with 50 mL of seed medium, which was the same as that previously reported
398 (Shin et al., 2016), and grown at 30 °C and 220 rpm for 17-18 hours.
399 Approximately 40 mL of seed medium was added as the inoculum to 400 mL of
400 fermentation medium (initial $OD_{600}$=1.5-2.0) with 25 μg/mL kanamycin in a 1.2
401 L fermenter. The fed-batch fermentation medium was the same as that used by
402 Shin et al., 2016, except that the biotin concentration was 1.8 mg/L. An
403 Eppendorf-DASGIP parallel bioreactor system (Hamburg, Germany) equipped
404 with eight 1.2-L jars was used for all fed-batch cultivation experiments. The
405 temperature and agitation were maintained at 30 °C and 1200 rpm, respectively,
406 and the pH was maintained at 7.0 by the addition of a 28% (v/v) ammonia
407 solution. Foaming was suppressed by adding 10% (v/v) antifoam 204 (Sigma–

Aldrich, St. Louis, MO, USA). A 50% (w/v) glucose solution was added when the residual glucose level was below than 5 g/L. Samples were taken every 12 hours to analyze the L-lysine, 5-aminovaleric acid, and valerolactam contents, the residual glucose was analyzed with a SBA-40E Biosensor analyzer (Jinan Yanhe Biotechnology Co., LTD, Jinan, China), and the $OD_{600}$ was measured with a cell density meter Ultrospec 10 (Biochrom, Cambridge, UK).

**2.7 Quantitative analysis of L-lysine, 5-AVA and valerolactam**

A high-performance liquid chromatography–mass spectrometry (LC–MS) instrument (Agilent 1290-6470, Agilent Technologies, Santa Clara, CA, USA) fitted with an EC-C18 column (4.6 × 100 mm; Agilent Technologies) was operated at 37 °C to determine the L-lysine, 5-AVA and valerolactam concentrations in the culture broth (flask culture and fed-batch culture). Samples were removed from the cultured medium and placed in 2.0 ml Eppendorf tubes, and 100 μL of supernatant was obtained by centrifugation at 11600 x *g* for 3 min. Then, the 100 μL of supernatant was treated with a freeze dryer (Christ Alpha-2LDplus, Osterode, Germany) for 2-3 hours and resuspended in 1 mL of 5% MeOH. This solution was diluted 1000-fold before each sample was subjected to LC–MS analysis. The method for valerolactam quantitation was modified based on a previous report (Chae et al., 2017). The mobile phase was composed of solvent A ($H_2O$, 0.1% formic acid) and solvent B (MeOH), and elution was performed with the following gradient: 0-10 min,

5%-30% B at 0.5 mL/min; and 10-16 min, 5% B at 0.5 mL/min. The eluent was directed to the mass spectrometer, which was operated in electrospray ionization (ESI) positive ion mode with the following conditions: gas temperature, 350 °C; gas flow, 10.0 L/min; nebulizer, 45 psi; and capillary voltage, 3.5 kV. Multiple reaction monitor (MRM) mode was selected as the scan mode to detect precursor-to-product ion transitions. The m/z transitions were 100.1 to 44.1 (fragmentor: 110; CE: 40) and 100.1 to 56.1 (fragmentor: 110; CE: 21). For the quantitation of L-lysine and 5-AVA, the mobile phase was applied from 0-10 min with 5% B (MeOH) at a flow rate of 0.2 mL/min. The same mass spectrometry parameters were used, except MRM mode was set to 147 to 130.1 (fragmentor: 80; CE: 9) and 147 to 84.1 (fragmentor: 80; CE: 17) for L-lysine, and the 5-AVA m/z transitions were 118 to 101(fragmentor: 80; CE: 9) and 118 to 55.1 (fragmentor: 80; CE: 2). Standards of L-lysine (Sigma–Aldrich), 5-AVA (Sigma–Aldrich) (each 5.0 mg/L, 2.5 mg/L, 1.25 mg/L, 0.625 mg/L and 0.3125 mg/L) and valerolactam (Sigma–Aldrich) (each 4.0 mg/L, 2.0 mg/L, 1.0 mg/L, 0.5 mg/L, 0.25 mg/L and 0.125 mg/L) were used to generate standard curves. Statistical analysis was performed with GraphPad Prism 8.0.1 (La Jolla, CA, USA), and the results are reported as the mean with SD (*n*=3).

## 3. Results

### 3.1. Construction of the valerolactam biosynthetic pathway in an L-lysine-

**producing *C. glutamicum* mutant.**

Three enzymatic reactions are needed to convert L-lysine into valerolactam (Fig. 1A). To eliminate the need to add extracellular L-lysine to the reaction, we constructed a chassis strain that produces L-lysine. We chose *C. glutamicum* ATCC13032 as the base strain for L-lysine production because it is Generally Recognized as Safe (GRAS) and is already considered a strain that can be used for industrial L-lysine production (Becker et al., 2011). The wild-type *lysC* in the genome of *C. glutamicum* ATCC13032 was replaced with a mutant *lysC* (C932T) to construct the mutant strain *C. glutamicum* XT1. The aspartokinase encoded by *lysC* is a key regulatory enzyme in L-lysine biosynthesis, and the point mutation C932T can increase L-lysine production by reducing feedback inhibition by L-lysine (Fig. 1B) (Ohnishi et al., 2002)(Becker et al., 2011). This strain produced 5.23 g/L L-lysine within 48 hours in flask culture (Fig. 1B). Using lysine-producing *C. glutamicum* XT1 as the chassis strain for valerolactam biosynthesis, we then designed, constructed, and tested various strategies for gene regulation to produce valerolactam.

Act, encoding the β-alanine CoA transferase from *Clostridium propionicum* (Chae et al., 2017), ORF26, encoding the acyl-CoA ligase from *Streptomyces aizunensis*, and CaiC, encoding a crotonobetaine CoA ligase from *E. coli* (Zhang et al., 2017b), have been reported to be catalysts for the cyclization step of valerolactam biosynthesis, and together with DavB and DavA from *P. putida*, they compose the valerolactam biosynthetic pathway. Act was selected first to

metabolically engineer a valerolactam biosynthetic pathway to improve the titer of valerolactam in *C. glutamicum* XT1.

The strengths of the previously characterized strong constitutive *C. glutamicum* promoters H1, H2, H9 and H10, which showed strength similar to or greater than the widely used strong promoter pH36 (Wei et al., 2018), were revalidated in *C. glutamicum* XT1 with mCherry as a reporter. As indicated by mCherry fluorescence, promoter H1 showed the highest strength (Fig. S1) and was selected to drive the valerolactam biosynthetic pathway genes for subsequent research. According to previous research, the high copy number plasmid pHCP was constructed based on pCES208; compared with pCES208 (4-5 copies/cell), the copy number of pHCP increased 10-fold (Choi et al., 2018). The strongest constitutive promoter, H1, was used to drive expression of DavA, DavB and Act, which were integrated into both pCES208 and pHCP to obtain pCES208-H1davAB-act and pHCP-H1davAB-act, respectively, whereas H1-driven DavA and DavB (no Act) were ligated into pCES208 to obtain pCES208-H1DavAB as a negative control. These plasmids (pCES208-H1DavAB, pCES208-H1davAB-act, and pHCP-H1davAB-act) were transformed into *C. glutamicum* XT1 yielding strains *C. glutamicum* Val-1, *C. glutamicum* Val-2, and *C. glutamicum* Val-3, respectively, to test their corresponding valerolactam titers.

In flask cultures, 0.73 g/L valerolactam was produced by *C. glutamicum* Val-2, which was 25-fold more than that with the same pathway genes in *E. coli* under flask culture conditions (29 mg/L) (Chae et al., 2017); moreover, 0.97 g/L

valerolactam was produced by *C. glutamicum* Val-3 (Fig. S2). In *C. glutamicum* Val-3, most of the L-lysine was transformed into 5-AVA by the overexpressed DavA and DavB by increasing the plasmid copy number, whereas in Val-2 there were approximately equal amounts of L-lysine and 5-AVA (Fig. S2). Hence, we concluded that the cyclization of 5-AVA into valerolactam by Act is the rate-limiting step for valerolactam biosynthesis.

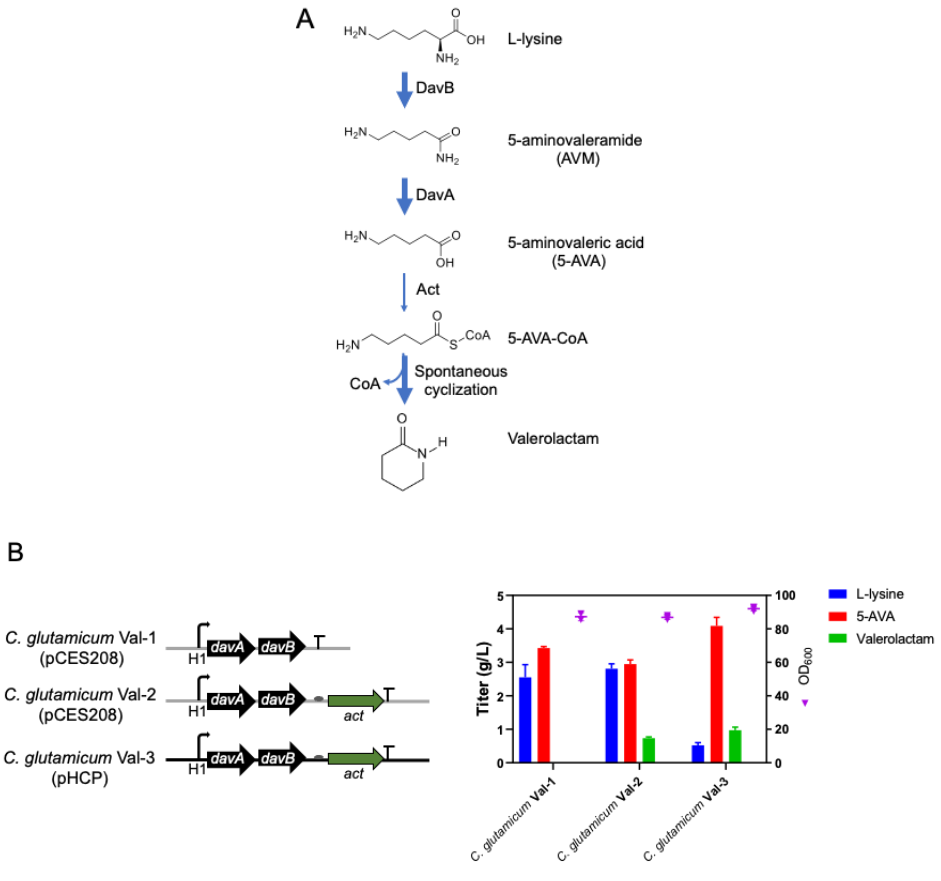


**Figure 1. (A)** The biosynthetic pathway of valerolactam from L-lysine. **(B)** L-lysine, 5-AVA, and valerolactam production by *C. glutamicum* XT1 mutants with different versions of the valerolactam biosynthetic pathway. 5-AVA (5-aminovaleric acid).

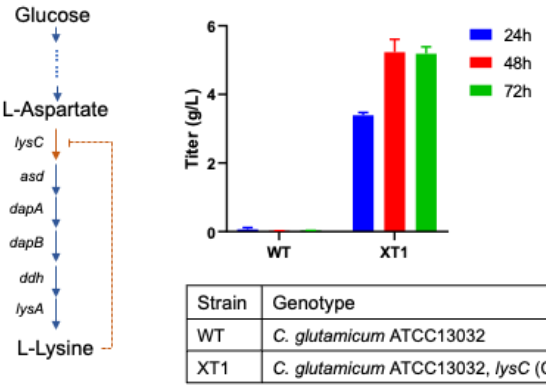


| Strain | Genotype |
|---|---|
| WT | *C. glutamicum* ATCC13032 |
| XT1 | *C. glutamicum* ATCC13032, *lysC* (C932T) |

507

508 **Figure S1**. The L-lysine biosynthetic pathway from glucose in

509 *Corynebacterium glutamicum* and the titer of L-lysine produced by *C.*

510 *glutamicum* ATCC13032 (WT) and mutant (XT1) in flask cultures.

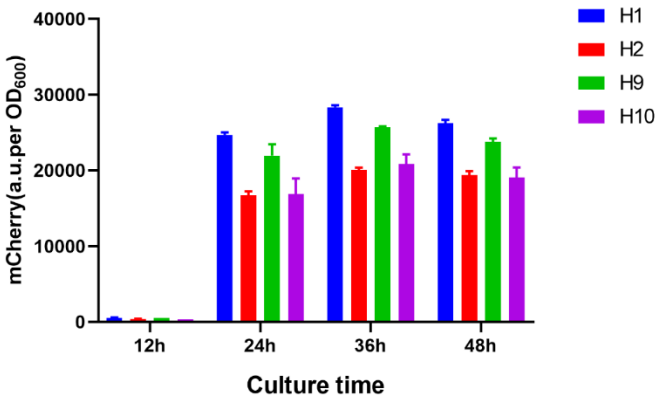


511

512 **Figure S2.** Strengths of the strong constitutive promoters evaluated in *C.*

513 *glutamicum* XT1.

514

515 **3.2 Design of a dynamic upregulation system to amplify the expression of**

516 **Act**

517 To further improve the titer of valerolactam, our primary task became how

518 to obtain much higher expression of Act than in *C. glutamicum* Val-3. We first

519 tried to add another strong promoter, H1, to drive Act to further increase its

520 expression level, resulting in plasmid pHCP-H1davAB-H1act (Fig. 2B). In

addition, a dynamic upregulation strategy was also used to further amplify the expression of Act. Previously this positive feedback loop (dynamic upregulation)-based gene amplifier was shown to dramatically increase the expression of the regulated GFP gene (Nistala et al., 2010). Thus, we designed the valerolactam biosensor ChnR/Pb system as a positive feedback amplifier to regulate the expression of Act (Fig. 2A). The promoter H1 was used to drive the expression of valerolactam biosynthetic pathway genes with Act regulated by the ChnR/Pb system to obtain the pHCP-H1davAB-Pb-act-chnR plasmid (Fig. 2). We hypothesized that the promoter H1 would initiate expression of Act and ChnR, and then the valerolactam produced from the cyclization reaction of 5-AVA would bind with ChnR to form a ChnR-valerolactam complex that would regulate expression of the Pb promoter (Zhang et al., 2017a), thus initiating the dynamic upregulation system (positive feedback amplifier) (Fig. 2A).

Comparing the valerolactam titers in the flask cultures of *C. glutamicum* Val-4 and *C. glutamicum* Val-5, which are *C. glutamicum* XT1 harboring pHCP-H1davAB-H1act and pHCP-H1davAB-Pb-act-chnR, respectively, with that from the *C. glutamicum* Val-3 control, 0.67 g/L and 0.15 g/L valerolactam were produced with *C. glutamicum* Val-4 and *C. glutamicum* Val-5, respectively, which were both lower than the valerolactam produced with the *C. glutamicum* Val-3 control (Fig. 2C). This decrease in valerolactam production with the extra H1 promoter for Act in *C. glutamicum* Val-4 may have been explained by (Rohles et al., 2022), who found that an additional promoter of the second gene

in a two-gene operon can sometimes decrease the expression levels of the genes. To our surprise, the valerolactam pathway dynamically upregulated in *C. glutamicum* Val-5 showed less valerolactam production than the control (Fig. 2C). We suspected that the main reason for this result was due to the lower sensitivity (1-50 mM) and poor dynamic output range (2.4) of the original valerolactam biosensor (ChnR/Pb system) (Zhang et al., 2017a), which limited the expression of Act.

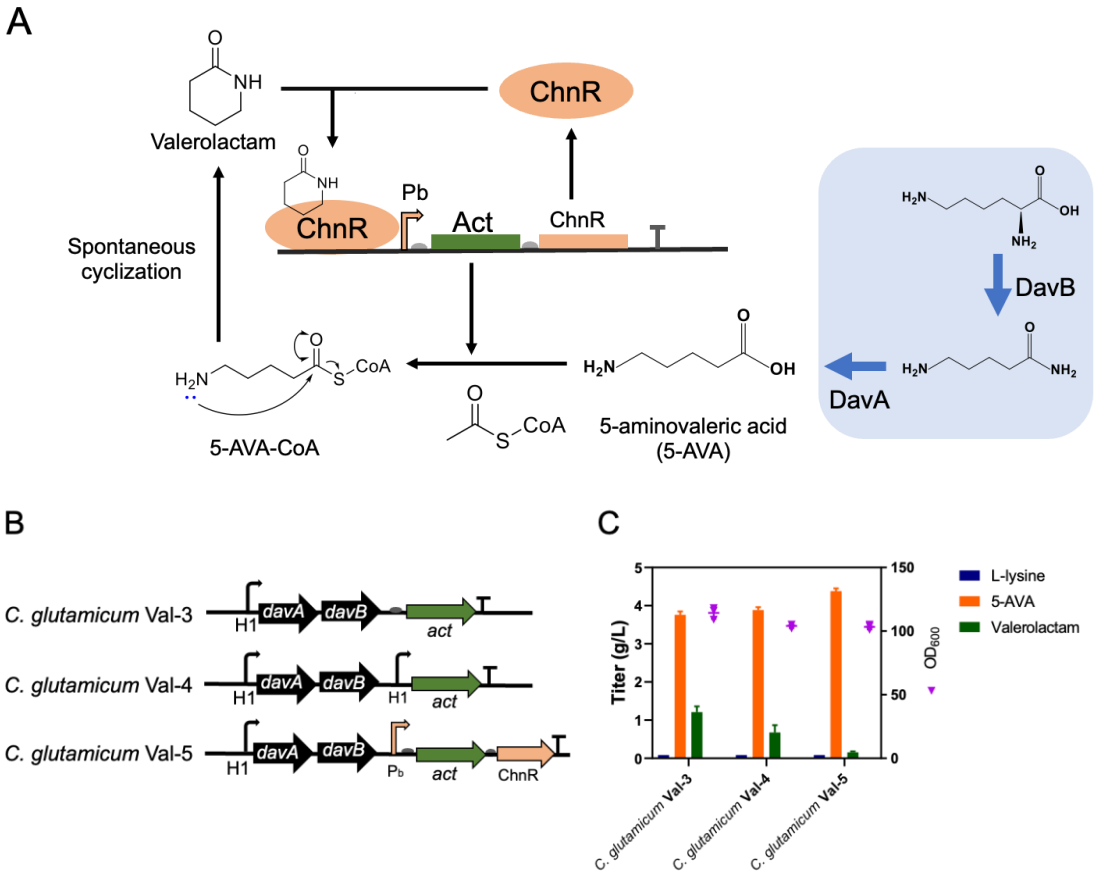


**Figure 2.** Valerolactam production and the dynamic regulatory system developed here. **(A)** Schematic of the ChnR/Pb system for dynamic upregulation of the expression of Act in the valerolactam biosynthetic pathway. **(B)** Valerolactam biosynthetic gene cluster with three different regulatory

systems. **(C)** Production of L-lysine, 5-AVA, and valerolactam in flask cultures at 48 hours. 5-AVA (5-aminovaleric acid).

### 3.3. Improving the sensitivity and dynamic output range of the valerolactam biosensor.

The sensitivity and dynamic output range of the biosensor in the ChnR/Pb system determine the expression time and maximum expression level of Act. To improve the sensitivity and dynamic output range of the biosensor, the binding affinities of the transcription factor ChnR for the promoter Pb and substrate valerolactam should be modified (Snoek et al., 2020). The original valerolactam biosensor (ChnR/Pb system) was characterized in *E. coli* DH10B (Zhang et al., 2017a), and mutant library construction, sorting and characterization of the valerolactam biosensor were also performed in *E. coli* DH10B. Cheng et al. proposed a putative ChnR binding region (5'-3': TTGTTTGGATC) in the promoter Pb (Cheng et al., 2000), so we constructed a Pb site-saturation mutagenesis library based on the predicted ChnR binding region with sfGFP as the reporter. The Pb mutant library was cultured with 1 mM valerolactam for 12 hours and then sorted by FACS for the mutants with the top 1% sfGFP signal (Fig. S3A). Approximately 500 colonies from the FACS-sorted group were further tested with 1 mM valerolactam. The biosensor mutant E1 (5'-3': TGTAGCCCACC) showed a higher sfGFP signal than the original biosensor pBbS-sfGFP after treatment with 1 mM valerolactam. The biosensor

with this Pb mutation (E1) was named pBbS-E1. The fluorescence output of strains harboring biosensor plasmids pBbS-E1 and pBbS-sfGFP were compared for valerolactam concentrations in the range 0-100 mM. The results from pBbS-E1 showed a linear correlation in the fluorescence intensity with 0-1 mM valerolactam, while there was no response from pBbS-sfGFP with 0-1 mM valerolactam (Fig. S3B), indicating the increased sensitivity of pBbS-E1 compared with the original biosensor pBbS-sfGFP. Moreover, the dynamic output range of pBbS-E1 was much higher than that of pBbS-sfGFP for 0-100 mM valerolactam (Fig. 3).

Engineering the valerolactam binding domain in the transcription factor ChnR should further increase the dynamic output range (Snoek et al., 2020)(Mannan et al., 2017); however, the valerolactam binding domain in ChnR is not yet defined. Therefore, a random ChnR mutagenesis library was constructed based on the pBbS-E1 plasmid by error-prone PCR (epPCR). This mutant library was then cultured with 1 mM valerolactam for FACS sorting. After two rounds of FACS sorting for the colonies with the top 1% sfGFP signal in response to 1 mM valerolactam, approximately 1000 colonies were randomly selected for testing with 1 mM valerolactam (Fig. S3A). There were three biosensor mutants that showed a higher sfGFP signal in response to 1 mM valerolactam than biosensor pBbS-E1: M-B1 (S63G and V121A), M-E5 (N22T and S63G) and M-A4 (T281N). The M-B1 mutant showed the largest dynamic output range with 0-1 mM valerolactam, which was 3.0-fold higher than the

pBbS-E1 control (Fig. S3C). We found that the valerolactam biosensors with these ChnR mutants had a higher dynamic output range with increased leaky expression, especially the biosensor with the M-B1 mutant, which showed the highest leaky expression among these biosensors (Fig. S3C). The output fluorescence signal intensity of the biosensor with the M-B1 mutant with 0 mM valerolactam was even higher than that of the control pBbS-E1 at 1 mM valerolactam (Fig. S3C). The leaky expression of this biosensor with the M-B1 mutant may help initiate the dynamic upregulation at an early stage and hence increase the expression of Act to a greater extent than the other ChnR mutants. The biosensor with this M-B1 mutation with the highest dynamic output range was named pBbS-E1B1 (Fig. 3) (ChnR-B1/Pb-E1 system) and was chosen for subsequent engineering.

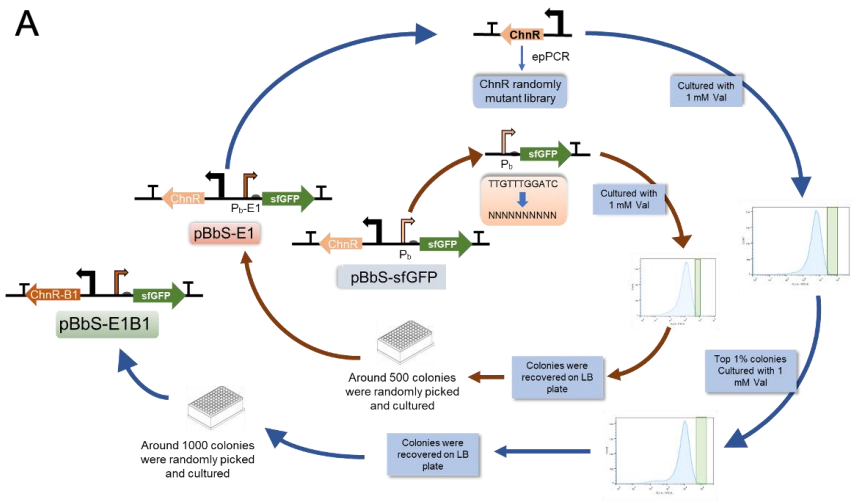

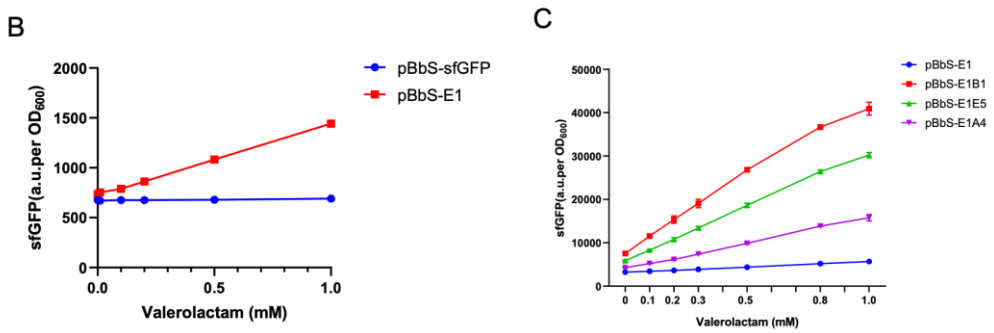


**Figure S3. (A)** Schematic of engineering the valerolactam biosensor. We started with the pBbS-sfGFP biosensor. Red arrow indicates engineering the ChnR binding site in Pb promoter. The Pb site-saturation mutagenesis library was sorted by FACS for the colonies with top 1% GFP signal, and these colonies were further verified in 96-well plates with 1 mM valerolactam to get biosensor pBbS-E1. Blue arrow indicates improving the binding affinity of ChnR for valerolactam (Val) by two rounds of FACS sorting. The ChnR mutants selected from the second round of FACS sorting were further verified in 96-well plates with 1 mM valerolactam to get the biosensor mutant pBbS-E1B1 with the highest fluorescence signal. **(B)** Comparison of the outputs of the biosensor mutant pBbS-E1 with the original valerolactam biosensor pBbS-sfGFP for 0-1 mM valerolactam. **(C)** Comparison of the output from promoter Pb with different ChnR mutants with the pBbS-E1 control for 0-1 mM valerolactam.

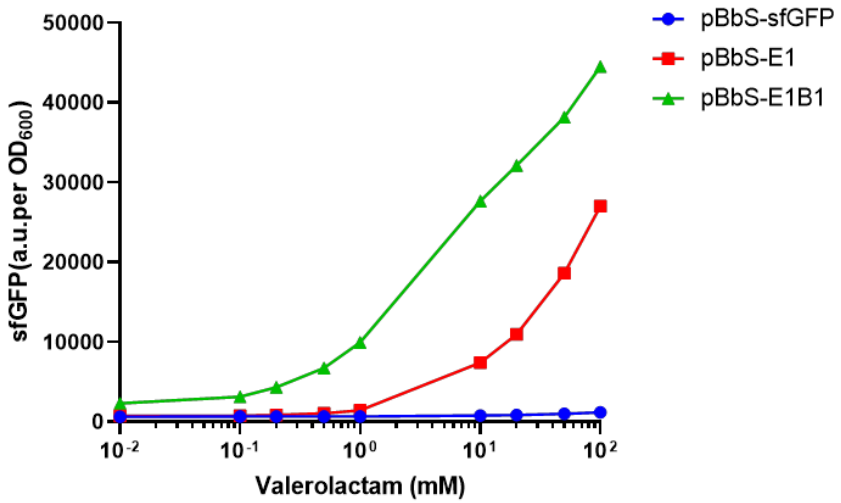


**Figure 3.** Comparison of the outputs of the evolved biosensor pBbS-E1 and pBbS-E1B1 with the original biosensor pBbS-sfGFP in different concentrations of valerolactam.

### 3.4. The ChnR-B1/Pb-E1 system improved valerolactam production.

The engineered ChnR-B1/Pb-E1 system (from pBbS-E1B1) can be used to increase the titer of valerolactam. ChnR-B1 and Pb-E1 were used to replace wild-type ChnR and Pb, respectively, in the dynamic upregulation pathway (Fig. 2). The Pb-E1 mutant without ChnR was used as a negative control to regulate the expression of Act, and the combinations of Pb-E1 with ChnR and Pb with ChnR-B1 were also constructed and tested (Fig. 4). These different combinations of ChnR and Pb helped us determine the best promoter regulator for our dynamic regulation system. The valerolactam biosynthetic pathway plasmids were transformed into *C. glutamicum* XT1, and *C. glutamicum* Val-3, with the highest titer of valerolactam thus far, was set as a control. After 48 hours of flask culture, *C. glutamicum* Val-9 with the ChnR-B1/Pb-E1 system

(pHCP-H1davAB-E1-act-B1) produced 2.46 g/L valerolactam, an increase in the titer of more than 100% compared with the *C. glutamicum* Val-3 control (1.21 g/L) (Fig. 4B).

We also noticed that *C. glutamicum* Val-8 with the ChnR-B1/Pb system (pHCP-H1davAB-Pb-act-B1) was able to produce much more valerolactam (2.11 g/L) than the *C. glutamicum* Val-3 control (Fig. 4B). In contrast, *C. glutamicum* Val-6 (Pb-E1 negative control) and *C. glutamicum* Val-7 (ChnR/Pb-E1 system) produced much less (0.11 g/L and 0.16 g/L, respectively) than the control. From these flask culture results, we found that the strains using ChnR-B1 for the dynamic upregulation of Act were able to produce more valerolactam than the *C. glutamicum* Val-3 control, while the strains with wild-type ChnR for the dynamic upregulation of Act produced a limited amount of valerolactam. These results indicate that the properties of the transcription factor ChnR play a key role in our designed dynamic upregulation system to increase the expression level of Act. Since *C. glutamicum* Val-9 with the ChnR-B1/Pb-E1 system regulates the expression of Act and produces a higher titer of valerolactam than the promoter H1 control, we were interested in whether this dynamic upregulation system can be used to increase the expression of the other enzymes (ORF26 and CaiC) to improve the production of valerolactam.

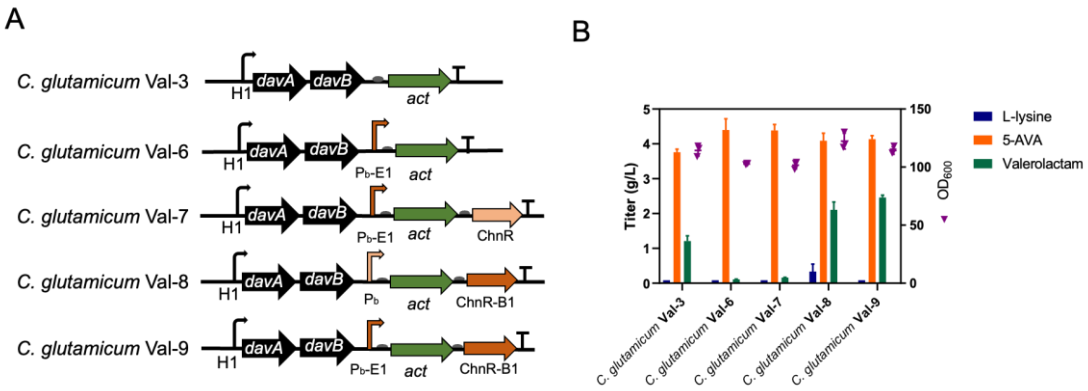


**Figure 4.** Dynamic upregulation of Act with the different regulator-promoter systems for valerolactam biosynthesis. **(A)** Design of the valerolactam pathway with different ChnR and Pb mutant combinations. **(B)** Flask culture results of the different valerolactam biosynthesis pathways indicated in **(A)**. 5-AVA (5-aminovaleric acid).

### 3.5. Dynamic upregulation of ORF26 and CaiC for valerolactam production in *C. glutamicum* XT1.

To test whether the engineered ChnR-B1/Pb-E1 system can be used for dynamic upregulation of the expression of ORF26 and CaiC in valerolactam biosynthesis, *C. glutamicum* codon optimized versions of ORF26 and CaiC were constructed as catalysts for the cyclization step in the valerolactam biosynthetic pathway. These genes were introduced into the various plasmids in place of *act* creating pHCP-H1davAB-orf26 and pHCP-H1davAB-caiC (the controls) and pHCP-H1davAB-E1-orf26-B1 and pHCP-H1davAB-E1-CaiC-B1 (ChnR-B1/Pb-E1 regulated systems) (Fig. 5A). After transformation into *C. glutamicum* XT1, flask culture was carried out for 48 hours. The results showed

683 that *C. glutamicum* Val-11 (*C. glutamicum* XT1 harboring pHCP-H1davAB-E1-
684 orf26-B1) and *C. glutamicum* Val-13 (*C. glutamicum* XT1 harboring pHCP-
685 H1davAB-E1-CaiC-B1) produced 2.90 g/L and 2.28 g/L valerolactam,
686 respectively, both of which generated more valerolactam than the promoter H1
687 controls *C. glutamicum* Val-10 (*C. glutamicum* XT1 harboring pHCP-H1davAB-
688 orf26) and *C. glutamicum* Val-12 (*C. glutamicum* XT1 harboring pHCP-
689 H1davAB-caiC), which produced 2.21 g/L and 1.39 g/L valerolactam,
690 respectively (Fig. 5B). We noticed that the ORF26 group produced the highest
691 titer of valerolactam compared with the Act and CaiC constructs (Fig. 4B and
692 Fig. 5B); however, *C. glutamicum* Val-11 did not show a significant improvement
693 in valerolactam production compared with *C. glutamicum* Val-10 (Fig. 5B), and
694 the solubility of ORF26 (Zhang et al., 2017b) may be the main reason for this
695 result.

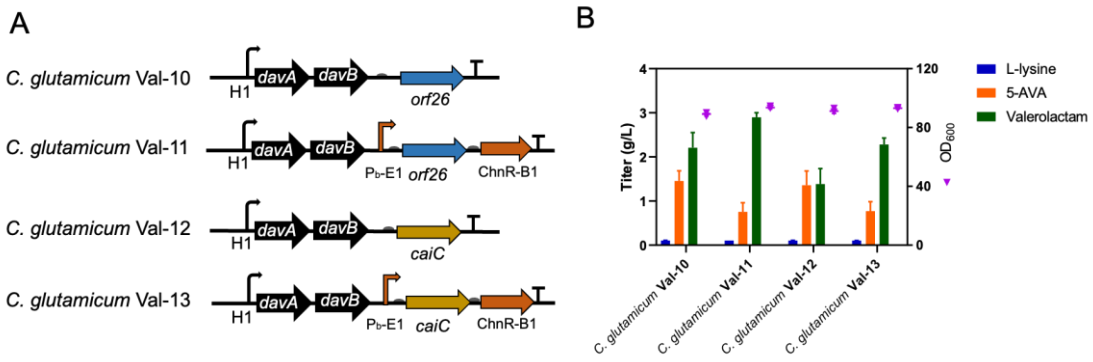

696

697 **Figure 5.** Dynamic upregulation of the ORF26 and CaiC with ChnR-B1/Pb-E1
698 system for valerolactam biosynthesis. 5-AVA (5-aminovaleric acid).

699

700 **3.6. Fed-batch fermentation for valerolactam biosynthesis in *C.***

***glutamicum* XT1.**

To demonstrate that dynamic regulation can further improve the titer of valerolactam in fed-batch cultivation, glucose-fed batch cultures of *C. glutamicum* Val-9 (Act), *C. glutamicum* Val-11 (ORF26) or *C. glutamicum* Val-13 (CaiC) were performed in a 1.2-L lab-scale bioreactor system, and 50% (w/v) glucose was added according to the glucose levels in the media. The time profiles of these three fed-batch cultures are shown in Fig. 6 (indicated as Act, ORF26, and CaiC, respectively). Growth of the Act, ORF26 and CaiC strains entered the stationary phase at 24 hours. Glucose feeding started immediately once there was less than 1 g/L glucose in the medium, and the cells continued to grow to an $OD_{600}$ of 211 (Act), 157 (ORF26), and 190 (CaiC) at 96 hours (Fig. 6). The valerolactam titers of these mutants reached 12.33 g/L (Act), 11.88 g/L (ORF26), and 12.15 g/L (CaiC) at the end of fed-batch fermentation (Fig. 6, Table 2), which are the highest levels reported thus far. In particular, the valerolactam titer of the Act mutants was 10-fold higher than that in previous research (1.18 g/L), which used a valerolactam biosynthetic pathway in *E. coli* with a constitutive promoter that drove the same enzymes used here (DavA, DavB, Act) (Chae et al., 2017). 5-AVA accumulated in these three cultures, indicating that the titer of valerolactam can be further increased by engineering the enzyme activity of Act/ORF26/CaiC (Fig. 6, Table 2).

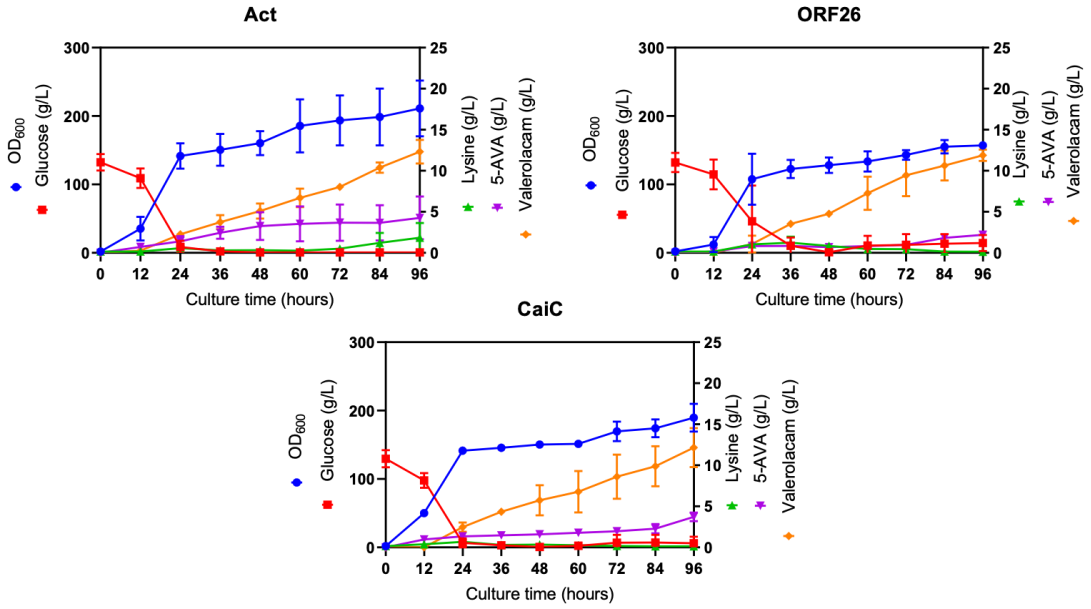


721

722 **Figure 6.** Fed-batch fermentation of valerolactam production in *C. glutamicum*

723 Val-9 (Act), *C. glutamicum* Val-11 (ORF26) and *C. glutamicum* Val-13 (CaiC).

724 (There are two replicates for *C. glutamicum* Val-11, and three replicates for *C.*

725 *glutamicum* Val-9 and *C. glutamicum* Val-13)

726

727 **Table 2.** Fermentation results summary of the *C. glutamicum* XT1 with different

728 valerolactam biosynthetic pathway.

| Strains | Valerolactam titer (g/L) | 5-aminovaleric acid titer (g/L) |
|---|---|---|
| *C. glutamicum* Val-9 (Act) | 12.33±1.44 | 4.26±2.61 |
| *C. glutamicum* Val-11 (ORF26) | 11.88±0.70 | 2.19±0.24 |
| *C. glutamicum* Val-13 (CaiC) | 12.15±2.37 | 3.71±0.52 |

## 4. Discussion

The complete biosynthesis of valerolactam has been studied in *E. coli*, and the major rate-limiting step in its production is the cyclization of 5-AVA to valerolactam (Gordillo Sierra and Alper, 2020)(Zhang et al., 2017b). In this study, we found that the Act-catalyzed activation of 5-AVA followed by the spontaneous cyclization to valerolactam was also a limiting step in our system (Fig. S2). A valerolactam biosensor-based dynamic upregulation system (positive feedback loop) was designed to enhance production of this rate-limiting enzyme (Fig. 2A), and the final titer of valerolactam from this pathway with dynamic upregulation of Act increased to 12.33 g/L in fed-batch culture. This dynamic upregulation system was also used to overexpress ORF26 and CaiC, which have been reported to be important for the cyclization of 5-AVA to valerolactam, and the valerolactam titers of these two strains reached 11.88 g/L and 12.15 g/L, respectively, in a glucose fed-batch fermentation, the titer of valerolactam with dynamic upregulation system in this research is also much higher than Cheng et al., reported 6.88 g/L valerolactam which was synthesized from L-lysine by a combination of enzymatic catalysis and pH optimization (Cheng et al., 2021).

To increase the titer of valerolactam, traditional metabolic engineering methods, such as optimizing the promoter activity and increasing the plasmid copy number, have been tested, and the results showed that these methods

751 contribute little to increasing the titer of valerolactam but instead to conversion
752 of L-lysine to 5-AVA (Fig. 2 and Fig. S2), the precursor to valerolactam. Thus,
753 we speculated that the cyclization of 5-AVA to valerolactam by Act limits the
754 production of valerolactam, and we therefore need to increase the expression
755 of Act to solve this bottleneck. A genetic signal amplifier was designed based
756 on a LuxR positive feedback loop and showed a great ability to increase the
757 expression of the regulated gene (Nistala et al., 2010). We developed the
758 ChnR/Pb system as a valerolactam biosensor. Thus, we first constructed a
759 gene amplifier in a positive feedback loop with the valerolactam biosensor
760 ChnR/Pb system to regulate the expression of Act (Fig. 2). However, the results
761 from flask culture indicated that the Act overexpressed by dynamic upregulation
762 (ChnR/Pb system) was not sufficient to improve the titer of valerolactam. We
763 found that the sensitivity and dynamic output range of the biosensor pBbS-
764 sfGFP (ChnR/Pb system) for valerolactam may limit the maximum expression
765 level of Act under the control of dynamic upregulation. Based on a previous
766 transcription factor engineering method (Snoek et al., 2020), a valerolactam
767 biosensor mutant with higher sensitivity and a larger dynamic output range was
768 obtained (pBbS-E1B1 in Fig. 3). After testing with different combinations of
769 promoter-regulator systems, compared with the strong constitutive control in *C.*
770 *glutamicum* Val-3, the titer of valerolactam was increased by 103% in *C.*
771 *glutamicum* Val-9 (ChnR-B1/Pb-E1 system) under the same culture conditions
772 (Fig. 4B). The flask culture results indicated that the dynamic upregulation

773 system with the ChnR-B1 mutation can significantly increase valerolactam
774 production, while the dynamic upregulation system designed based on wild-
775 type ChnR showed no effect on valerolactam biosynthesis (Fig. 2B and Fig. 4B).
776 In addition, we noticed that the titer of valerolactam from *C. glutamicum* Val-7
777 (ChnR/Pb-E1 system) was similar to that from *C. glutamicum* Val-5 (ChnR/Pb
778 system); however, the dynamic output range of biosensor pBbS-E1 (ChnR/Pb-
779 E1 system) with valerolactam was much higher than that of pBbS-sfGFP
780 (ChnR/Pb system). We suspect that the performance of our designed dynamic
781 upregulation system, a positive feedback amplifier for regulating the expression
782 of the rate-limiting enzymes, is mainly affected by the properties of the
783 transcription factor ChnR-B1. Furthermore, our dynamic upregulation system
784 was used to amplify the expression of ORF26 and CaiC for valerolactam
785 biosynthesis, and the titer of valerolactam increased by approximately 31% and
786 64%, respectively, compared with that of the strong promoter H1 control under
787 flask culture conditions (Fig. 5B). From the flask culture and fed-batch
788 fermentation results, 5-AVA accumulated as a byproduct (Fig. 5B, Table 2), and
789 the lower catalytic activity of these enzymes to activate 5-AVA for its cyclization
790 into valerolactam may be the main reason. Previous research from our lab
791 showed that ORF26 is insoluble, which may affect the growth of *C. glutamicum*
792 Val-11 in the fed-batch fermentation (Fig. 6), has an optimal pH of 8.0 and
793 catalyzes significant ATP and ADP hydrolysis (Zhang et al., 2017b), while *C.*
794 *glutamicum* growth should occur at pH 7.0. Thus, engineering an ORF26

mutant with reduced ATP and ADP hydrolysis, an optimal pH of 7.0 and increased solubility may further increase the titer of valerolactam from *C. glutamicum*. In addition, our engineered valerolactam biosensor pBbS-E1B1 showed a higher dynamic output range for caprolactam than valerolactam (Fig. S4), and there was no effect of caprolactam on the growth *C. glutamicum* (Fig. S5); thus, we suppose that our dynamic upregulation system (ChnR-B1/Pb-E1) can also be used to design a method for caprolactam biosynthesis in *C. glutamicum*.

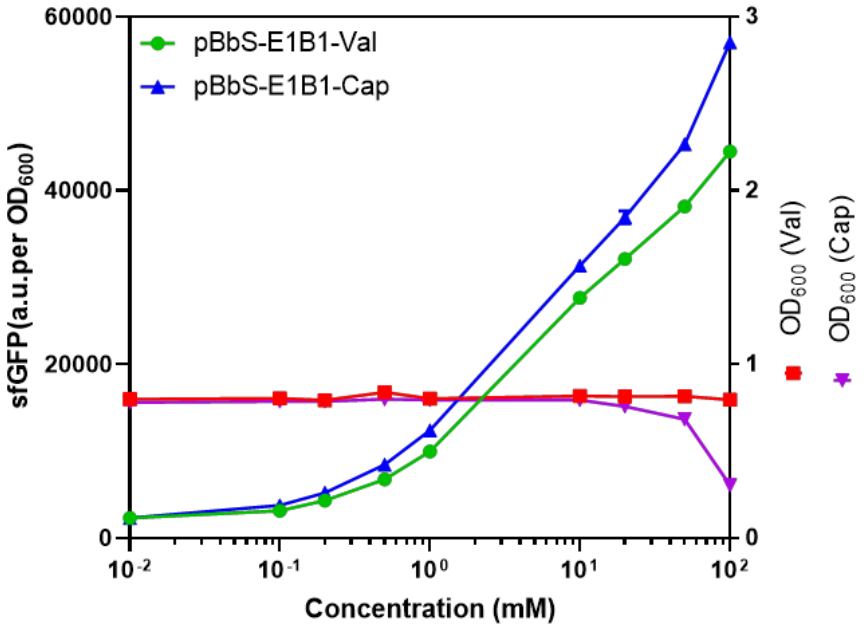


**Figure S4.** Biosensor characterization of pBbS-E1B1 sensitivity to valerolactam (Val) and caprolactam (Cap) in *E. coli*.

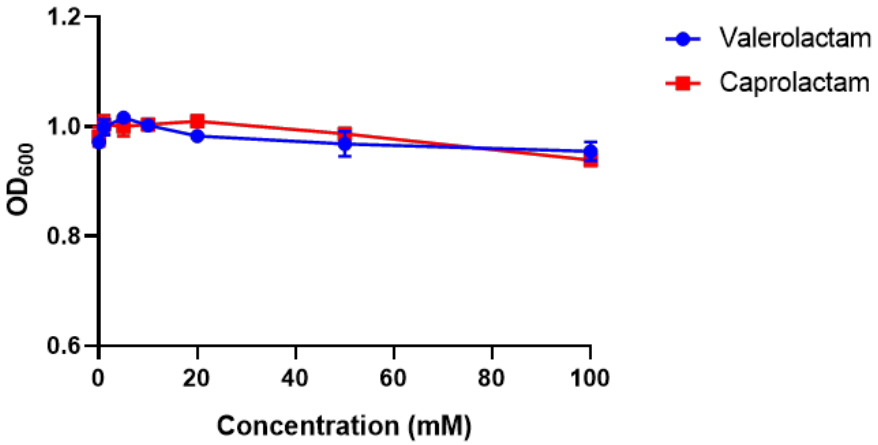


**Figure S5.** The effect of valerolactam and caprolactam on growth. of *C. glutamicum* XT1.

## 5. References

Becker, J., Zelder, O., Häfner, S., Schröder, H., Wittmann, C., 2011. From zero to hero-Design-based systems metabolic engineering of *Corynebacterium glutamicum* for l-lysine production. Metab Eng. 13, 159–168. https://doi.org/10.1002/ccd.27579

Brockman, I.M., Prather, K.L.J., 2015. Dynamic metabolic engineering: New strategies for developing responsive cell factories. Biotechnol J. 10, 1360. https://doi.org/10.1002/BIOT.201400422

Chae, T.U., Ko, Y.S., Hwang, K.S., Lee, S.Y., 2017. Metabolic engineering of *Escherichia coli* for the production of four-, five- and six-carbon lactams. Metab Eng. 41, 82–91. https://doi.org/10.1016/j.ymben.2017.04.001

Cheng, J., Tu, W., Luo, Z., Liang, L., Gou, X., Wang, X., Liu, C., Zhang, G., 2021. Coproduction of 5-aminovalerate and δ-valerolactam for the

synthesis of nylon 5 from L-lysine in *Escherichia coli*. Front Bioeng Biotechnol. 9, 1–9. https://doi.org/10.3389/fbioe.2021.726126

Cheng, Q., Thomas, S.M., Kostichka, K., Valentine, J.R., Nagarajan, V., 2000. Genetic analysis of a gene cluster for cyclohexanol oxidation in *Acinetobacter* sp. Strain SE19 by in vitro transposition. J Bacteriol. 182, 4744–4751.

Choi, J.W., Yim, S.S., Jeong, K.J., 2018. Development of a high-copy-number plasmid via adaptive laboratory evolution of *Corynebacterium glutamicum*. Appl Microbiol Biotechnol. 102, 873–883. https://doi.org/10.1007/s00253-017-8653-2

Dahl, R.H., Zhang, F., Alonso-Gutierrez, J., Baidoo, E., Batth, T.S., Redding-Johanson, A.M., Petzold, C.J., Mukhopadhyay, A., Lee, T.S., Adams, P.D., Keasling, J.D., 2013. Engineering dynamic pathway regulation using stress-response promoters. Nat Biotechnol. 31, 1039–1046. https://doi.org/10.1038/nbt.2689

Gordillo Sierra, A.R., Alper, H.S., 2020. Progress in the metabolic engineering of bio-based lactams and their ω-amino acids precursors. Biotechnol Adv. 43, 107587. https://doi.org/10.1016/J.BIOTECHADV.2020.107587

Green, M.R., Sambrook, J., 2012. Molecular cloning: a laboratory manual, Fourth edition, Cold Spring Harbor Laboratory Press, Cold Spring Harbor, New York (2012).

Jones, J.A., Toparlak, T.D., Koffas, M.A.G., 2015. Metabolic pathway balancing

847 and its role in the production of biofuels and chemicals. Curr Opin
848 Biotechnol. 33, 52–59. https://doi.org/10.1016/J.COPBIO.2014.11.013
849 Mannan, A.A., Liu, D., Zhang, F., Oyarzún, D.A., 2017. Fundamental design
850 principles for transcription-factor-based metabolite biosensors. ACS Synth
851 Biol. 6, 1851–1859. https://doi.org/10.1021/acssynbio.7b00172
852 Matsu-Ura, T., Dovzhenok, A.A., Coradetti, S.T., Subramanian, K.R., Meyer,
853 D.R., Kwon, J.J., Kim, C., Salomonis, N., Glass, N.L., Lim, S., Hong, C.I.,
854 2018. Synthetic gene network with positive feedback loop amplifies
855 cellulase gene expression in *Neurospora crassa*. ACS Synth Biol. 7, 1395–
856 1405. https://doi.org/10.1021/acssynbio.8b00011
857 Nistala, G.J., Wu, K., Rao, C. V., Bhalerao, K.D., 2010. A modular positive
858 feedback-based gene amplifier. J Biol Eng. 4, 1–8.
859 https://doi.org/10.1186/1754-1611-4-4
860 Ohnishi, J., Mitsuhashi, S., Hayashi, M., Ando, S., Yokoi, H., Ochiai, K., Ikeda,
861 M., 2002. A novel methodology employing *Corynebacterium glutamicum*
862 genome information to generate a new L-lysine-producing mutant. Appl
863 Microbiol Biotechnol. 58, 217–223. https://doi.org/10.1007/S00253-001-
864 0883-6
865 Park, J.U., Jo, J.H., Kim, Y.J., Chung, S.S., Lee, J.H., Lee, H.H., 2008.
866 Construction of heat-inducible expression vector of *Corynebacterium*
867 *glutamicum* and *C. ammoniagenes*: fusion of lambda operator with
868 promoters isolated from *C. ammoniagenes*. J Microbiol Biotechnol. 18,

639–647.

Park, S.J., Oh, Y.H., Noh, W., Kim, H.Y., Shin, J.H., Lee, E.G., Lee, S., David, Y., Baylon, M.G., Song, B.K., Jegal, J., Lee, S.Y., Lee, S.H., 2014. High-level conversion of L-lysine into 5-aminovalerate that can be used for nylon 6,5 synthesis. Biotechnol J. 9, 1322–1328. https://doi.org/10.1002/biot.201400156

Rohles, C., Pauli, S., Gießelmann, G., Kohlstedt, M., Becker, J., Wittmann, C., 2022. Systems metabolic engineering of *Corynebacterium glutamicum* eliminates all by-products for selective and high-yield production of the platform chemical 5-aminovalerate. Metab Eng. 73, 168–181. https://doi.org/10.1016/J.YMBEN.2022.07.005

Rohles, C.M., Gießelmann, G., Kohlstedt, M., Wittmann, C., Becker, J., 2016. Systems metabolic engineering of *Corynebacterium glutamicum* for the production of the carbon-5 platform chemicals 5-aminovalerate and glutarate. Microb Cell Fact. 15, 1–13. https://doi.org/10.1186/s12934-016-0553-0

Ruan, Y., Zhu, L., Li, Q., 2015. Improving the electro-transformation efficiency of *Corynebacterium glutamicum* by weakening its cell wall and increasing the cytoplasmic membrane fluidity. Biotechnol Lett. 37, 2445–2452. https://doi.org/10.1007/s10529-015-1934-x

Schäfer, A., Tauch, A., Jäger, W., Kalinowski, J., Thierbach, G., Pühler, A., 1994. Small mobilizable multi-purpose cloning vectors derived from the

*Escherichia coli* plasmids pK18 and pK19: selection of defined deletions in the chromosome of *Corynebacterium glutamicum*. Gene. 145, 69–73. https://doi.org/10.1016/0378-1119(94)90324-7

Shin, J.H., Park, S.H., Oh, Y.H., Choi, J.W., Lee, M.H., Cho, J.S., Jeong, K.J., Joo, J.C., Yu, J., Park, S.J., Lee, S.Y., 2016. Metabolic engineering of *Corynebacterium glutamicum* for enhanced production of 5-aminovaleric acid. Microb Cell Fact. 15, 1–13. https://doi.org/10.1186/s12934-016-0566-8

Snoek, T., Chaberski, E.K., Ambri, F., Kol, S., Bjørn, S.P., Pang, B., Barajas, J.F., Welner, D.H., Jensen, M.K., Keasling, J.D., 2020. Evolution-guided engineering of small-molecule biosensors. Nucleic Acids Res. 48, 1–14. https://doi.org/10.1093/nar/gkz954

Wei, L., Xu, N., Wang, Y., Zhou, W., Han, G., Ma, Y., Liu, J., 2018. Promoter library-based module combination (PLMC) technology for optimization of threonine biosynthesis in *Corynebacterium glutamicum*. Appl Microbiol Biotechnol. 102, 4117–4130. https://doi.org/10.1007/s00253-018-8911-y

Yang, Y., Lin, Y., Wang, Jian, Wu, Y., Zhang, R., Cheng, M., Shen, X., Wang, Jia, Chen, Z., Li, C., Yuan, Q., Yan, Y., 2018. Sensor-regulator and RNAi based bifunctional dynamic control network for engineered microbial synthesis. Nat Commun. 9, 1–10. https://doi.org/10.1038/s41467-018-05466-0

Yeom, S.-J., Kim, M., Kwon, K.K., Fu, Y., Rha, E., Park, S.-H., Lee, H., Kim, H.,

Lee, D.-H., Kim, D.-M., Lee, S.-G., 2018. A synthetic microbial biosensor for high-throughput screening of lactam biocatalysts. Nat Commun. 9, 5053. https://doi.org/10.1038/s41467-018-07488-0

Zhang, F., Carothers, J.M., Keasling, J.D., 2012. Design of a dynamic sensor-regulator system for production of chemicals and fuels derived from fatty acids. Nat Biotechnol. 30, 354–359. https://doi.org/10.1038/nbt.2149

Zhang, J., Barajas, J.F., Burdu, M., Ruegg, T.L., Dias, B., Keasling, J.D., 2017a. Development of a transcription factor-based lactam biosensor. ACS Synth Biol. 6, 439–445. https://doi.org/10.1021/acssynbio.6b00136

Zhang, J., Barajas, J.F., Burdu, M., Wang, G., Baidoo, E.E., Keasling, J.D., 2017b. Application of an acyl-CoA ligase from *Streptomyces aizunensis* for lactam biosynthesis. ACS Synth Biol. 6, 884–890. https://doi.org/10.1021/acssynbio.6b00372

**Author contributions**

Xixi Zhao: Conceptualization, Methodology, Validation, Formal analysis, Investigation, Writing-original Draft, Visualization. Yanling Wu: Methodology, Validation, Investigation. Tingye Feng: Validation, Investigation. Junfeng Shen: Resources. Huan Lu: Validation. Yunfeng Zhang: Validation. Howard C. Chou: Conceptualization, Writing-review & editing. Xiaozhou Luo: Conceptualization, Writing-review & editing, Supervision, Project administration, Funding acquisition. Jay D. Keasling: Conceptualization, Writing-review & editing,

Supervision, Funding acquisition.

**Acknowledgement**

This work is supported by the National Key R&D Program of China (2020YFA0907700), National Natural Science Foundation of China (32101201), Guangdong Basic and Applied Basic Research Foundation (2021B1515020049 and 2019A1515110549), Shenzhen Institute of Synthetic Biology Scientific Research Program (JCHZ20200004), China Postdoctoral Science Foundation (2019M653121) and Shenzhen Science and Technology Program (ZDSYS20210623091810032 and CYJ20190807154003687). We thank Prof. Sang Yup Lee of the Korea Advanced Institutes of Science and Technology for providing the pCES208 plasmid. We thank Dr. Haibing He for helpful discussion and Miss Zhenqin Wei for helping organization the meeting about this project.

**Conflict of Interest**

X.L. has a financial interest in Demetrix and Synceres. J.D.K. has a financial interest in Amyris, Lygos, Demetrix, Maple Bio, Napigen, Apertor Pharma, Ansa Biotechnologies, Berkeley Yeast, and Zero Acre Farms.

954 **Supplementary Material**

955 **Table S1.** Plasmids used in this study

| Plasmids | Description | Source |
|---|---|---|
| pK18mobsacB | Kana$^r$, *sacB* from *B.subtilis* | Schäfer et al., 1994 |
| pK18-lysC | pK18mobsacB derivate, harboring *lysC* gene with point mutation at C932T and 588 bp *lysC* downstream fragment from the *C. glutamicum* ATCC13032 genome | This study |
| pEC-XK99E | *E. coli* and *C. glutamicum* shuttle vector, Kana$^r$ | Lab Stock |
| pH1-mCherry | pEC-XK99E derivate, H1-mCherry | This study |
| pH2-mCherry | pEC-XK99E derivate, H2-mCherry | This study |
| pH9-mCherry | pEC-XK99E derivate, H9-mCherry | This study |
| pH10-mCherry | pEC-XK99E derivate, H10-mCherry | This study |
| pCES208 | Shuttle vector between *E. coli* and *C. glutamicum*, Kana$^r$ | Park et al., 2008 |
| pCES208- | pCES208 derivate, H1, codon-optimized | This |

| | | |
|---|---|---|
| H1davAB | *davA*, *davB* | study |
| pCES208-H1davAB-act | pCES208 derivate, H1, codon-optimized *davA*, *davB* and *act* | This study |
| pHCP | pCES208 derivate, *parB* nonsense mutation, Kana$^r$ | This study |
| pHCP-H1davAB-act | pHCP derivate, H1, codon-optimized *davA*, *davB* and *act* | This study |
| pHCP-H1davAB-H1act | pHCP derivate, H1, codon-optimized *davA*, *davB* and H1-*act* | This study |
| pHCP-H1davAB-Pb-act-chnR | pHCP derivate, H1, codon-optimized *davA*, *davB* and Pb-*act*-chnR | This study |
| pBbSlactam | Lactam biosensor, harboring the *chnR* from *Acinetobacter sp.* and mCherry under control of Pb (the promoter of *chnB* from *Acinetobacter sp.*), Cm$^R$ | Zhang et al., 2017a |
| pBbS-sfGFP | pBbSlactam derivate, mCherry was replaced with sfGFP | This study |
| pBbS-E1 | pBbS-sfGFP derivate, with mutation in the Pb of ChnR binding site, and sfGFP under control of the Pb mutant (Pb-E1) | This study |
| pBbS-E1B1 | pBb-E1 derivate, with a *chnR* mutant (ChnR-M-B1) | This study |
| pBbS-E1E5 | pBb-E1 derivate, with a *chnR* mutant (ChnR-M-E5) | This study |
| pBbS-E1A4 | pBb-E1 derivate, with a *chnR* mutant (ChnR- | This |

| | | |
|---|---|---|
| | M-A4) | study |
| pHCP-H1davAB-E1-act | pHCP derivate, H1, codon-optimized *davA*, *davB* and Pb-E1-*act* | This study |
| pHCP-H1davAB-E1-act-chnR | pHCP derivate, H1, codon-optimized *davA*, *davB* and Pb-E1-*act*-chnR | This study |
| pHCP-H1davAB-Pb-act-B1 | pHCP derivate, H1, codon-optimized *davA*, *davB* and Pb-*act*-ChnR-B1 | This study |
| pHCP-H1davAB-E1-act-B1 | pHCP derivate, H1, codon-optimized *davA*, *davB* and Pb-E1-*act*-ChnR-B1 | This study |
| pHCP-H1davAB-orf26 | pHCP derivate, H1, codon-optimized *davA*, *davB* and *orf26* | This study |
| pHCP-H1davAB-E1-orf26-B1 | pHCP derivate, H1, codon-optimized *davA*, *davB* and Pb-E1-*orf26*-ChnR-B1 | This study |
| pHCP-H1davAB-caiC | pHCP derivate, H1, codon-optimized *davA*, *davB* and *caiC* | This study |
| pHCP-H1davAB-E1-caiC-B1 | pHCP derivate, H1, codon-optimized *davA*, *davB* and Pb-E1-*caiC*-ChnR-B1 | This study |

956

957 **Table S2.** Primers used in this study

| Primer | Sequence (5' to 3') |
|---|---|
| P1 | cgtaatcatggtcatagctg |
| P2 | agtcgacctgcaggcatg |
| P3 | atgcctgcaggtcgactATGGCCCTGGTCGTACAG |

| | |
|---|---|
| P4 | CGAGGGCAGGTGAAGATGATGTCGGTGGTGC |
| P5 | ATCTTCACCTGCCCTCGTTC |
| P6 | ctatgaccatgattacgCATCATGGACGAACTCAACG |
| P7 | GCTATATATGCTTATACTGGGCTAAATTAGAGCCTTAGCGAAAGGATGG GCatgcgtaaaggagaagaag |
| P8 | cgactctagtttgtatagttcatccatg |
| P9 | actatacaaactagagtcgacctgcagg |
| P10 | TATAAGCATATATAGCCGGCGCAAGCAAGTACGAGACTCAAGAGCGAG Cattcaccaccctgaattgac |
| P11 | GTCGAGGAATACTGTATACTATTTAAAATTCATTGGATAGCAAAGGACG GATatgcgtaaaggagaag |
| P12 | TATACAGTATTCCTCGACAGAATACCAGGCACAGTAAGTCGAGACAGA GCattcaccaccctgaattgac |
| P13 | CATTCTGGTAAGGTACGATCCTAGAGTCTTAAGAGAACGGAAAGGAATT GCatgcgtaaaggagaagaag |
| P14 | GTACCTTACCAGAATGTCGCCCTGAAAACTAATATGTATACCATGGGAG Cattcaccaccctgaattgac |
| P15 | GCGTATGGTAAGCTCTGTTATGTATAGTCCGAGCACGGCGAAAGGATA CTCatgcgtaaaggagaagaag |
| P16 | AGAGCTTACCATACGCCGCCGGCTTAGAGCCGACCGGTAAGGGTTGA GCattcaccaccctgaattgac |
| P17 | ccaccgCAGTAGGCtCAACTGATTCG |
| P18 | ttgAgcctactgcggtggcctgattc |
| P19 | GCTATATATGCTTATACTGGGCTAAATTAGAGCCTTAGCGAAAGGATGG GCATGCATCACCATCACCATCATC |

| | |
|---|---|
| P20 | ATTTTCCTCCTTTttagcctttacgcaggtgc |
| P21 | taaaggctaaAAAGGAGGAAAATCatgaac |
| P22 | TGTATGTCCTCCTGGACTTCttaatctgccagggcgatc |
| P23 | AAGTCCAGGAGGACATACAATGAAGCGCCCTCTCGAAGG |
| P24 | tactgccgccaggcagcggccgcTTAGATGACGTTCTTCTCC |
| P25 | cgctgcctggcggcagtag |
| P26 | TATAAGCATATATAGCCGGCGCAAGCAAGTACGAGACTCAAGAGCGAG Ccagcttttgttccctttagtg |
| P27 | tactgccgccaggcagcggccgcttaatctgccagggcgatcg |
| P28 | AGTATAAGCATATATAGCCGGCGCAAGCAAGTACGAGACTCAAGAGCG AGCttaatctgccagggcgatcg |
| P29 | gtgatatcccgcggccattaatctgccagggcgatcg |
| P30 | tggccgcgggatatcactag |
| P31 | tATGTCCTCCTGGACTTCtgaatttattcaaaatctgc |
| P32 | AAGTCCAGGAGGACATACAATGCATCACCATCACCATCATCATAAGCGC CCTCTCGAAG |
| P33 | gtctgtgctcatATTCATCCTTTTTAGATGACGTTCTTCTCC |
| P34 | AAAGGATGAATatgagcacagacaaagc |
| P35 | actgccgccaggcagcggccgctcaaaaaacaatagaggag |
| P36 | AAGTCCAGGAGGACATACAATGCATCACCATCACCATCATCATACCGCA AAAATCTTTGCCG |
| P37 | actgccgccaggcagcggccgcTTATTCGGCTGCCATGCGGG |
| P38 | gctcatATTCATCCTTTTTATTCGGCTGCCATGCG |
| P39 | gattaaGAAGTCCAGGAGGACATACAATGGACATTATCGGTGGC |
| P40 | actgccgccaggcagcggccgcTTACTTGAGGTTCTTGC |

| | |
|---|---|
| P41 | gtctgtgctcatATTCATCCTTTTTACTTGAGGTTCTTGCGG |
| P42 | tttgtacagttcatccatac |
| P43 | atgcgtaaaggcgaagagc |
| P44 | tggatgaactgtacaaatgaggatccaaactcgagtaagg |
| P45 | tcttcgcctttacgcatggtaccctccattacgac |
| P46 | tctcttttagttgcaagcttc |
| P47 | gcagatgaagaagcttgcaactaaaagagaNNNNNNNNNNNagttacccaaaatcgttg |
| P48 | agagtcaattcagggtggtg |
| P49 | gagattggtgtgttcctgtc |
| P50 | aggaacacaccaatctcgtgtctg |
| P51 | caccctgaattgactctcttc |

**Table S3.** Sequence of codon optimized *davA* and *davB* genes from *P. putida*, *act* gene from *C. propionicum*, *orf26* gene from *S. aizunensis*, *caiC* gene from *E. coli*.

| Gene | Codon optimized sequence |
|---|---|
| *davA* | atgcgcatcgcactgtaccaaggcgcacccaagccactagacgttcctggtaaccttcaacggctgcg<br>ccaccaggcgcagctggcagctgaacgcggagctcagttgctggtgtgcccagagatgttcctcaccg<br>gctacaacattggcctggcccaagtcgaacgtctcgccgaagccgcagatggcccagcagcaatga<br>ccgtggtcgaaatcgctcaggctcaccgcatcgcaattgtttacggttacccggagcgcggtgatgacg<br>gagctatctacaactccgttcagttgatcgatgcgcatggacgatctctgtcaaattatcgcaagacgca<br>cttgttcggtgaactcgatcgctcgatgttctcccctggtgcggaccacttcccagtcgtggaactggaag<br>gctggaaggttggacttcttatctgttacgacatcgagttcccagagaacgcccgtcgactagcgttggat |

| | |
|---|---|
| | ggagccgagcttatccttgtgcccaccgctaacatgactccgtacgattttacctgccaagtgactgtccg<br>tgcgagggcacaggaaaatcagtgctacctcgtatatgcaaactactgcggtgctgaagacgagattg<br>aatattgtgggcaatctagcattattggaccggatggctccttgctcgctatggccggtcgcgatgaatgc<br>cagttgcttgcagagcttgagcatgagcgggtcgttcaggggcgtacagcttttccttatttaaccgacctc<br>cgtcaggagctgcacctgcgtaaaggctaa |
| *davB* | atgaacaagaagaatcgacaccccgccgacggcaagaagccgattaccattttcggaccagatttcc<br>cttttgctttcgatgattggctagaacacccagcaggcctgggaagcattccagctgagcgccatggag<br>aagaggtggctatcgtcggagctggtatcgctggcctcgtagcggcatacgagctgatgaagctgggc<br>ctcaagcctgtggtgtatgaggcttccaagctcggcggccggctccgctcccaagccttcaatggaact<br>gacgggatcgttgccgagctgggtggcatgcgcttcccagtgtcttccactgccttctaccactacgtcga<br>caaattgggcctggaaacgaaacccttccccaatcctttgaccccagcttccggaagtacggttattgat<br>cttgaaggacagacctattacgccgagaaacctacagaccttccacaactgtttcatgaggttgccgac<br>gcatgggctgatgctctggagtcgggtgcgcagttcgccgatatccagcaggcaatccgcgatcgtgat<br>gtaccacgccttaaggaattatggaacaagttggttccactgtgggacgaccgtaccttctacgacttcgt<br>cgctacctctcgctcctttgctaaactgagctttcaacacagagaagtgtttggccaggtcggtttcggcac<br>cggcggttgggattcggacttccctaacagtatgttggaaatcttccgcgtggttatgaccaactgcgacg<br>accaccagcacctggttgttgggggtgtggaacaagtcccacaaggaatctggcgccacgtgccgga<br>acgttgtgtgcattggccagaagggactagcctgagcacgctgcatggtggcgcaccgcgtaccggtg<br>tcaagcgcattgcccgcgcatccgatggccgcttggcagtcacggacaactggggtgatacccgcca<br>ctattccgcagtactagctacctgtcagacatggttgcttaccactcaaatcgactgcgaagaatctctgtt<br>ctcgcaaaagatgtggatggcactggaccggacccgctacatgcagtcgtctaaaacctttgtcatggt<br>cgacaggccgttctggaaggataaggaccctgagaccggtcgtgacctgctgagcatgaccctcact<br>gatcgtctcactcgcggcacttatctttttgataacggtaacgataaacccggggtgatctgcctgtcatac<br>tcatggatgtctgatgcgctgaagatgctgccacacccggtggagaagcgcgtacagcttgccctggat<br>gcgctcaagaagatttatccgaaaaccgatatcgcaggccatatcatcggcgatccaatcacggtttcc |

| | |
|---|---|
| | tgggaggccgacccctactttctcggcgcgttcaaaggcgcgttaccgggtcattaccgctacaaccag<br>cgaatgtacgcgcacttcatgcagcaggatatgccggcagagcagcgcggtatttttattgctggtgatg<br>acgtgtcatggacccctgcctgggttgaaggcgcggtccagacatctctgaacgcagtgtggggtatca<br>tgaatcactttggtgggcacacccacccagacaatccaggcccgggagatgtgttcaacgagatcgg<br>cccgatcgccctggcagattaa |
| *act* | atgaagcgccctctcgaaggcatccgtgtgctggacctcacccaagcttactccggcccattctgcacta<br>tgaacctcgcagatcatggcgccgaggtcatcaagatcgaacgccccggttccggtgatcagacccg<br>cggctggggtcctatggaaaacgactactccggctactacgcatacatcaaccgcaacaagaagggt<br>atcactttaaatctcgcatccgaagagggcaagaaggtgttcgcagagctggtcaagtccgccgacgt<br>catttgcgagaactacaaggtgggcgtgctggaaaagctgggcttctcctacgaggttttaaaggagct<br>caatccacgtatcatctacggctccatctccggcttcggtttaactggcgaactgtcctctcgcccttgctac<br>gatatcgtggcacaagctatgtccggcatgatgtccgtgaccggcttcgcagatggtcctccttgcaaga<br>tcggtccttccgtgggcgactcctataccggtgcatacctctgcatgggcgtgctcatggctttatacgagc<br>gcgagaagactggcgtgggtcgtcgcattgacgtcggcatggtcgacactttattctccactatggagaa<br>cttcgtggtggagtacaccatcgctggtaagcacccacaccgcgctggtaaccaagatccatccatcg<br>ccccttttcgactccttccgtgccaaggactccgacttcgtcatgggctgcggcaccaacaaaatgttcgc<br>cggtctgtgcaaggccatgggccgcgaggatttaatcgacgatccacgcttcaacaccaatttaaacc<br>gctgcgacaactatttaaacgatttaaagccaatcattgaggagtggacccagaccaagaccgtggca<br>gagctggaggaaatcatctgcggtttatccatcccattcggccctattttaactatcccagagatttccgag<br>cactctctgaccaaggagcgcaatatgctctgggaagtgtaccaacccggtatggatcgcaccatccg<br>cattcccggttcccctatcaagattcacggtgaggaggacaaggcacagaaaggcgccccaattttag<br>gcgaagacaacttcgcagtgtacgcagagatcctcggtctgtccgtcgaagagatcaagtctttagagg<br>agaagaacgtcatctaa |
| *orf26* | atgaccgcaaaaatctttgccgtggactccgtccgcccaatcgacgagttcgaacaagatgcactgcg<br>cgtcgccgacgtgattcgcgaacgtggcgtgtgtttaggcgatcgcgtgatgctcaaggctggtaactcc |

| | |
|---|---|
| | gcatcttacgtgtgcgtgctgtacgcactcatgcacattggtgcctccatcgtgctggtggaccagcaag<br>aacataaggaagagacccgccgcattgcactgcgcaccggtgtgaaggtgaccttcgtggacgatga<br>gaccccaatcgatcaagacgccgatcctatccatttatacgagctcatggtggcaacccagaaccgtc<br>cacctatggactccgctttatccttcgatgcttggggcgaactgtccgacggtttaattatgtggacctccg<br>gctccaccggttctccaaagggcgtcgtgaagtccggcggtaaatttctggcaaatttacgtcgcaacg<br>cacaccaagtgggccaccgcccagacgatgttttaatgccactgctcccattcgcccatcagtatggttt<br>atccatggtgctgattgcttggctgacccgctgctctctcgtgatcgccccataccgtcgtttagatcgcgct<br>ttacgtatggcacgcgattccggcaccaccgtgatcgacgcaaccccatcctcctaccgctctatcctcg<br>gtttagtcacccgcaaaccagctttacgtgcacatttagctggtacccgtatgttctgcgtgggcgcagca<br>ccactcgacgcaccactggtggaatcctacgtgcaagaattcggtctgccattattagattcttacggctc<br>caccgaactgaacaacatcgcctttgccactctggataacccagtgtcttgtggccgcgcaatggaggg<br>tatcggtttacgtatcgtggatgaggatggccgcgaagtcgcagctggtcagcccggtgaaattgaagt<br>ggacacccccgatgcactggagggtcagatcgccgaagatggctccatcatcccagcaccaactgg<br>ctggcaacgcaccggcgatttaggtcacctcgatgcagacggcaacctctacgttttaggccgcaagttt<br>gccgtgcaccgcatgggttacactttatacccagagctgatcgaacgcaaagtggccgcagagggct<br>gtcctacccgcatcgtgccactcccagatgagctgcgcggttcccagctcgtgttcttcgtggaggatgat<br>gagcagcgcgatgccggttactggcgtgaacgtctgtgtggcttattaccagcattcgaacagccaaac<br>aaggtggtggttttagagcaattccctctcaaccgcaacggcaagccagataagaaggaactgaccc<br>gcatggcagccgaataa |
| *caiC* | atggacattatcggtggccagcatttacgccaaatgtgggacgacctcgcagatgtctacggtcacaag<br>accgctttaatttgcgaatcctccggtggcgtcgtgaatcgttactcctacctcgagctcaaccaagaaat<br>caatcgcaccgccaatctgttctacactttaggcatccgcaagggcgacaaggtggcactgcatttaga<br>caactgccccgaattcatcttctgctggttcggtttagcaaaaatcggcgcaatcatggtgcctatcaatg<br>cccgtttactgtgtgaggaatccgcatggattttacagaactcccaagcttgtttactggtgacctctgccc<br>agttttacccaatgtaccagcagatccaacaagaagacgcaacccagctgcgccacatctgtctcacc |

| | |
|---|---|
| | gatgtggcactccccgctgacgatggtgtctcctcctttacccagctgaaaaaccagcaacccgctacc<br>ctctgctacgcaccaccactgtccaccgacgataccgcagaaattttatttacttctggcaccacctctcg<br>ccctaagggcgtcgtgattacccactataatttacgcttcgctggttactactccgcttggcaatgcgccct<br>ccgcgacgatgacgtgtacctcaccgtgatgccagccttccacatcgactgtcaatgcactgcagcaat<br>ggcagcattctctgccggcgccaccttcgtgctcgtggagaaatactccgcacgcgccttttggggcca<br>agtgcagaagtatcgcgccaccgtcaccgagtgtattccaatgatgatccgtactttaatggtgcagcca<br>ccttccgccaacgatcagcagcatcgcctccgcgaagtgatgttttatttaaatttatccgagcaagaaa<br>aggacgcattctgcgagcgcttcggcgtgcgtttactgacctcctatggcatgaccgagaccatcgtgg<br>gtatcattggcgatcgccccggtgataagcgccgttggccttctatcggtcgcgtgggcttctgctacgaa<br>gccgaaattcgcgacgatcacaaccgccctctccccgctggtgaaatcggcgaaatctgcatcaagg<br>gcattcccggtaagaccattttcaaggaatactttctgaacccacaagctactgccaaggtgctggagg<br>ccgatggctggctgcataccggtgataccggctatcgcgacgaggaagatttcttctacttcgtggaccg<br>ccgctgcaacatgatcaagcgtggcggcgagaacgtgtcttgcgtcgagctggagaacatcatcgca<br>gcccatccaaagatccaagatatcgtggtggtgggcatcaaagactccatccgcgatgaagccatca<br>aggcattcgtcgtgctcaacgagggtgagactctgtccgaggaggagttcttccgcttctgcgagcaaa<br>acatggccaagttcaaggtcccttcctatttagaaatccgcaaggatttaccacgcaactgctccggcaa<br>gatcatccgcaagaacctcaagtaa |

963

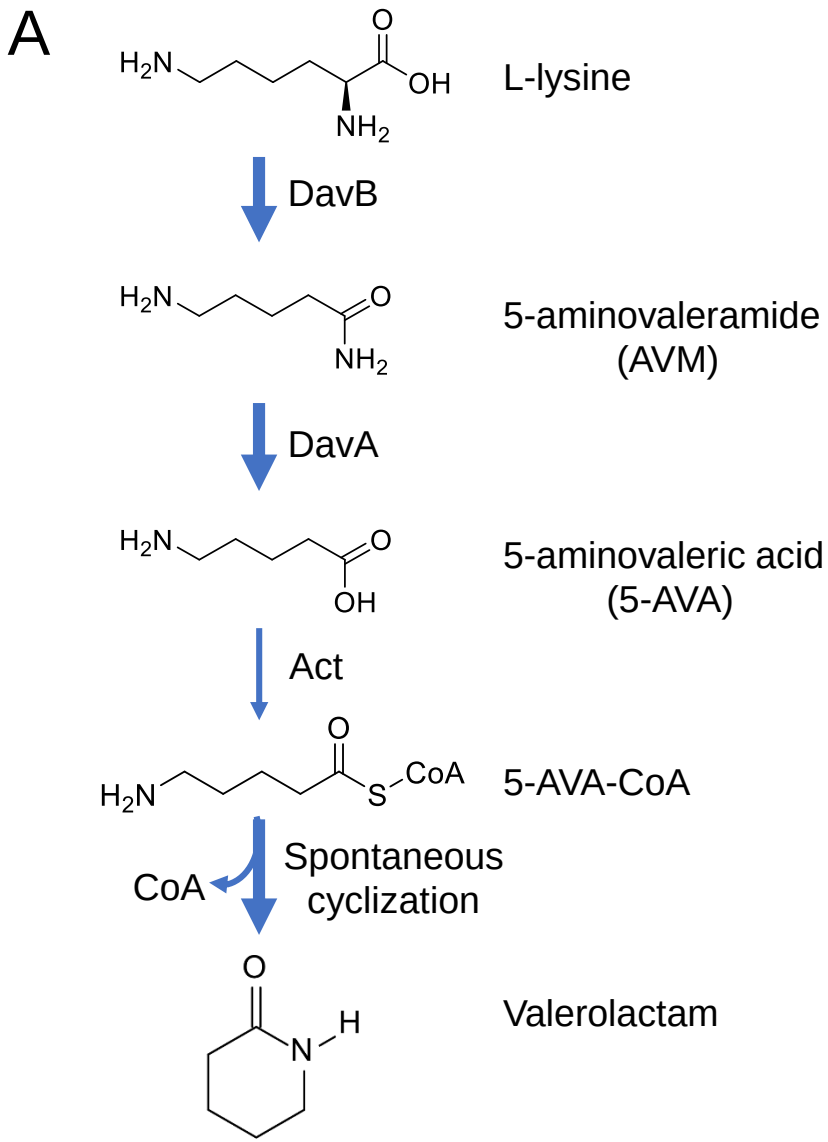


**Figure 1. (A)** The biosynthetic pathway of valerolactam from L-lysine.

B

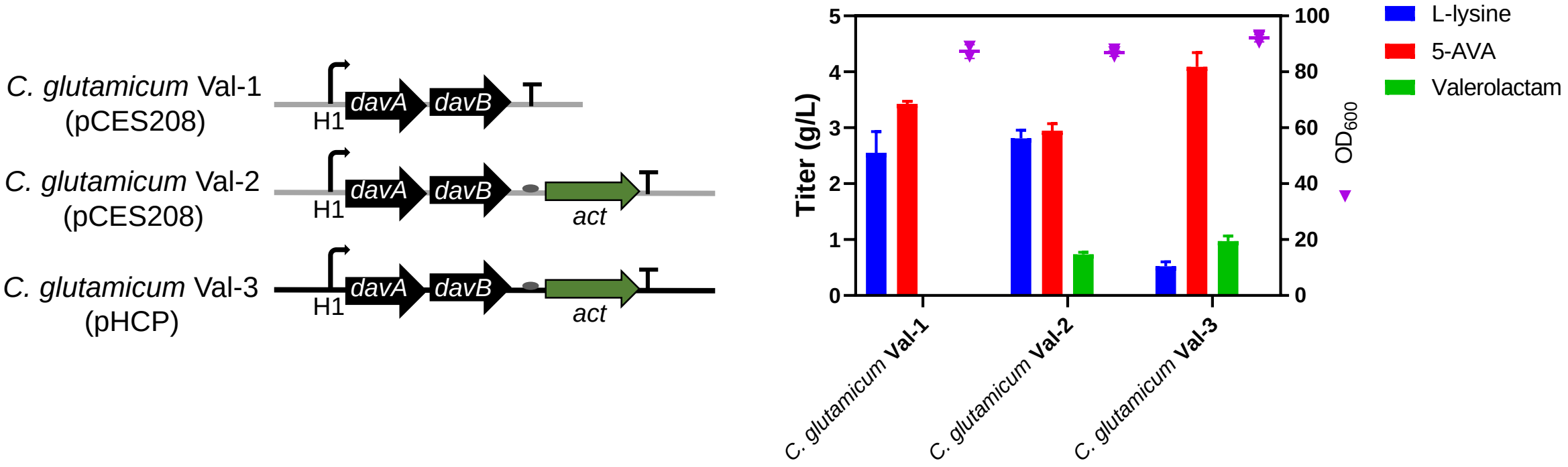


**Figure 1**. **(B)** L-lysine, 5-AVA, and valerolactam production by *C. glutamicum* XT1 mutants with different versions of the valerolactam biosynthetic pathway. 5-AVA (5-aminovaleric acid).

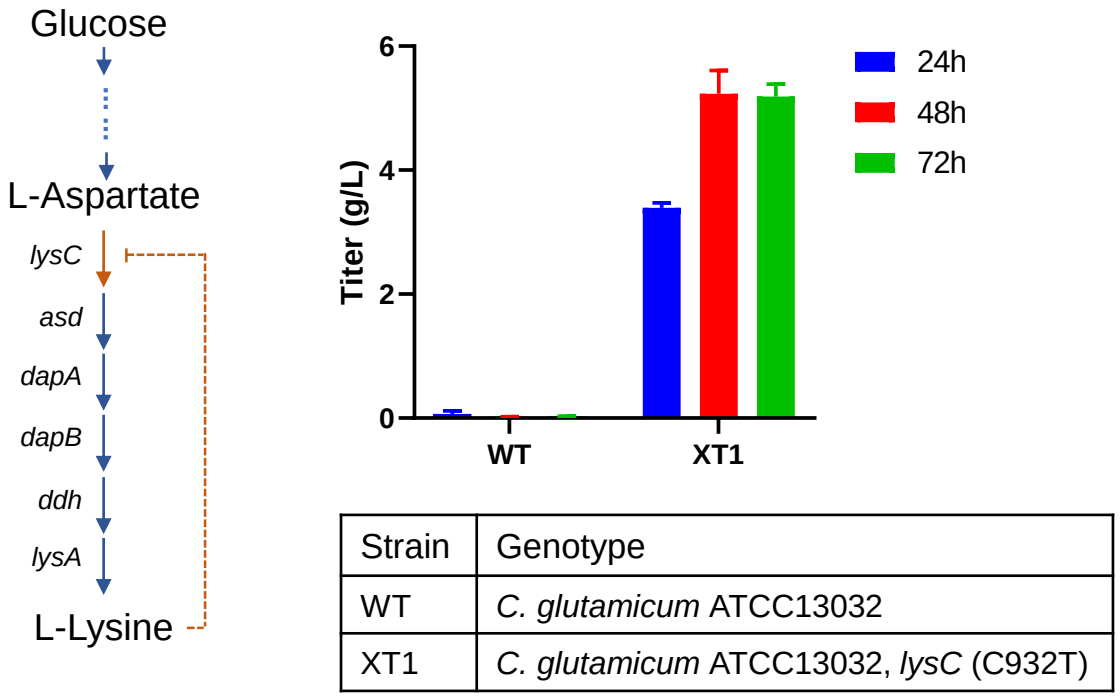


| Strain | Genotype |
|---|---|
| WT | *C. glutamicum* ATCC13032 |
| XT1 | *C. glutamicum* ATCC13032, *lysC* (C932T) |

**Figure S1.** The L-lysine biosynthetic pathway from glucose in *Corynebacterium glutamicum* and the titer of L-lysine produced by *C. glutamicum* ATCC13032 (WT) and mutant (XT1) in flask cultures.

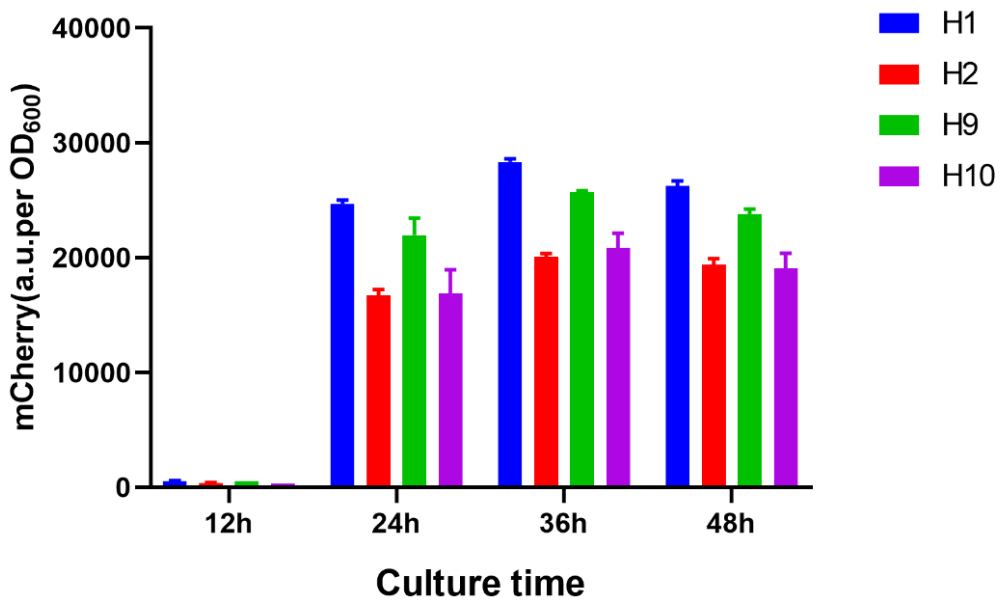


**Figure S2.** Strengths of the strong constitutive promoters evaluated in *C. glutamicum* XT1.

A

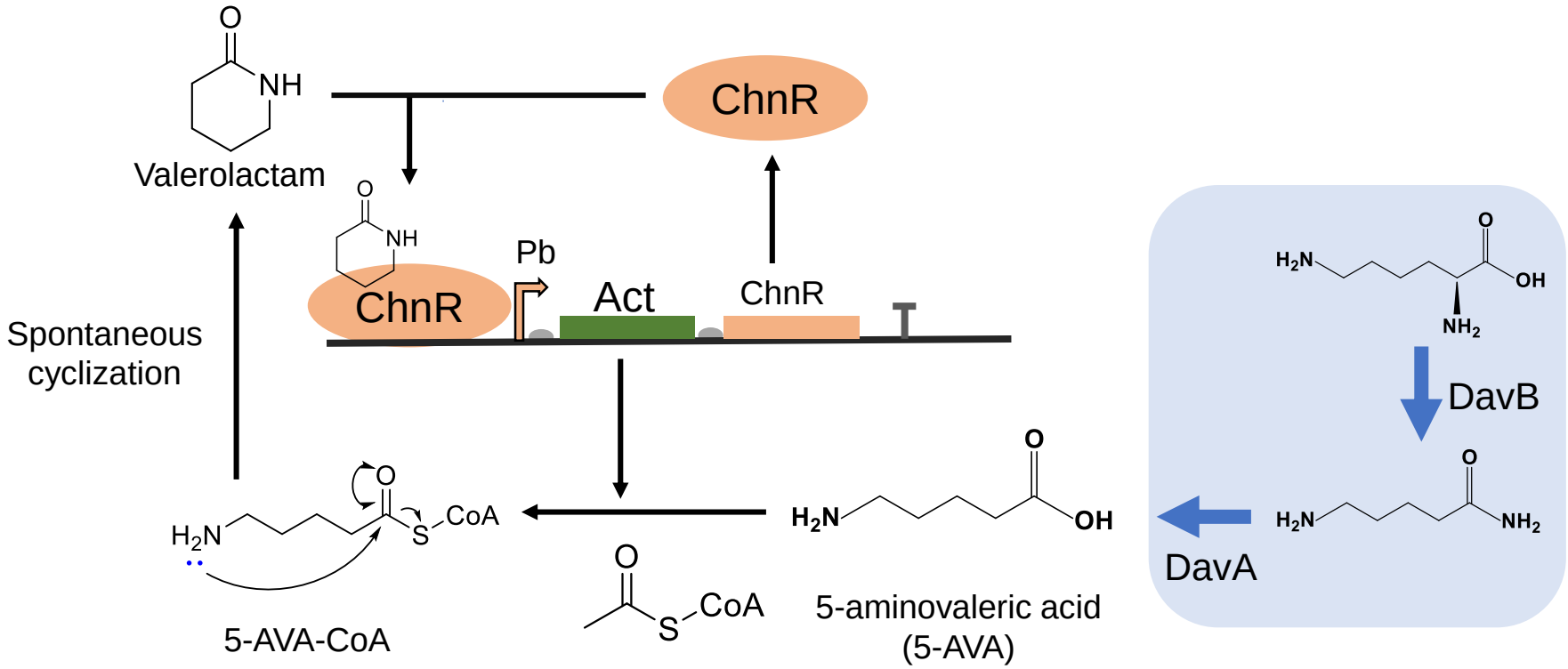


**Figure 2.** Valerolactam production and the dynamic regulatory system developed here. **(A)** Schematic of the ChnR/Pb system for dynamic upregulation of the expression of Act in the valerolactam biosynthetic pathway.

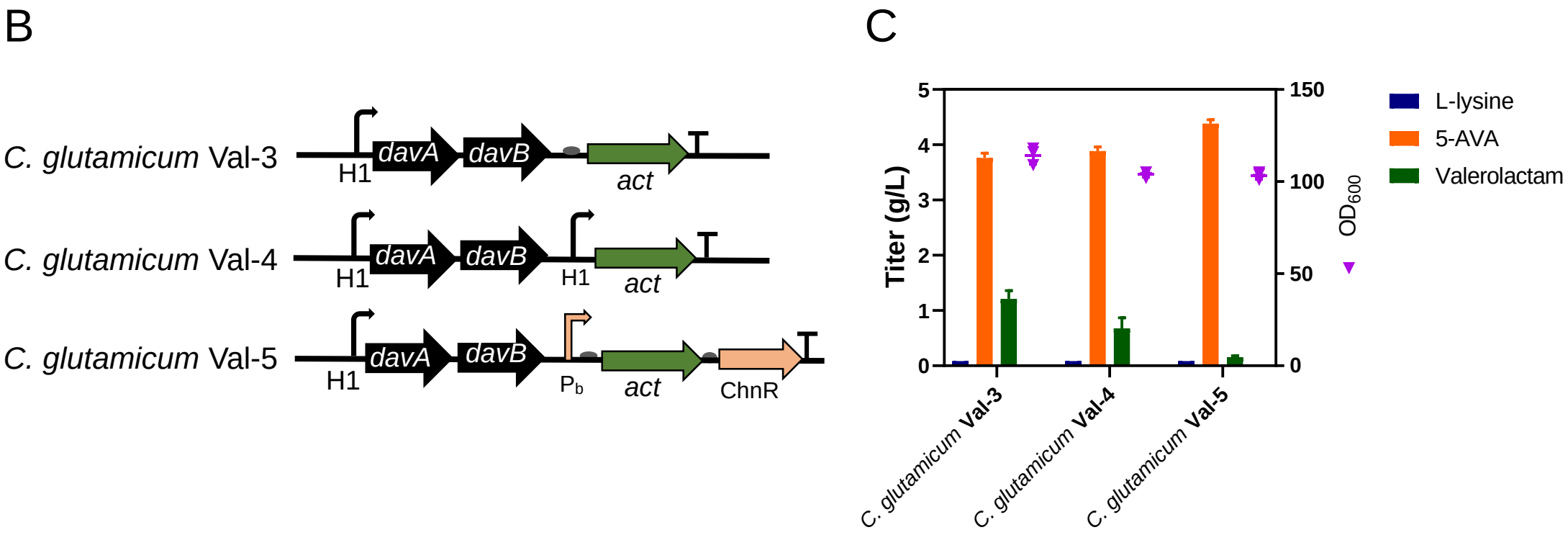


**Figure 2. (B)** Valerolactam biosynthetic gene cluster with three different regulatory systems. **(C)** Production of L-lysine, 5-AVA, and valerolactam in flask cultures at 48 hours. 5-AVA (5-aminovaleric acid).

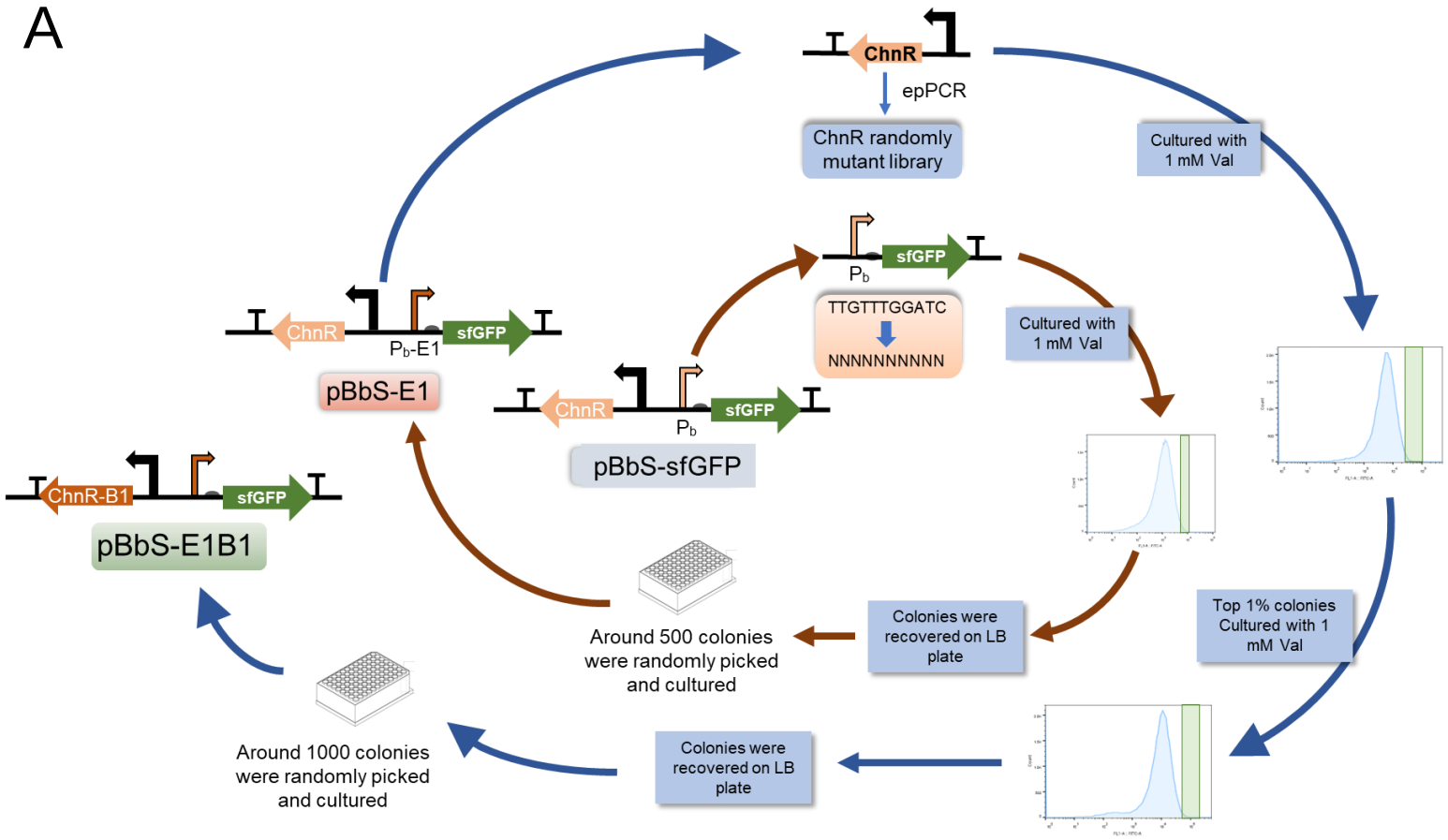


**Figure S3. (A)** Schematic of engineering the valerolactam biosensor. We started with the pBbS-sfGFP biosensor. Red arrow indicates engineering the ChnR binding site in Pb promoter. The Pb site-saturation mutagenesis library was sorted by FACS for the colonies with top 1% GFP signal, and these colonies were further verified in 96-well plates with 1 mM valerolactam to get biosensor pBbS-E1. Blue arrow indicates improving the binding affinity of ChnR for valerolactam (Val) by two rounds of FACS sorting. The ChnR mutants selected from the second round of FACS sorting were further verified in 96-well plates with 1 mM valerolactam to get the biosensor mutant pBbS-E1B1 with the highest fluorescence signal.

B

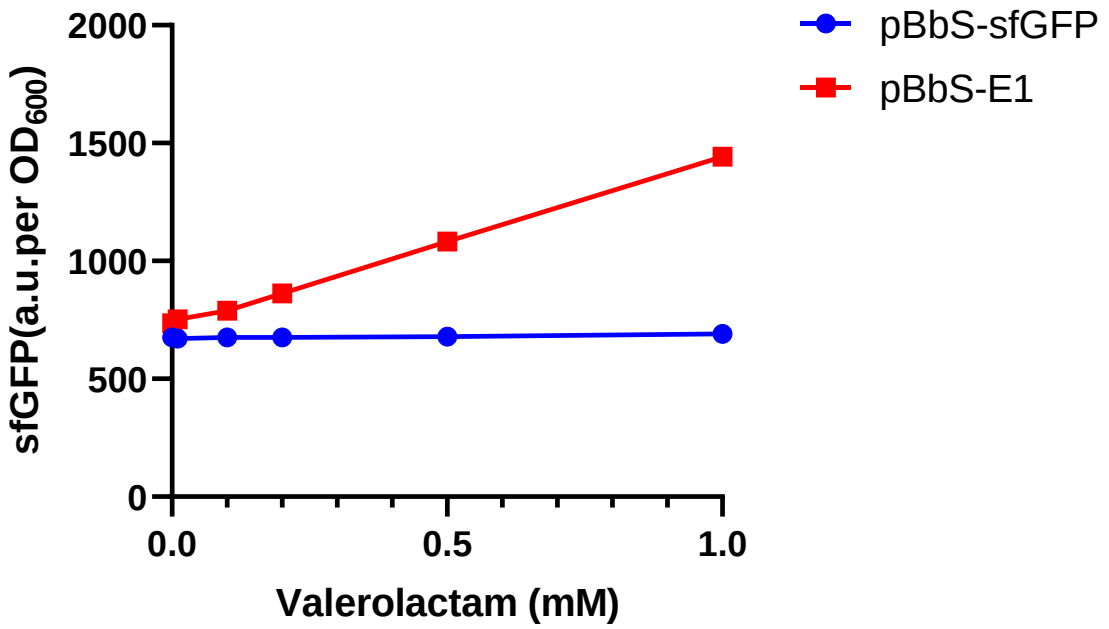


C

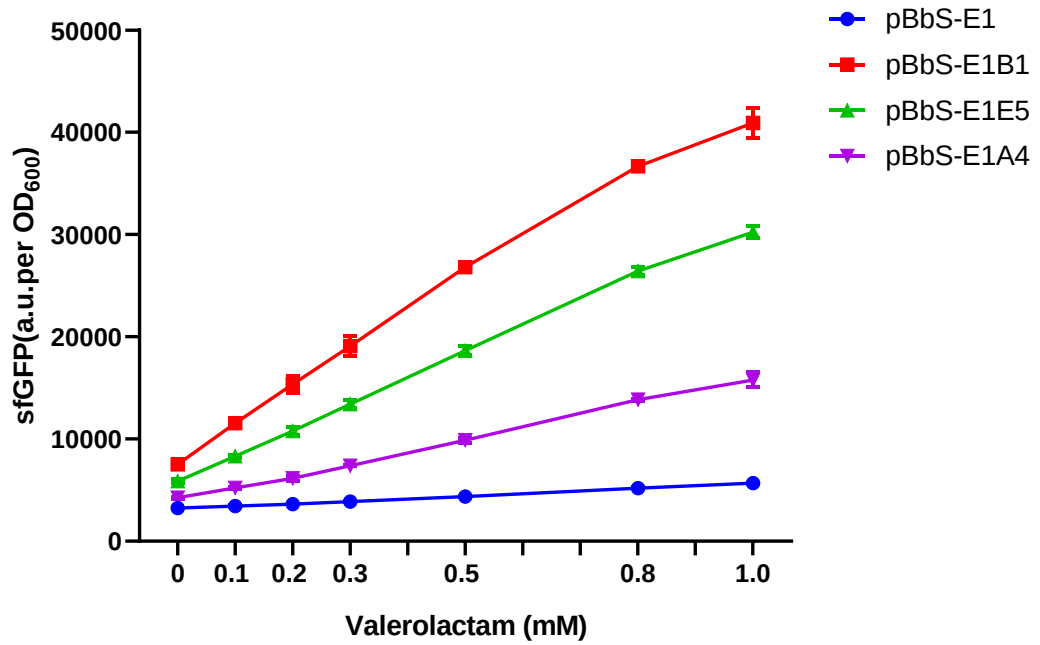


**Figure S3. (B)** Comparison of the outputs of the biosensor mutant pBbS-E1 with the original valerolactam biosensor pBbS-sfGFP for 0-1 mM valerolactam. **(C)** Comparison of the output from promoter Pb with different ChnR mutants with the pBbS-E1 control for 0-1 mM valerolactam.

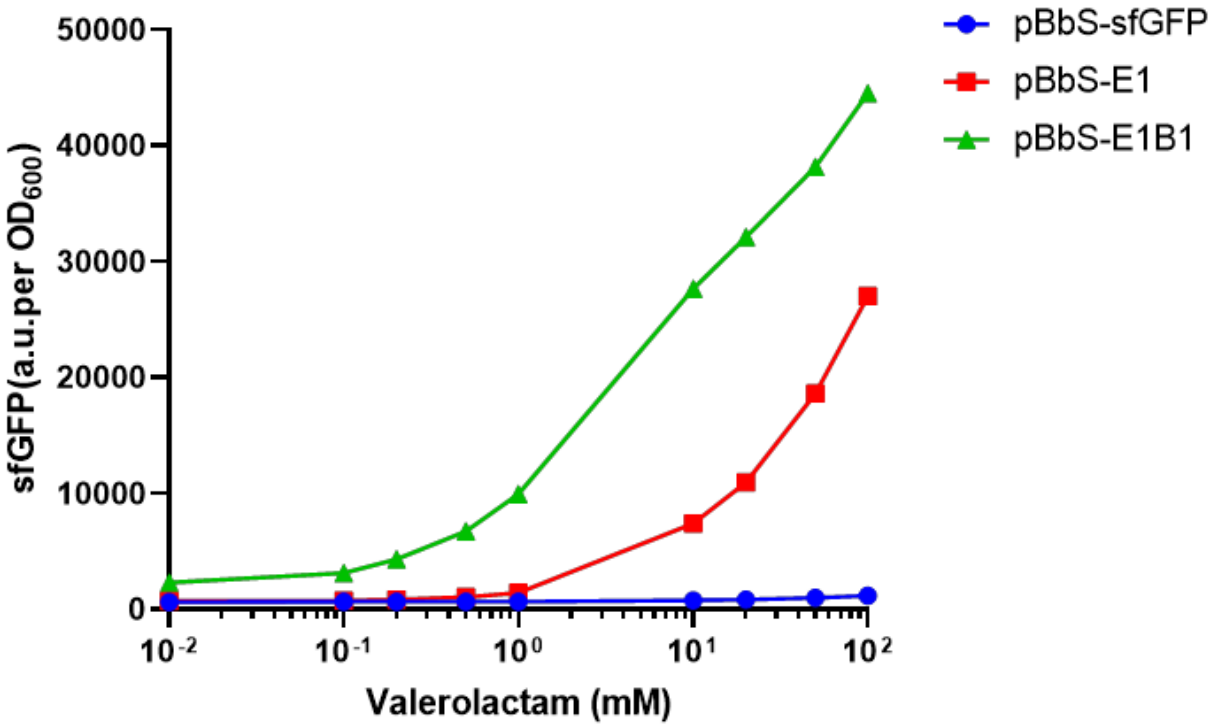


**Figure 3.** Comparison of the outputs of the evolved biosensor pBbS-E1 and pBbS-E1B1 with the original biosensor pBbS-sfGFP in different concentrations of valerolactam.

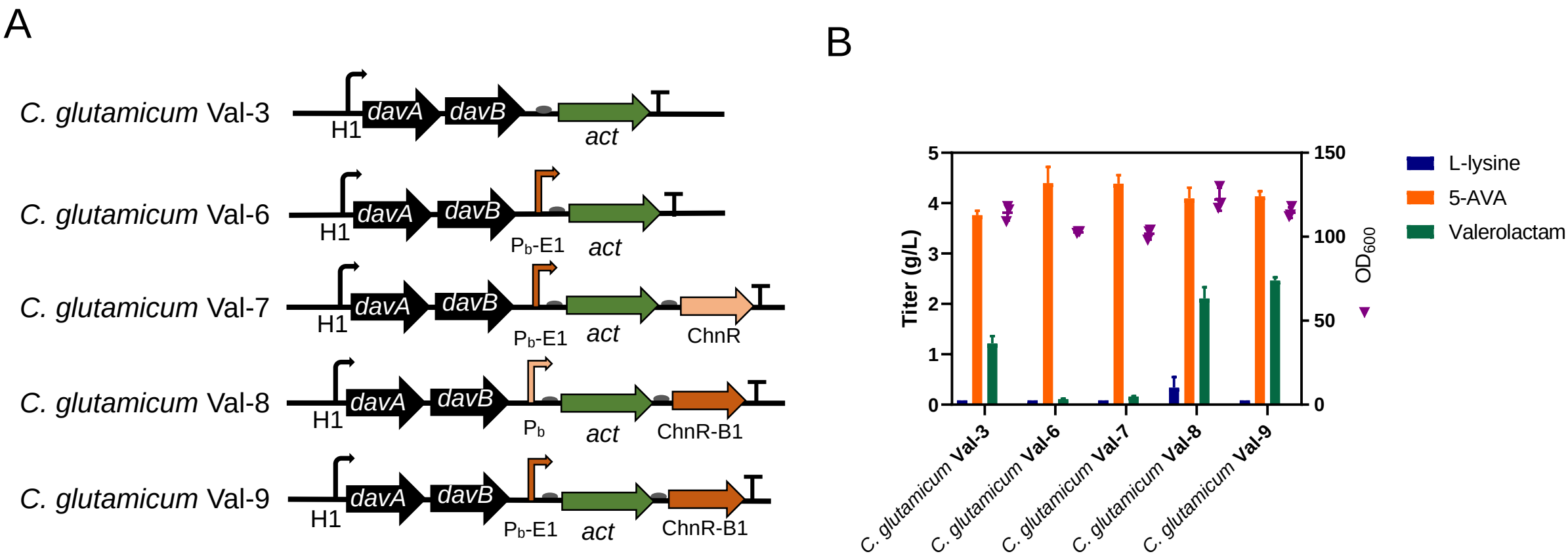


**Figure 4.** Dynamic upregulation of Act with the different regulator-promoter systems for valerolactam biosynthesis. **(A)** Design of the valerolactam pathway with different ChnR and Pb mutant combinations. **(B)** Flask culture results of the different valerolactam biosynthesis pathways indicated in **(A)**. 5-AVA (5-aminovaleric acid).

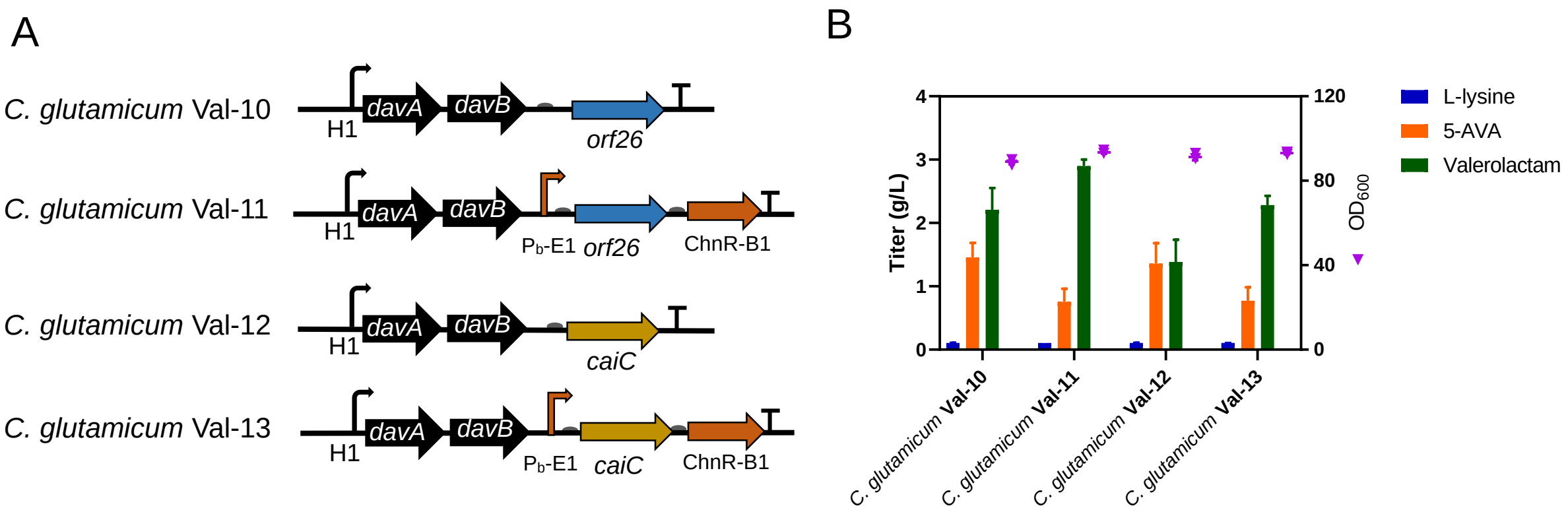


**Figure 5.** Dynamic upregulation of the ORF26 and CaiC with ChnR-B1/Pb-E1 system for valerolactam biosynthesis. 5-AVA (5-aminovaleric acid).

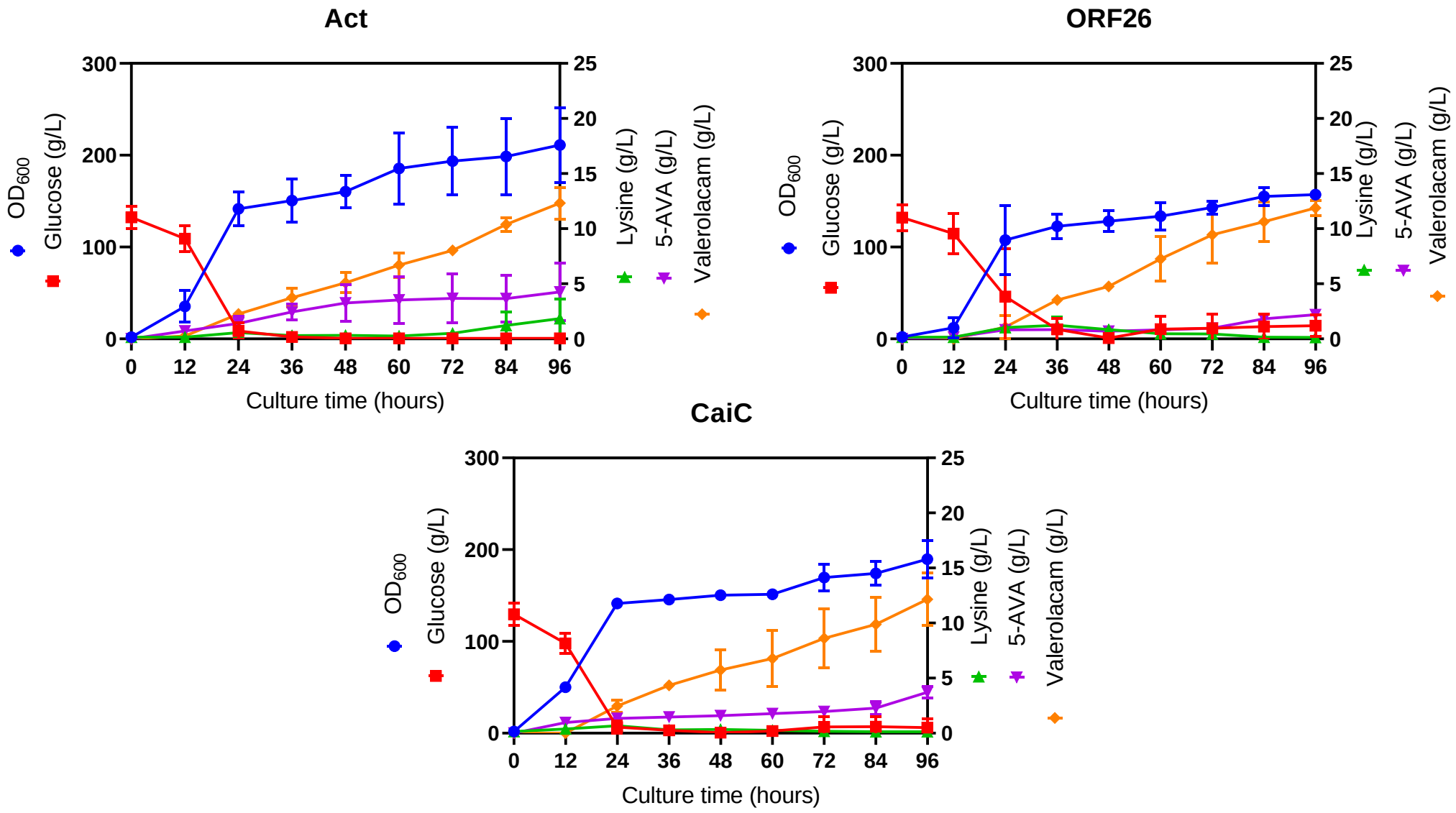


**Figure 6.** Fed-batch fermentation of valerolactam production in *C. glutamicum* Val-9 (Act), *C. glutamicum* Val-11 (ORF26) and *C. glutamicum* Val-13 (CaiC). (There is two replicates for *C. glutamicum* Val-11, three replicates for *C. glutamicum* Val-9 and *C. glutamicum* Val-13 )

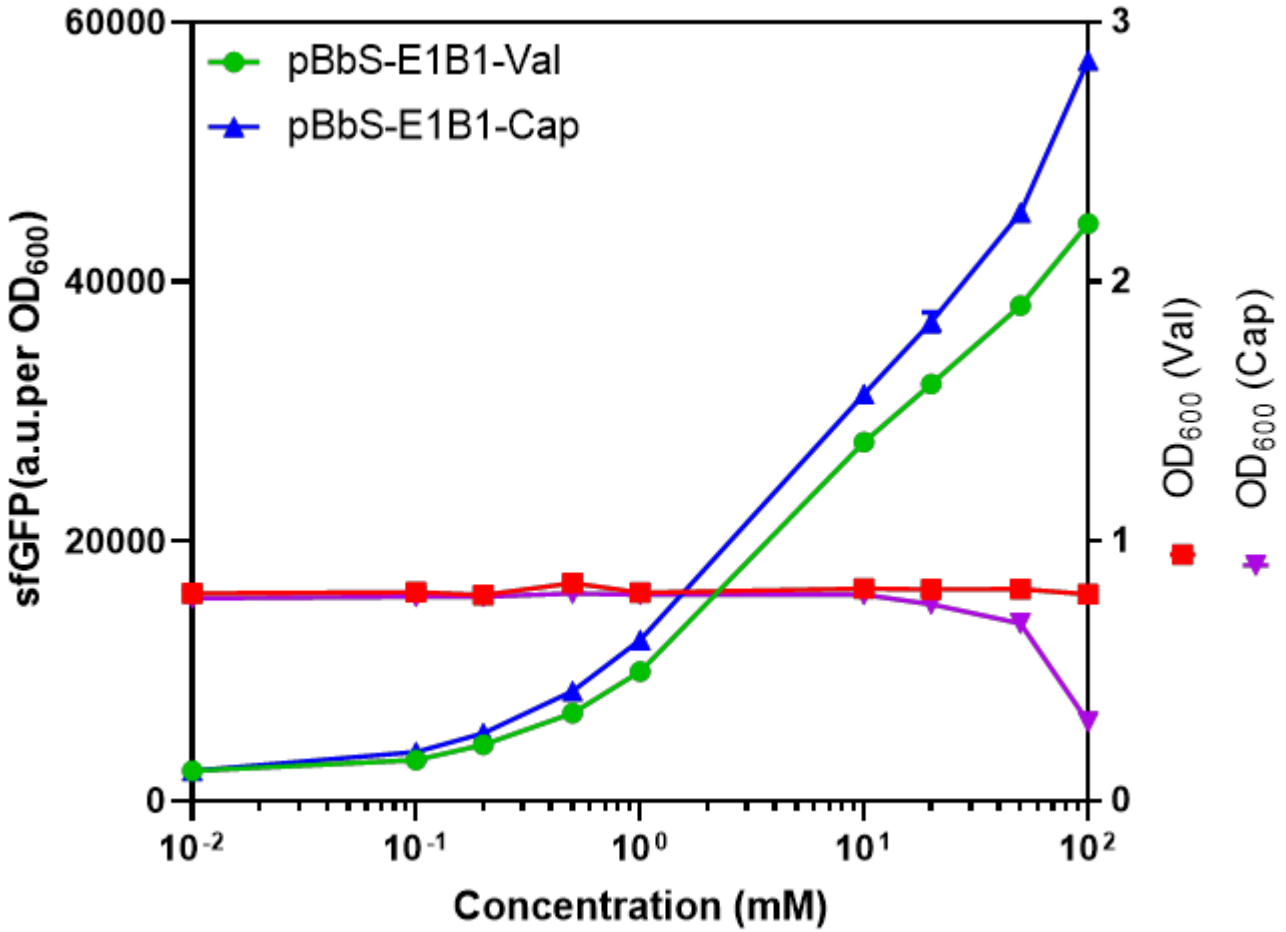


**Figure S4.** Biosensor characterization of pBbS-E1B1 sensitivity to valerolactam (Val) and caprolactam (Cap) in *E. coli*.

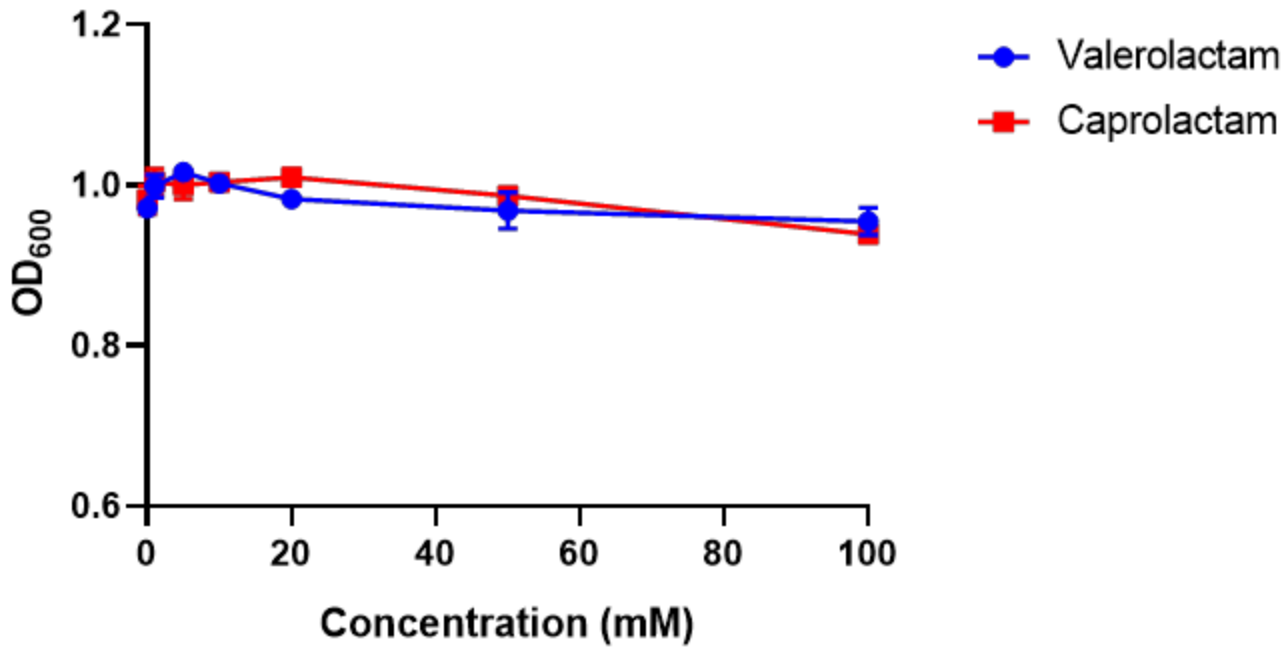


**Figure S5.** The effect of valerolactam and caprolactam on growth. of *C. glutamicum* XT1.

# Dynamic upregulation of the rate-limiting enzyme for valerolactam biosynthesis in *Corynebacterium glutamicum*

Xixi Zhao[a,b,1], Yanling Wu[a,b,c,1], Tingye Feng[a,b], Junfeng Shen[a,b], Huan Lu[a,b], Yunfeng Zhang[a,b], Howard H. Chou[a,b,c,d], Xiaozhou Luo[a,b,c,d]*, Jay D. Keasling[a,e,f,g,h,i]

[a]Center for Synthetic Biochemistry, Shenzhen Institute of Synthetic Biology, Shenzhen Institutes of Advanced Technology, Chinese Academy of Sciences, Shenzhen 518055, China.

[b]CAS Key Laboratory of Quantitative Engineering Biology, Shenzhen Institute of Synthetic Biology, Shenzhen Institutes of Advanced Technology, Chinese Academy of Sciences, Shenzhen 518055, China.

[c]University of Chinese Academy of Sciences, Beijing 100049, China

[d]Shenzhen Key Laboratory for the Intelligent Microbial Manufacturing of Medicines, Shenzhen Institutes of Advanced Technology, Chinese Academy of Sciences, Shenzhen 518055, China.

[e]Joint BioEnergy Institute, Lawrence Berkeley National Laboratory, Emeryville, CA 94608, USA.

[f]Biological Systems and Engineering Division, Lawrence Berkeley National Laboratory, Berkeley, CA 94720, USA.

[g]QB3 Institute, University of California, Berkeley, Berkeley, CA 94720, USA.

[h]Department of Chemical and Biomolecular Engineering and Department of Bioengineering, University of California, Berkeley, Berkeley, CA 94720, USA.

[i]The Novo Nordisk Foundation Center for Biosustainability, Technical University Denmark, Kemitorvet, Building 220, Kongens Lyngby 2800, Denmark.

[1]These authors contributed equally to this work.

*Corresponding author: xz.luo@siat.ac.cn

**Abstract**

Valerolactam is a monomer used to manufacture high-value nylon-5 and nylon-6,5. However, the biological production of valerolactam has been limited by the inadequate efficiency of enzymes to cyclize 5-aminovaleric acid to produce valerolactam. In this study, we engineered *Corynebacterium glutamicum* with a valerolactam biosynthetic pathway consisting of DavAB from *Pseudomonas putida* to convert L-lysine to 5-aminovaleric acid and β-alanine CoA transferase (Act) from *Clostridium propionicum* to produce valerolactam from 5-aminovaleric acid. Most of the L-lysine was converted into 5-aminovaleric acid, but promoter optimization and increasing the copy number of Act were insufficient to significantly improve the titer of valerolactam. To eliminate the bottleneck at Act, we designed a dynamic upregulation system (a positive feedback loop based on the valerolactam biosensor ChnR/Pb). We used laboratory evolution to engineer ChnR/Pb to have higher sensitivity and a higher dynamic output range, and the engineered ChnR-B1/Pb-E1 system was used to overexpress the rate-limiting enzymes (Act/ORF26/CaiC) that cyclize 5-aminovaleric acid into valerolactam. In glucose fed-batch culture, we obtained 12.33 g/L valerolactam from the dynamic upregulation of Act, 11.88 g/L using ORF26, and 12.15 g/L using CaiC. Our engineered biosensor (ChnR-B1/Pb-E1 system) was also sensitive to 0.01-100 mM caprolactam, which suggests that this dynamic upregulation system can be used to enhance caprolactam biosynthesis in the future.

**Keywords**: Dynamic regulation, valerolactam, biosensor engineering, *Corynebacterium glutamicum*.

## 1. Introduction

Lactams are used as monomers for the synthesis of industrial polyamides (nylon-4, nylon-5, nylon-6, nylon-6,5, etc.) (Yeom et al., 2018)(Chae et al., 2017)(Zhang et al., 2017b). Nylons are widely used in automobile parts, carpets, and packaging due to their high tensile strength, good elasticity, and excellent abrasion resistance. The global market for nylon-6 (with caprolactam as the monomer) was estimated at USD 15 billion in 2019, and the market is growing, propelled, in part, by an increasing demand for lightweight vehicles (Gordillo Sierra and Alper, 2020). Nylon-6,5 can be synthesized using valerolactam and caprolactam as monomers and has different properties than nylon-6 due to the addition of valerolactam (Park et al., 2014). Valerolactam and caprolactam are currently produced by petrochemical processes that require high temperatures and harsh acidic conditions, are energy intensive, and produce large amounts of waste. Biosynthesis of these lactams will alleviate many of these issues (Gordillo Sierra and Alper, 2020).

The biosynthetic pathway to produce valerolactam from lysine has three enzymes, DavB (L-lysine monooxygenase) and DavA (5-aminovaleramide amidohydrolase) from *Pseudomonas putida* and an enzyme for the cyclization step of 5-aminovaleric acid (5-AVA) to valerolactam (Chae et al., 2017)(Zhang et al., 2017b). Recently, *Corynebacterium glutamicum* was engineered to produce 48.3 g/L 5-AVA by balancing the expression of heterologous *davAB*

genes from *P. putida*, reducing the formation of the byproduct glutarate, increasing 5-AVA export and reducing 5-AVA reimport (Rohles et al., 2022). Additionally, *Escherichia coli* WL3110 was engineered with the same pathway to produce 90.59 g/L 5-AVA from 120 g/L L-lysine (Park et al., 2014). While 5-AVA has been produced in high titer, there has been less progress in producing valerolactam. When Act (β-alanine CoA transferase) was used for the cyclization step, 1.18 g/L valerolactam was synthesized from glucose in *Escherichia coli* (Chae et al., 2017), and 705 mg/L valerolactam was synthesized from 10 g/L L-lysine when DavB, DavA, and ORF26 (acyl-CoA ligase) were co-expressed in *E. coli* (Zhang et al., 2017b). The limited titer of the biosynthesized valerolactam is due to the inefficiency of the cyclization of 5-AVA to valerolactam (Zhang et al., 2017b)(Gordillo Sierra and Alper, 2020).

In traditional metabolic engineering strategies, heterologously expressed pathway genes are modulated by increasing the DNA copy number, optimizing promoter and ribosome binding strength, and engineering pathway enzymes to maximize the production of the target chemicals (Brockman and Prather, 2015). These strategies can effectively improve titer, rate, and yield of the desired final product. Additionally, dynamic regulation systems have been effective for increasing the titer of products through the upregulation or downregulation of pathway genes by internally sensing metabolite levels in real time (Zhang et al., 2012)(Dahl et al., 2013)(Jones et al., 2015)(Yang et al., 2018). For example, the transcription factor CatR has been designed for the dynamic upregulation

of salicylate biosynthesis in the muconic acid biosynthetic pathway, and this strategy successfully increased the muconic acid titer by 5.87-fold compared with static control (Yang et al., 2018). Another strategy for dynamic regulation has been designed based on a positive feedback loop, in which the gene product enhances its own production directly or indirectly by amplifying the expression level of enzymes for its production. In *Neurospora crassa*, the transcription factor CLR-2 was placed under the control of *Pcbh-1*, which is a target of CLR-2. The expression level of CLR-2 was significantly increased using this positive feedback loop and hence amplified the expression of approximately 50% of 78 lignocellulosic degradation-related genes, which revealed a previously unappreciated role of CLR-2 in the lignocellulosic degradation gene network (Matsu-Ura et al., 2018). Finally, a LuxR-based positive feedback loop was designed as a genetic signal amplifier, and the maximum expression level of the output signal was substantially increased in the strains with a positive feedback loop compared to those without (Nistala et al., 2010). In light of the previously reported biosensors for various lactams (ChnR/Pb system), we reasoned that it should be possible to increase the titer of valerolactam by dynamically upregulating the rate-limiting cyclization step.

*C. glutamicum* was chosen as the host to produce valerolactam because it is known to produce high levels of lysine and 5-AVA (Fig. 1A)(Becker et al., 2011)(Shin et al., 2016) (Chae et al., 2017)(Zhang et al., 2017b)(Rohles et al., 2022). We engineered wild-type *C. glutamicum* with *davAB* and *act* by

traditional metabolic engineering to increase its production of valerolactam. The lactam biosensor was then optimized and used to control the expression of the cyclization enzyme, leading to a 10-fold improvement in valerolactam production during fed-batch fermentation (Chae et al., 2017).

## 2. Materials and Methods

### 2.1 Experimental materials

All bacterial strains and plasmids used in this study are listed in Table 1 and Table S1 respectively. All primers were synthesized at GENEWIZ (Suzhou, China) and are listed in Table S2. The valerolactam biosynthetic pathway genes *davB* and *davA* from *Pseudomonas putida* KT2440, *act* from *Clostridium propionicum*, *orf26* from *Streptomyces aizunensis*, and *caiC* from *Escherichia coli* were codon optimized for all *C. glutamicum* and synthesized at GENEWIZ (Suzhou, China) (the sequences of the *C. glutamicum*-codon optimized versions of *davB* and *davA* from *P. putida* were the same as those described by (Shin et al., 2016)). The sequences of the *C. glutamicum* codon-optimized genes are listed in Table S3.

**Table 1** Bacterial strains used in this study.

| Strain | Description | Source |
|---|---|---|
| *E. coli* DH5α | General cloning purpose. Genotype: F⁻ φ80*lac*ZΔM15 Δ(*lac*ZYA-*arg*F) | Lab stock |

| | | |
|---|---|---|
| | U169 *rec*A1 *end*A1 *hsd*R17($r_K^-$, $m_K^+$) *pho*A *sup*E44 *thi*-1 *gyr*A96 *rel*A1 $\lambda^-$ | |
| *E. coli* DH10B | $F^-$*mcr*A Δ(*mrr-hsd*RMS-*mcr*BC) φ80*lac*ZΔM15 Δ*lac*X74 *rec*A1 *end*A1 *ara*D139 Δ(*ara-leu*)7697 *gal*U *gal*K $\lambda^-$*rps*L($Str^R$) *nup*G | Lab stock |
| *C. glutamicum* ATCC 13032 | Wilt type | Lab stock |
| *C. glutamicum* XT1 | *C. glutamicum* ATCC 13032 derivate, *lysC* (C932T) | This study |
| *C. glutamicum* Val-1 | *C. glutamicum* XT1 harboring pCES208-H1davAB | This study |
| *C. glutamicum* Val-2 | *C. glutamicum* XT1 harboring pCES208-H1davAB-act | This study |
| *C. glutamicum* Val-3 | *C. glutamicum* XT1 harboring pHCP-H1davAB-act | This study |
| *C. glutamicum* Val-4 | *C. glutamicum* XT1 harboring pHCP-H1davAB-H1act | This study |
| *C. glutamicum* Val-5 | *C. glutamicum* XT1 harboring pHCP-H1davAB-Pb-act-chnR | This study |
| *C. glutamicum* Val-6 | *C. glutamicum* XT1 harboring pHCP-H1davAB-E1-act | This study |
| *C. glutamicum* Val-7 | *C. glutamicum* XT1 harboring pHCP-H1davAB-E1-act-chnR | This study |
| *C. glutamicum* | *C. glutamicum* XT1 harboring pHCP- | This |

| | | |
|---|---|---|
| Val-8 | H1davAB-Pb-act-B1 | study |
| *C. glutamicum* Val-9 | *C. glutamicum* XT1 harboring pHCP-H1davAB-E1-act-B1 | This study |
| *C. glutamicum* Val-10 | *C. glutamicum* XT1 harboring pHCP-H1davAB-orf26 | This study |
| *C. glutamicum* Val-11 | *C. glutamicum* XT1 harboring pHCP-H1davAB-E1-orf26-B1 | This study |
| *C. glutamicum* Val-12 | *C. glutamicum* XT1 harboring pHCP-H1davAB-caiC | This study |
| *C. glutamicum* Val-13 | *C. glutamicum* XT1 harboring pHCP-H1davAB-E1-caiC-B1 | This study |

Luria-Bertani (LB) broth or plates (1.5%, w/v, agar) containing appropriate antibiotics were used for *E. coli* inoculation, plasmid propagation, and transformation. Kanamycin (50 μg/mL) and chloramphenicol (25 μg/mL) were added to the medium when necessary. *E. coli* DH5α was used for general cloning purposes, and *E. coli* DH10B was used for biosensor characterization and mutant library construction and sorting.

*Corynebacterium glutamicum* ATCC13032 was used as the base strain for the construction of the L-lysine-producing and valerolactam-producing chassis strains. LBHIS (tryptone 5 g/L, yeast extract 2.5 g/L, NaCl 5 g/L, BHI 18.5 g/L, sorbitol 91 g/L, pH=7.2) broth or plates with 25 μg/mL kanamycin were used for

148 the cultivation or transformation of *C. glutamicum*.

149

150 **2.2 Genetic manipulation**

151 All DNA manipulation was performed according to standard protocols (Green
152 and Sambrook, 2012). Phanta DNA polymerase (Vazyme, Biotech, Co., Ltd.,
153 China) was used for DNA fragment amplification by polymerase chain reaction
154 (PCR, ThermoFisher ProFlex PCR system). The kits for DNA fragment
155 purification and gel extraction were purchased from Omega Bio-Tek Inc.
156 (Norcross, GA, USA). The plasmid miniprep kit was purchased from TIANGEN
157 Biotech (Beijing, China), and the Gibson assembly reaction kit was purchased
158 from New England Biolabs (NEB, Ipswich, MA, USA).

159 The plasmid pK18mobsacB was used for point mutation of the *lysC* gene in the
160 *C. glutamicum* ATCC13032 genome. The primers P1 and P2 were used to
161 amplify the pK18 backbone from pK18mobsacB, primers P3 and P4 with a point
162 mutation (C932T, red font) were used to amplify part of *lysC* from the *C.*
163 *glutamicum* ATCC13032 genome, and primers P5 with a point mutation (C932T,
164 red font) and P6 were used to amplify the other part of *lysC* and 588 bp of the
165 *lysC* downstream fragment from the *C. glutamicum* ATCC13032 genome; the
166 **pK18-lysC** plasmid was obtained by Gibson assembly of the above three
167 fragments. Then, pK18-lysC was transformed into *C. glutamicum* ATCC13032.
168 After double crossover homologous recombination driven by sucrose selection
169 based on the function of *sacB* (Schäfer et al., 1994), we obtained the ***C.***

170 ***glutamicum* XT1** (*lysC*: C932T) strain with sequence confirmation.

171 For promoter strength analysis in *C. glutamicum* XT1, primers P7 (containing
172 part of the H1 sequence) and P8 were used to amplify the H1-mCherry fragment
173 from pBbSlactam, primers P9 and P10 (containing part of the H1 sequence)
174 were used to amplify the pEC backbone from pEC-XK99E, and then Gibson
175 assembly of the above two fragments was performed to obtain **pH1-mCherry**.
176 Primers P11 (containing part of the H2 sequence) and P8 were used to amplify
177 the H2-mCherry fragment from pBbSlactam, primers P12 (containing part of the
178 H2 sequence) and P9 were used to amplify the pEC backbone from pEC-
179 XK99E, and Gibson assembly of the above two fragments was used to obtain
180 **pH2-mCherry**. Primers P13 (containing part of the H9 sequence) and P8 were
181 used to amplify the H9-mCherry fragment from pBbSlactam, primers P14
182 (containing part of the H9 sequence) and P9 were used to amplify the pEC
183 backbone from pEC-XK99E, and Gibson assembly of the above two fragments
184 was performed to obtain **pH9-mCherry**. Primers P15 (containing part of the
185 H10 sequence) and P8 were used to amplify the H10-mCherry fragment from
186 pBbSlactam, primers P16 (containing part of the H9 sequence) and P9 were
187 used to amplify the pEC backbone from pEC-XK99E, and Gibson assembly of
188 the above two fragments was performed to obtain **pH10-mCherry**.

189 To construct the high copy number plasmids derived from pCES208 (a kind gift
190 from Prof. Sang Yup Lee's Lab, (Park et al., 2008)), it was necessary to

191 introduce a nonsense mutation in the *parB* locus (Choi et al., 2018). Primers
192 P17 (with point mutation of *parB*, red font) and P18 (with point mutation of *parB*,
193 red font) were used to insert the point mutation into *parB*. Then, Gibson
194 assembly of this single PCR fragment was performed to obtain the **pHCP**
195 plasmid, and pCES208 and pHCP were used as backbones to construct the
196 valerolactam biosynthetic pathway. Primers P19 (containing part of the H1
197 sequence) and P20 (containing part of the RBS for *davB* and the RBS sequence
198 is from (Shin et al., 2016)) were used to amplify H1-*davA* from the synthesized
199 codon-optimized *davA* plasmid. Primers P21 (containing the RBS for *davB*) and
200 P22 (containing the RBS (Rohles et al., 2016) for *act*/*orf26*/*caiC*) were used to
201 amplify the *davB* fragment from the synthesized codon-optimized *davB* plasmid.
202 Primers P23 and P24 were used to amplify the *act* fragment from the
203 synthesized codon-optimized *act* plasmid, and then primers P19 and P24 were
204 used for fusion PCR of the H1-*davA*, *davB* and *act* fragments to obtain the H1-
205 davAB-act fragment. Primers P25 and P26 were used to amplify the pHCP
206 backbone from the pHCP plasmid, and then Gibson assembly of the pHCP
207 backbone and H1-davAB-act was performed to obtain the **pHCP-H1davAB-act**
208 plasmid. For pCES208-H1davAB-act plasmid construction, primers P25 and
209 P26 were used to amplify the pCES208 backbone from the pCES208 plasmid,
210 and then Gibson assembly of the pCES208 backbone with the H1-davAB-act
211 fragment was performed to obtain the plasmid. For pCES208-H1davAB plasmid
212 construction, primer P19 and primer P27 were used to amplify the H1davAB

fragment from H1davAB-act, and then Gibson assembly of pCES208 with H1davAB was performed to obtain the plasmid.

For pHCP-H1davAB-H1act plasmid construction, primers P21 and P28 were used to amplify *davB*-H1 from the synthesized codon-optimized *davB* plasmid. Primer P19 and primer P24 were used to amplify the H1-*act* fragment from the synthesized codon-optimized *act* plasmid, and then primers P19 and P24 were used for fusion PCR of the H1-*davA*, *davB*-H1 and H1-*act* fragments to obtain the H1-davAB-H1-act fragment. Gibson assembly of the H1-davAB-H1-act fragment with the pHCP backbone was used to obtain the plasmid.

For pHCP-H1davAB-Pb-act-chnR plasmid construction, primers P21 and P29 were used to amplify *davB*-Pb from the synthesized codon-optimized *davB* plasmid. Primers P30 and P31 were used to amplify the Pb fragment from pBbSlactam, primers P32 and P33 were used to amplify the Pb-*act* fragment from the synthesized codon-optimized *act* plasmid, primers P34 and P35 were used to amplify the *chnR* fragment from pBbSlactam, primers P19 and P29 were used for fusion PCR of H1-*davA* and *davB*-Pb to obtain the H1-davAB-Pb fragment, primers P30 and P35 were used for fusion PCR of Pb, Pb-*act* and *chnR* to obtain the Pb-*act*-chnR fragment, and then Gibson assembly of the H1-davAB-Pb, Pb-*act*-chnR and pHCP backbone was used to obtain the plasmid.

For construction of the other valerolactam biosynthetic pathway, many of the same primers were used to amplify the mutants from the different templates.

For example, for pHCP-H1davAB-E1act construction, primers P30 and P31 were used to amplify Pb-E1 from the pBbS-E1 plasmid, primers P32 and P24 were used to amplify *act* from the synthesized codon-optimized *act* plasmid, and primers P30 and P24 were used for fusion PCR of Pb-E1 and *act* fragments to obtain the E1-act fragment. Gibson assembly of H1-*davA*, *davB*, and E1-act was carried out to obtain **pHCP-H1davAB-E1act**.

For construction of dynamic regulation of *act* by ChnR/Pb-E1 system. Primers P30 and P35 were used for fusion PCR of Pb-E1, Pb-*act* and *chnR* to obtain the E1-*act*-chnR fragment, and then Gibson assembly of the H1-davAB-Pb, E1-*act*-chnR and pHCP backbone was performed to obtain **pHCP-H1davAB-E1-act-chnR**.

For construction of dynamic regulation of *act* by ChnR-B1/Pb system. Primers P34 and P35 were used to amplify the *chnR*-B1 fragment from pBbS-E1B1, then primers P30 and P35 were used for fusion PCR of Pb, Pb-*act* and *chnR*-B1 to obtain the Pb-*act*-B1 fragment. Next, Gibson assembly of the H1-davAB-Pb, Pb-*act*-B1 and pHCP backbone was performed to obtain **pHCP-H1davAB-Pb-act-B1**.

For construction of dynamic regulation of *act* by ChnR-B1/Pb-E1 system. Primers P30 and P35 were used for fusion PCR of Pb-E1, Pb-*act* and *chnR*-B1 to obtain the E1-*act*-B1 fragment, and then Gibson assembly of the H1-davAB-Pb, E1-*act*-B1 and pHCP backbone was performed to obtain **pHCP-H1davAB-**

**E1-act-B1**.

For construction of ORF26 as the catalysts for the cyclization step of valerolactam biosynthesis. Primers P36 and P37 were used to amplify the *orf26* fragment from the synthesized codon-optimized orf26 plasmid, then primers P19 and P37 were used for fusion PCR of the H1-*davA*, *davB* and *orf26* fragments to obtain the H1-davAB-orf26 fragment. Next, Gibson assembly of the pHCP backbone and H1-davAB-orf26 was used to obtain the **pHCP-H1davAB-orf26** plasmid.

For construction of dynamic regulation of *orf26* by ChnR-B1/Pb-E1 system. Primers P36 and P38 were used to amplify Pb-orf26 from the synthesized codon-optimized orf26 plasmid, and primers P30 and P35 were used for fusion PCR of Pb-E1, Pb-*orf26* and *chnR*-B1 to obtain the E1-orf26-B1 fragment. Then, Gibson assembly of the H1-davAB-Pb, E1-*orf26*-B1 and pHCP backbone was performed to obtain the **pHCP-H1davAB-E1-orf26-B1** plasmid.

For construction of CaiC as the catalysts for the cyclization step of valerolactam biosynthesis Primers P39 and P40 were used to amplify the *caiC* fragment from the synthesized codon-optimized *caiC* plasmid, then primers P19 and P40 were used for fusion PCR of the H1-*davA*, *davB* and *caiC* fragments to obtain the H1-davAB-caiC fragment. Next, Gibson assembly of the pHCP backbone and H1-davAB-caiC was used to obtain the **pHCP-H1davAB-caiC** plasmid.

For construction of dynamic regulation of *caiC* by ChnR-B1/Pb-E1 system.

Primers P39 and P41 were used to amplify Pb-*caiC* from the synthesized codon-optimized *caiC* plasmid, and primers P30 and P35 were used for fusion PCR of Pb-E1, Pb-*caiC* and *chnR*-B1 to obtain E1-*caiC*-B1. Then, Gibson assembly of the H1-davAB-Pb, E1-*caiC*-B1 and pHCP backbone was performed to obtain **pHCP-H1davAB-E1-caiC-B1**.

All the above Gibson assembly reactions were transformed into *E. coli* DH5α, and the plasmids were sequenced.

### 2.3 Promoter analysis

The constructed pH1-mCherry, pH2-mCherry, pH9-mCherry, and pH10-mCherry plasmids were transformed into *C. glutamicum* XT1 using electro transformation (Ruan et al., 2015). Three randomly selected colonies from each plate were inoculated into 3 mL of LBHIS with 25 μg/mL kanamycin and incubated at 30 °C and 200 rpm shaking for 16-18 hours. Then the cells were inoculated (1:100) into 96-deep well plates containing 1 mL of LBHIS and 25 μg/mL kanamycin. The cells in the 96-deep well plates were cultured in a high-speed shaker at 30 °C and 800 rpm. One hundred microliters of culture medium were removed at 12 h, 24 h, 36 h, and 48 h for mCherry fluorescence signal analysis ($\lambda_{ex}$=575 nm, $\lambda_{em}$=620 nm) with an Infinite 200 PRO (TECAN, San Jose, CA).

### 2.4 Mutant library construction and biosensor engineering

298 For valerolactam biosensor engineering, the primers P42 and P43 were used
299 to amplify sfGFP from pMD19-sfGFP, which was a kind gift from Prof. Fu's
300 laboratory (SIAT, Shenzhen, China). The primers P44 and P45 were used to
301 amplify the backbone from pBbSlactam, and then Gibson assembly of the
302 backbone and sfGFP was performed to obtain pBbS-sfGFP. Primers P46 and
303 P47 (N in red font was indicated as the putative binding site of the transcription
304 factor ChnR (Cheng et al., 2000), Table S2) were used to amplify the Pb site-
305 saturated mutant library fragments followed by Gibson assembly and
306 transformation into *E. coli* DH10B to obtain the Pb mutant library. Then, 20-30
307 colonies were randomly selected for sequencing to analyze the quality of the
308 library. *E. coli* DH10B with the Pb mutant library was sorted with 1 mM
309 valerolactam by fluorescence-activated cell sorting (FACS, BD Aria III, San
310 Jose, USA) to obtain the colonies with the highest 1% sfGFP signal. These
311 colonies were plated on LB agar with 25 μg/mL chloramphenicol. Approximately
312 500 colonies were randomly placed into 96-deep well plates with 1 mL of LB
313 (including 25 μg/mL chloramphenicol and 1 mM valerolactam) and cultured for
314 12 hours at 37 °C and 800 rpm in a high-speed shaker. Samples (100 μL) were
315 then placed into 96-well plates for sfGFP fluorescence analysis ($\lambda_{ex}$=488 nm,
316 $\lambda_{em}$=520 nm). A mutant Pb-E1 (5'-3': TGTAGCCCACC) showed a much higher
317 sfGFP signal in response to 1 mM valerolactam than the wild type (5'-3':
318 ttgtttggatc). The plasmid with this mutation was named pBbS-E1.
319 Primers P48 and P49 were used for error-prone PCR (epPCR) of the *chnR*

gene to engineer the transcription factor ChnR to generate a mutant with a higher binding affinity for valerolactam. epPCR was performed according to the instruction manual of the GeneMorph II Random Mutagenesis Kit (Agilent Technologies, #200550). To obtain a library with both low and medium mutation frequencies of ChnR, 4 tubes (50 μL) were used for epPCR with 300 ng-500 ng of target DNA, which were conducted as follows: 95 °C for 2 min, 23× (95 °C for 30 s, 55 °C for 30 s, 72 °C for 1 min and 15 s), and 72 °C for 10 min. The epPCR products were subjected to gel extraction for library construction. Primers P50 and P51 were used to amplify the E1 backbone from pBbS-E1 followed by Gibson assembly of the *chnR* epPCR products and E1 backbone, and the Gibson reaction products were transformed into *E. coli* DH10B competent cells to obtain the ChnR random mutant library (~1*10^6 colonies were obtained). Approximately 40 colonies from the ChnR library were randomly selected for sequencing to assess the quality of the mutant library. The library was cultured with 1 mM valerolactam for 12 h, and the colonies with the top 1% sfGFP signal were sorted by FACS. These colonies were recultured with 1 mM valerolactam for a second round of FACS. Approximately 1000 colonies from the second round of FACS were randomly placed into 96-deep well plates with 1 mL of LB (including 25 μg/mL chloramphenicol and 1 mM valerolactam) and cultured for 12 hours at 37 °C and 800 rpm in a high-speed shaker. Then, 100 μL samples were placed in 96-well plates for sfGFP fluorescence analysis ($\lambda_{ex}$=488 nm, $\lambda_{em}$=520 nm), and a new mutant, ChnR-B1

(S63G, V121A) showed a much higher sfGFP signal to 1 mM valerolactam than the control pBbS-E1. The plasmid with this ChnR (S63G, V121A) mutation was named pBbS-E1B1.

### 2.5 Flask culture of the *C. glutamicum* strains to produce L-lysine and recombinant *C. glutamicum* XT1 to produce valerolactam

To compare the L-lysine production by *C. glutamicum* ATCC13032 and XT1, the strains from the glycerol stock were cultured on LBHIS agar for 24 hours, and then three randomly picked colonies were recultured on new LBHIS agar for 24 hours for the second round of activation. Three colonies each of *C. glutamicum* WT and XT1 from the second-round activation plates were cultured in LBHIS medium at 30 °C and 200 rpm shaking for 17-18 hours as the seed culture. For flask culture, the seed culture was added to a 250 mL flask containing 25 mL of growth medium (100 g/L glucose, 1 g/L $MgSO_4$, 1 g/L $K_2HPO_4$, 1 g/L $KH_2PO_4$, 1 g/L urea, 40 g/L $(NH_4)_2SO_4$, 10 g/L yeast extract, 100 μg/mL biotin, 10 mg/L β-alanine, 10 mg/L thiamine HCl, 10 mg/L nicotinic acid, 1.3 mg/L $(NH_4)_6MoO_{24}$, 40 mg/L $CaCl_2$, 10 mg/L $FeSO_4$, 10 mg/L $MnSO_4$, 5 mg/L $CuSO_4$, 10 mg/L $ZnSO_4$, and 5 mg/L $NiCl_2$) to have an initial $OD_{600}$=0.1, which was modified based on previous research (Shin et al., 2016). Each flask contained 0.75 g of $CaCO_3$ to maintain the pH at ~7.0 during cultivation, and the flasks were cultured at 30 °C with shaking at 220 rpm. Then, 500 μL samples were removed at 24 hours, 48 hours and 72 hours for quantitative analysis of L-lysine.

To examine whether increasing the expression of valerolactam biosynthetic pathway genes can improve valerolactam production, the plasmids pCES208-H1davAB, pCES208-H1davAB-act and pHCP-H1davAB-act were transformed into *C. glutamicum* XT1. To compare the strong constitutive promoter and the dynamically upregulated system of *act* for valerolactam biosynthesis, the pHCP-H1davAB-act, pHCP-H1davAB-H1act, and pHCP-H1davAB-Pb-act-chnR plasmids were transformed into *C. glutamicum* XT1. To compare the engineered biosensor system-assisted dynamic upregulation of *act* for valerolactam biosynthesis, the pHCP-H1davAB-E1-act, pHCP-H1davAB-E1-act-chnR, pHCP-H1davAB-Pb-act-B1, and pHCP-H1davAB-E1-act-B1 plasmids were transformed into *C. glutamicum* XT1. To determine whether the engineered biosensor system could assist in the dynamic upregulation of ORF26 and CaiC to produce more valerolactam than the strong consistent promoter, the plasmids pHCP-H1davAB-orf26 and pHCP-H1davAB-E1-orf26-B1, pHCP-H1davAB-caiC, and pHCP-H1davAB-E1-caiC-B1 were transformed into *C. glutamicum* XT1. Three randomly selected colonies from the above transformation plates were cultured in LBHIS medium with 25 μg/mL kanamycin at 30 °C and 200 rpm shaking for 17-18 hours as seed culture. For flask cultures, the seed culture was added to a 250 mL flask containing 25 mL of fermentation medium to have an initial $OD_{600}$=0.1, the fermentation medium was the same as the L-lysine production medium, plus 25 μg/mL kanamycin. Each flask contained 0.75 g of $CaCO_3$ to maintain the pH at ~7.0 during cultivation. The

386 culture conditions were 30 °C at 220 rpm for 48 hours, and 1 mL samples were
387 removed for measuring the $OD_{600}$ and quantitative analysis of L-lysine, 5-AVA
388 and valerolactam.
389
390 **2.6 Fed-batch fermentation to produce valerolactam**
391 The glycerol stocks of *C. glutamicum* XT1 pHCP-H1davAB-E1-act-B1, *C.*
392 *glutamicum* XT1 pHCP-H1davAB-E1-orf26-B1, and *C. glutamicum* XT1 pHCP-
393 H1davAB-E1-caiC-B1 were first cultured on LBHIS agar with 25 μg/mL
394 kanamycin, and after 24 hours, the activated colonies were transferred to a new
395 LBHIS plate with 25 μg/mL kanamycin for the second generation cultures. The
396 second generation cultures were collected and inoculated into a 250 mL flask
397 with 50 mL of seed medium, which was the same as that previously reported
398 (Shin et al., 2016), and grown at 30 °C and 220 rpm for 17-18 hours.
399 Approximately 40 mL of seed medium was added as the inoculum to 400 mL of
400 fermentation medium (initial $OD_{600}$=1.5-2.0) with 25 μg/mL kanamycin in a 1.2
401 L fermenter. The fed-batch fermentation medium was the same as that used by
402 Shin et al., 2016, except that the biotin concentration was 1.8 mg/L. An
403 Eppendorf-DASGIP parallel bioreactor system (Hamburg, Germany) equipped
404 with eight 1.2-L jars was used for all fed-batch cultivation experiments. The
405 temperature and agitation were maintained at 30 °C and 1200 rpm, respectively,
406 and the pH was maintained at 7.0 by the addition of a 28% (v/v) ammonia
407 solution. Foaming was suppressed by adding 10% (v/v) antifoam 204 (Sigma–

Aldrich, St. Louis, MO, USA). A 50% (w/v) glucose solution was added when the residual glucose level was below than 5 g/L. Samples were taken every 12 hours to analyze the L-lysine, 5-aminovaleric acid, and valerolactam contents, the residual glucose was analyzed with a SBA-40E Biosensor analyzer (Jinan Yanhe Biotechnology Co., LTD, Jinan, China), and the $OD_{600}$ was measured with a cell density meter Ultrospec 10 (Biochrom, Cambridge, UK).

**2.7 Quantitative analysis of L-lysine, 5-AVA and valerolactam**

A high-performance liquid chromatography–mass spectrometry (LC–MS) instrument (Agilent 1290-6470, Agilent Technologies, Santa Clara, CA, USA) fitted with an EC-C18 column (4.6 × 100 mm; Agilent Technologies) was operated at 37 °C to determine the L-lysine, 5-AVA and valerolactam concentrations in the culture broth (flask culture and fed-batch culture). Samples were removed from the cultured medium and placed in 2.0 ml Eppendorf tubes, and 100 μL of supernatant was obtained by centrifugation at 11600 x *g* for 3 min. Then, the 100 μL of supernatant was treated with a freeze dryer (Christ Alpha-2LDplus, Osterode, Germany) for 2-3 hours and resuspended in 1 mL of 5% MeOH. This solution was diluted 1000-fold before each sample was subjected to LC–MS analysis. The method for valerolactam quantitation was modified based on a previous report (Chae et al., 2017). The mobile phase was composed of solvent A ($H_2O$, 0.1% formic acid) and solvent B (MeOH), and elution was performed with the following gradient: 0-10 min,

5%-30% B at 0.5 mL/min; and 10-16 min, 5% B at 0.5 mL/min. The eluent was directed to the mass spectrometer, which was operated in electrospray ionization (ESI) positive ion mode with the following conditions: gas temperature, 350 °C; gas flow, 10.0 L/min; nebulizer, 45 psi; and capillary voltage, 3.5 kV. Multiple reaction monitor (MRM) mode was selected as the scan mode to detect precursor-to-product ion transitions. The m/z transitions were 100.1 to 44.1 (fragmentor: 110; CE: 40) and 100.1 to 56.1 (fragmentor: 110; CE: 21). For the quantitation of L-lysine and 5-AVA, the mobile phase was applied from 0-10 min with 5% B (MeOH) at a flow rate of 0.2 mL/min. The same mass spectrometry parameters were used, except MRM mode was set to 147 to 130.1 (fragmentor: 80; CE: 9) and 147 to 84.1 (fragmentor: 80; CE: 17) for L-lysine, and the 5-AVA m/z transitions were 118 to 101(fragmentor: 80; CE: 9) and 118 to 55.1 (fragmentor: 80; CE: 2). Standards of L-lysine (Sigma–Aldrich), 5-AVA (Sigma–Aldrich) (each 5.0 mg/L, 2.5 mg/L, 1.25 mg/L, 0.625 mg/L and 0.3125 mg/L) and valerolactam (Sigma–Aldrich) (each 4.0 mg/L, 2.0 mg/L, 1.0 mg/L, 0.5 mg/L, 0.25 mg/L and 0.125 mg/L) were used to generate standard curves. Statistical analysis was performed with GraphPad Prism 8.0.1 (La Jolla, CA, USA), and the results are reported as the mean with SD (*n*=3).

## 3. Results

### 3.1. Construction of the valerolactam biosynthetic pathway in an L-lysine-

**producing *C. glutamicum* mutant.**

Three enzymatic reactions are needed to convert L-lysine into valerolactam (Fig. 1A). To eliminate the need to add extracellular L-lysine to the reaction, we constructed a chassis strain that produces L-lysine. We chose *C. glutamicum* ATCC13032 as the base strain for L-lysine production because it is Generally Recognized as Safe (GRAS) and is already considered a strain that can be used for industrial L-lysine production (Becker et al., 2011). The wild-type *lysC* in the genome of *C. glutamicum* ATCC13032 was replaced with a mutant *lysC* (C932T) to construct the mutant strain *C. glutamicum* XT1. The aspartokinase encoded by *lysC* is a key regulatory enzyme in L-lysine biosynthesis, and the point mutation C932T can increase L-lysine production by reducing feedback inhibition by L-lysine (Fig. 1B) (Ohnishi et al., 2002)(Becker et al., 2011). This strain produced 5.23 g/L L-lysine within 48 hours in flask culture (Fig. 1B). Using lysine-producing *C. glutamicum* XT1 as the chassis strain for valerolactam biosynthesis, we then designed, constructed, and tested various strategies for gene regulation to produce valerolactam.

Act, encoding the β-alanine CoA transferase from *Clostridium propionicum* (Chae et al., 2017), ORF26, encoding the acyl-CoA ligase from *Streptomyces aizunensis*, and CaiC, encoding a crotonobetaine CoA ligase from *E. coli* (Zhang et al., 2017b), have been reported to be catalysts for the cyclization step of valerolactam biosynthesis, and together with DavB and DavA from *P. putida*, they compose the valerolactam biosynthetic pathway. Act was selected first to

metabolically engineer a valerolactam biosynthetic pathway to improve the titer of valerolactam in *C. glutamicum* XT1.

The strengths of the previously characterized strong constitutive *C. glutamicum* promoters H1, H2, H9 and H10, which showed strength similar to or greater than the widely used strong promoter pH36 (Wei et al., 2018), were revalidated in *C. glutamicum* XT1 with mCherry as a reporter. As indicated by mCherry fluorescence, promoter H1 showed the highest strength (Fig. S1) and was selected to drive the valerolactam biosynthetic pathway genes for subsequent research. According to previous research, the high copy number plasmid pHCP was constructed based on pCES208; compared with pCES208 (4-5 copies/cell), the copy number of pHCP increased 10-fold (Choi et al., 2018). The strongest constitutive promoter, H1, was used to drive expression of DavA, DavB and Act, which were integrated into both pCES208 and pHCP to obtain pCES208-H1davAB-act and pHCP-H1davAB-act, respectively, whereas H1-driven DavA and DavB (no Act) were ligated into pCES208 to obtain pCES208-H1DavAB as a negative control. These plasmids (pCES208-H1DavAB, pCES208-H1davAB-act, and pHCP-H1davAB-act) were transformed into *C. glutamicum* XT1 yielding strains *C. glutamicum* Val-1, *C. glutamicum* Val-2, and *C. glutamicum* Val-3, respectively, to test their corresponding valerolactam titers.

In flask cultures, 0.73 g/L valerolactam was produced by *C. glutamicum* Val-2, which was 25-fold more than that with the same pathway genes in *E. coli* under flask culture conditions (29 mg/L) (Chae et al., 2017); moreover, 0.97 g/L

valerolactam was produced by *C. glutamicum* Val-3 (Fig. S2). In *C. glutamicum* Val-3, most of the L-lysine was transformed into 5-AVA by the overexpressed DavA and DavB by increasing the plasmid copy number, whereas in Val-2 there were approximately equal amounts of L-lysine and 5-AVA (Fig. S2). Hence, we concluded that the cyclization of 5-AVA into valerolactam by Act is the rate-limiting step for valerolactam biosynthesis.

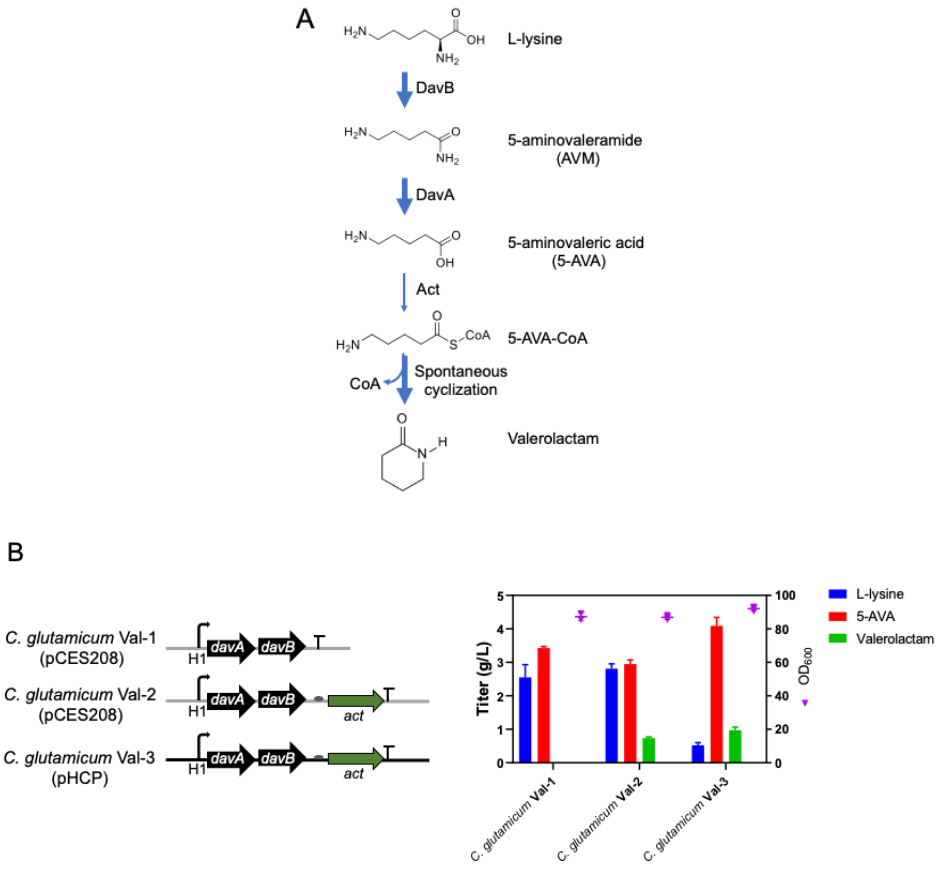


**Figure 1. (A)** The biosynthetic pathway of valerolactam from L-lysine. **(B)** L-lysine, 5-AVA, and valerolactam production by *C. glutamicum* XT1 mutants with different versions of the valerolactam biosynthetic pathway. 5-AVA (5-aminovaleric acid).

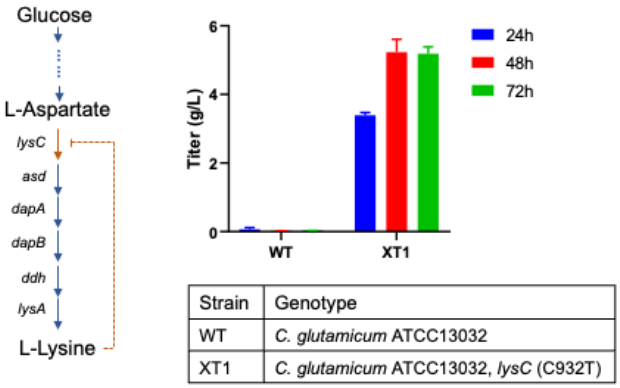


| Strain | Genotype |
|---|---|
| WT | *C. glutamicum* ATCC13032 |
| XT1 | *C. glutamicum* ATCC13032, *lysC* (C932T) |

507

508 **Figure S1**. The L-lysine biosynthetic pathway from glucose in

509 *Corynebacterium glutamicum* and the titer of L-lysine produced by *C.*

510 *glutamicum* ATCC13032 (WT) and mutant (XT1) in flask cultures.

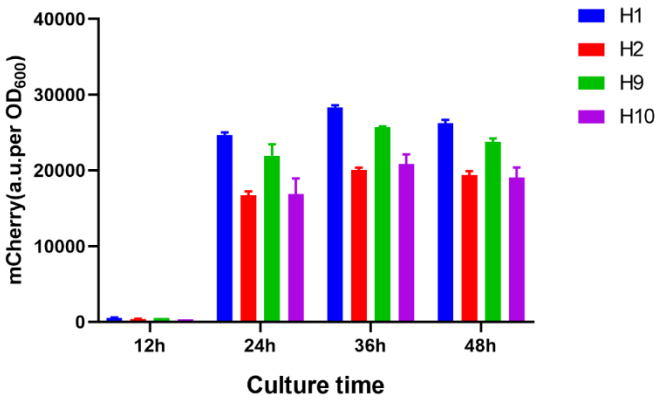


511

512 **Figure S2.** Strengths of the strong constitutive promoters evaluated in *C.*

513 *glutamicum* XT1.

514

515 **3.2 Design of a dynamic upregulation system to amplify the expression of**

516 **Act**

517 To further improve the titer of valerolactam, our primary task became how

518 to obtain much higher expression of Act than in *C. glutamicum* Val-3. We first

519 tried to add another strong promoter, H1, to drive Act to further increase its

520 expression level, resulting in plasmid pHCP-H1davAB-H1act (Fig. 2B). In

addition, a dynamic upregulation strategy was also used to further amplify the expression of Act. Previously this positive feedback loop (dynamic upregulation)-based gene amplifier was shown to dramatically increase the expression of the regulated GFP gene (Nistala et al., 2010). Thus, we designed the valerolactam biosensor ChnR/Pb system as a positive feedback amplifier to regulate the expression of Act (Fig. 2A). The promoter H1 was used to drive the expression of valerolactam biosynthetic pathway genes with Act regulated by the ChnR/Pb system to obtain the pHCP-H1davAB-Pb-act-chnR plasmid (Fig. 2). We hypothesized that the promoter H1 would initiate expression of Act and ChnR, and then the valerolactam produced from the cyclization reaction of 5-AVA would bind with ChnR to form a ChnR-valerolactam complex that would regulate expression of the Pb promoter (Zhang et al., 2017a), thus initiating the dynamic upregulation system (positive feedback amplifier) (Fig. 2A).

Comparing the valerolactam titers in the flask cultures of *C. glutamicum* Val-4 and *C. glutamicum* Val-5, which are *C. glutamicum* XT1 harboring pHCP-H1davAB-H1act and pHCP-H1davAB-Pb-act-chnR, respectively, with that from the *C. glutamicum* Val-3 control, 0.67 g/L and 0.15 g/L valerolactam were produced with *C. glutamicum* Val-4 and *C. glutamicum* Val-5, respectively, which were both lower than the valerolactam produced with the *C. glutamicum* Val-3 control (Fig. 2C). This decrease in valerolactam production with the extra H1 promoter for Act in *C. glutamicum* Val-4 may have been explained by (Rohles et al., 2022), who found that an additional promoter of the second gene

in a two-gene operon can sometimes decrease the expression levels of the genes. To our surprise, the valerolactam pathway dynamically upregulated in *C. glutamicum* Val-5 showed less valerolactam production than the control (Fig. 2C). We suspected that the main reason for this result was due to the lower sensitivity (1-50 mM) and poor dynamic output range (2.4) of the original valerolactam biosensor (ChnR/Pb system) (Zhang et al., 2017a), which limited the expression of Act.

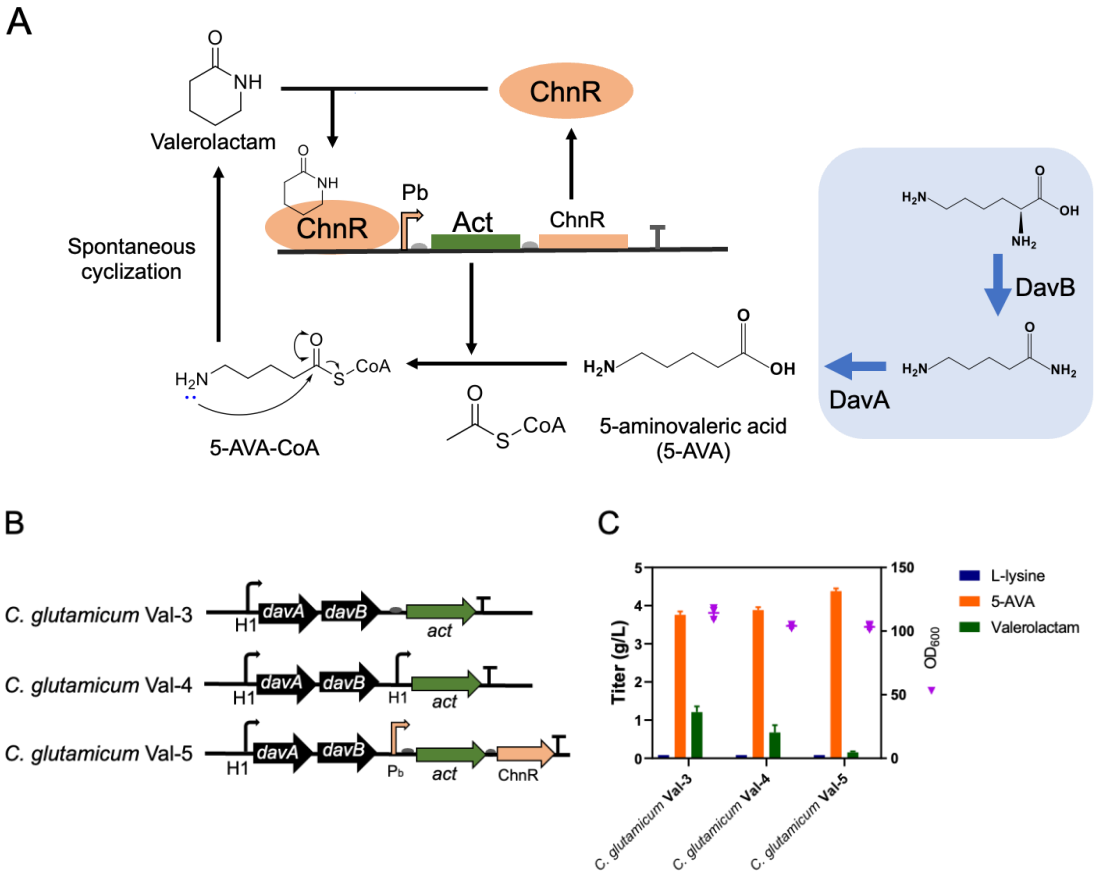


**Figure 2.** Valerolactam production and the dynamic regulatory system developed here. **(A)** Schematic of the ChnR/Pb system for dynamic upregulation of the expression of Act in the valerolactam biosynthetic pathway. **(B)** Valerolactam biosynthetic gene cluster with three different regulatory

systems. **(C)** Production of L-lysine, 5-AVA, and valerolactam in flask cultures at 48 hours. 5-AVA (5-aminovaleric acid).

### 3.3. Improving the sensitivity and dynamic output range of the valerolactam biosensor.

The sensitivity and dynamic output range of the biosensor in the ChnR/Pb system determine the expression time and maximum expression level of Act. To improve the sensitivity and dynamic output range of the biosensor, the binding affinities of the transcription factor ChnR for the promoter Pb and substrate valerolactam should be modified (Snoek et al., 2020). The original valerolactam biosensor (ChnR/Pb system) was characterized in *E. coli* DH10B (Zhang et al., 2017a), and mutant library construction, sorting and characterization of the valerolactam biosensor were also performed in *E. coli* DH10B. Cheng et al. proposed a putative ChnR binding region (5'-3': TTGTTTGGATC) in the promoter Pb (Cheng et al., 2000), so we constructed a Pb site-saturation mutagenesis library based on the predicted ChnR binding region with sfGFP as the reporter. The Pb mutant library was cultured with 1 mM valerolactam for 12 hours and then sorted by FACS for the mutants with the top 1% sfGFP signal (Fig. S3A). Approximately 500 colonies from the FACS-sorted group were further tested with 1 mM valerolactam. The biosensor mutant E1 (5'-3': TGTAGCCCACC) showed a higher sfGFP signal than the original biosensor pBbS-sfGFP after treatment with 1 mM valerolactam. The biosensor

with this Pb mutation (E1) was named pBbS-E1. The fluorescence output of strains harboring biosensor plasmids pBbS-E1 and pBbS-sfGFP were compared for valerolactam concentrations in the range 0-100 mM. The results from pBbS-E1 showed a linear correlation in the fluorescence intensity with 0-1 mM valerolactam, while there was no response from pBbS-sfGFP with 0-1 mM valerolactam (Fig. S3B), indicating the increased sensitivity of pBbS-E1 compared with the original biosensor pBbS-sfGFP. Moreover, the dynamic output range of pBbS-E1 was much higher than that of pBbS-sfGFP for 0-100 mM valerolactam (Fig. 3).

Engineering the valerolactam binding domain in the transcription factor ChnR should further increase the dynamic output range (Snoek et al., 2020)(Mannan et al., 2017); however, the valerolactam binding domain in ChnR is not yet defined. Therefore, a random ChnR mutagenesis library was constructed based on the pBbS-E1 plasmid by error-prone PCR (epPCR). This mutant library was then cultured with 1 mM valerolactam for FACS sorting. After two rounds of FACS sorting for the colonies with the top 1% sfGFP signal in response to 1 mM valerolactam, approximately 1000 colonies were randomly selected for testing with 1 mM valerolactam (Fig. S3A). There were three biosensor mutants that showed a higher sfGFP signal in response to 1 mM valerolactam than biosensor pBbS-E1: M-B1 (S63G and V121A), M-E5 (N22T and S63G) and M-A4 (T281N). The M-B1 mutant showed the largest dynamic output range with 0-1 mM valerolactam, which was 3.0-fold higher than the

pBbS-E1 control (Fig. S3C). We found that the valerolactam biosensors with these ChnR mutants had a higher dynamic output range with increased leaky expression, especially the biosensor with the M-B1 mutant, which showed the highest leaky expression among these biosensors (Fig. S3C). The output fluorescence signal intensity of the biosensor with the M-B1 mutant with 0 mM valerolactam was even higher than that of the control pBbS-E1 at 1 mM valerolactam (Fig. S3C). The leaky expression of this biosensor with the M-B1 mutant may help initiate the dynamic upregulation at an early stage and hence increase the expression of Act to a greater extent than the other ChnR mutants. The biosensor with this M-B1 mutation with the highest dynamic output range was named pBbS-E1B1 (Fig. 3) (ChnR-B1/Pb-E1 system) and was chosen for subsequent engineering.

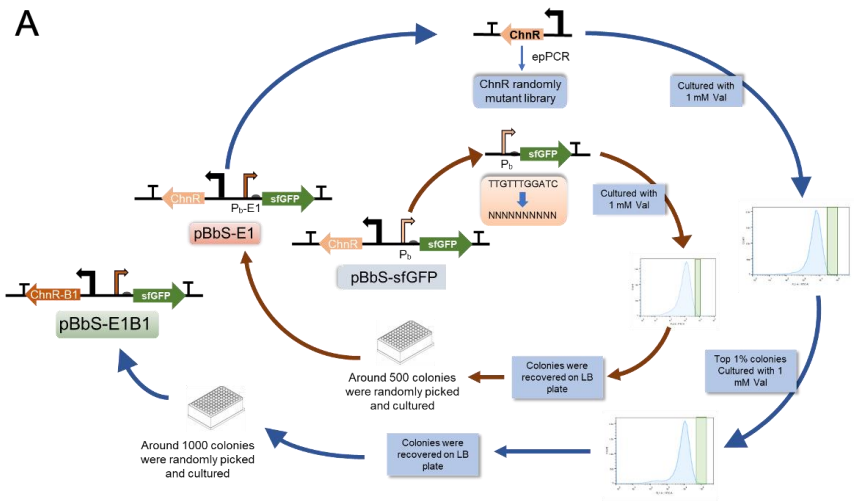

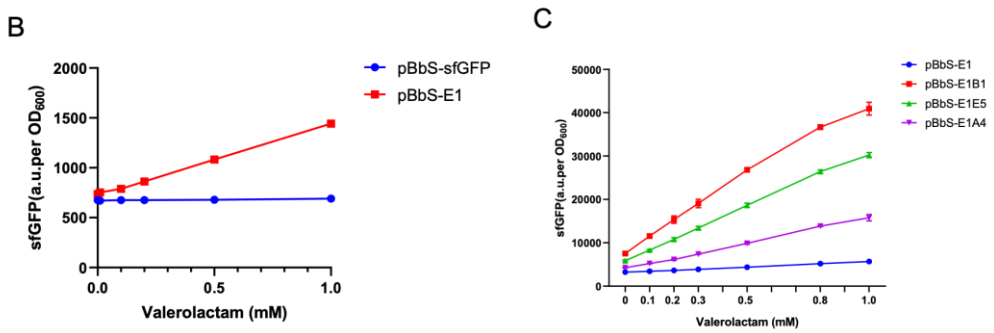


**Figure S3. (A)** Schematic of engineering the valerolactam biosensor. We started with the pBbS-sfGFP biosensor. Red arrow indicates engineering the ChnR binding site in Pb promoter. The Pb site-saturation mutagenesis library was sorted by FACS for the colonies with top 1% GFP signal, and these colonies were further verified in 96-well plates with 1 mM valerolactam to get biosensor pBbS-E1. Blue arrow indicates improving the binding affinity of ChnR for valerolactam (Val) by two rounds of FACS sorting. The ChnR mutants selected from the second round of FACS sorting were further verified in 96-well plates with 1 mM valerolactam to get the biosensor mutant pBbS-E1B1 with the highest fluorescence signal. **(B)** Comparison of the outputs of the biosensor mutant pBbS-E1 with the original valerolactam biosensor pBbS-sfGFP for 0-1 mM valerolactam. **(C)** Comparison of the output from promoter Pb with different ChnR mutants with the pBbS-E1 control for 0-1 mM valerolactam.

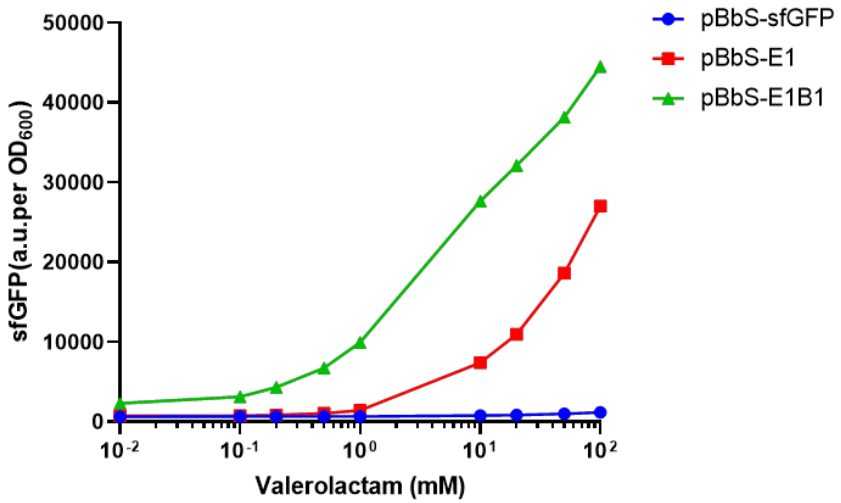


**Figure 3.** Comparison of the outputs of the evolved biosensor pBbS-E1 and pBbS-E1B1 with the original biosensor pBbS-sfGFP in different concentrations of valerolactam.

### 3.4. The ChnR-B1/Pb-E1 system improved valerolactam production.

The engineered ChnR-B1/Pb-E1 system (from pBbS-E1B1) can be used to increase the titer of valerolactam. ChnR-B1 and Pb-E1 were used to replace wild-type ChnR and Pb, respectively, in the dynamic upregulation pathway (Fig. 2). The Pb-E1 mutant without ChnR was used as a negative control to regulate the expression of Act, and the combinations of Pb-E1 with ChnR and Pb with ChnR-B1 were also constructed and tested (Fig. 4). These different combinations of ChnR and Pb helped us determine the best promoter regulator for our dynamic regulation system. The valerolactam biosynthetic pathway plasmids were transformed into *C. glutamicum* XT1, and *C. glutamicum* Val-3, with the highest titer of valerolactam thus far, was set as a control. After 48 hours of flask culture, *C. glutamicum* Val-9 with the ChnR-B1/Pb-E1 system

(pHCP-H1davAB-E1-act-B1) produced 2.46 g/L valerolactam, an increase in the titer of more than 100% compared with the *C. glutamicum* Val-3 control (1.21 g/L) (Fig. 4B).

We also noticed that *C. glutamicum* Val-8 with the ChnR-B1/Pb system (pHCP-H1davAB-Pb-act-B1) was able to produce much more valerolactam (2.11 g/L) than the *C. glutamicum* Val-3 control (Fig. 4B). In contrast, *C. glutamicum* Val-6 (Pb-E1 negative control) and *C. glutamicum* Val-7 (ChnR/Pb-E1 system) produced much less (0.11 g/L and 0.16 g/L, respectively) than the control. From these flask culture results, we found that the strains using ChnR-B1 for the dynamic upregulation of Act were able to produce more valerolactam than the *C. glutamicum* Val-3 control, while the strains with wild-type ChnR for the dynamic upregulation of Act produced a limited amount of valerolactam. These results indicate that the properties of the transcription factor ChnR play a key role in our designed dynamic upregulation system to increase the expression level of Act. Since *C. glutamicum* Val-9 with the ChnR-B1/Pb-E1 system regulates the expression of Act and produces a higher titer of valerolactam than the promoter H1 control, we were interested in whether this dynamic upregulation system can be used to increase the expression of the other enzymes (ORF26 and CaiC) to improve the production of valerolactam.

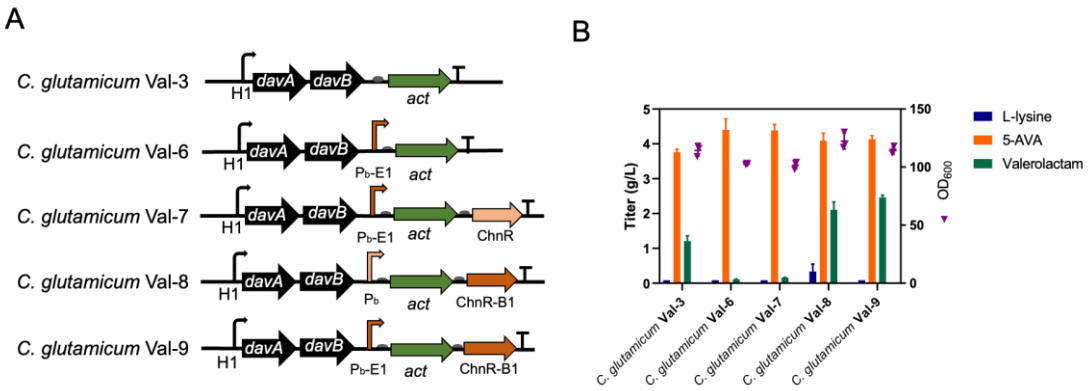


**Figure 4.** Dynamic upregulation of Act with the different regulator-promoter systems for valerolactam biosynthesis. **(A)** Design of the valerolactam pathway with different ChnR and Pb mutant combinations. **(B)** Flask culture results of the different valerolactam biosynthesis pathways indicated in **(A)**. 5-AVA (5-aminovaleric acid).

### 3.5. Dynamic upregulation of ORF26 and CaiC for valerolactam production in *C. glutamicum* XT1.

To test whether the engineered ChnR-B1/Pb-E1 system can be used for dynamic upregulation of the expression of ORF26 and CaiC in valerolactam biosynthesis, *C. glutamicum* codon optimized versions of ORF26 and CaiC were constructed as catalysts for the cyclization step in the valerolactam biosynthetic pathway. These genes were introduced into the various plasmids in place of *act* creating pHCP-H1davAB-orf26 and pHCP-H1davAB-caiC (the controls) and pHCP-H1davAB-E1-orf26-B1 and pHCP-H1davAB-E1-CaiC-B1 (ChnR-B1/Pb-E1 regulated systems) (Fig. 5A). After transformation into *C. glutamicum* XT1, flask culture was carried out for 48 hours. The results showed

683 that *C. glutamicum* Val-11 (*C. glutamicum* XT1 harboring pHCP-H1davAB-E1-
684 orf26-B1) and *C. glutamicum* Val-13 (*C. glutamicum* XT1 harboring pHCP-
685 H1davAB-E1-CaiC-B1) produced 2.90 g/L and 2.28 g/L valerolactam,
686 respectively, both of which generated more valerolactam than the promoter H1
687 controls *C. glutamicum* Val-10 (*C. glutamicum* XT1 harboring pHCP-H1davAB-
688 orf26) and *C. glutamicum* Val-12 (*C. glutamicum* XT1 harboring pHCP-
689 H1davAB-caiC), which produced 2.21 g/L and 1.39 g/L valerolactam,
690 respectively (Fig. 5B). We noticed that the ORF26 group produced the highest
691 titer of valerolactam compared with the Act and CaiC constructs (Fig. 4B and
692 Fig. 5B); however, *C. glutamicum* Val-11 did not show a significant improvement
693 in valerolactam production compared with *C. glutamicum* Val-10 (Fig. 5B), and
694 the solubility of ORF26 (Zhang et al., 2017b) may be the main reason for this
695 result.

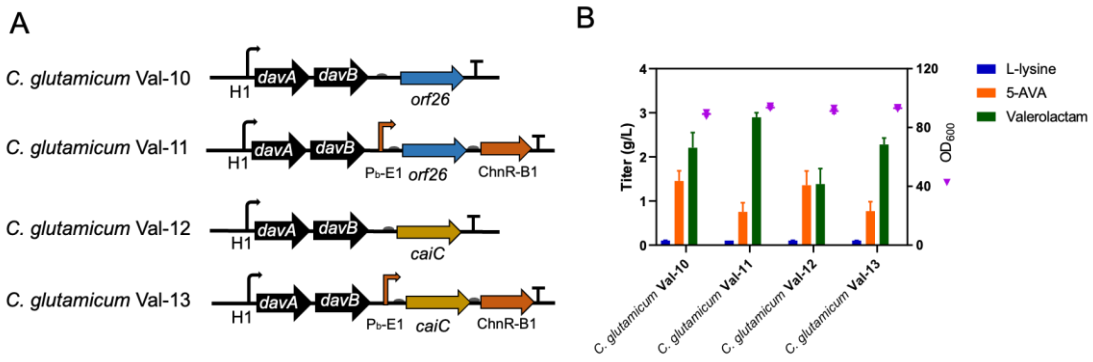

696

697 **Figure 5.** Dynamic upregulation of the ORF26 and CaiC with ChnR-B1/Pb-E1
698 system for valerolactam biosynthesis. 5-AVA (5-aminovaleric acid).

699

700 **3.6. Fed-batch fermentation for valerolactam biosynthesis in *C.***

***glutamicum* XT1.**

To demonstrate that dynamic regulation can further improve the titer of valerolactam in fed-batch cultivation, glucose-fed batch cultures of *C. glutamicum* Val-9 (Act), *C. glutamicum* Val-11 (ORF26) or *C. glutamicum* Val-13 (CaiC) were performed in a 1.2-L lab-scale bioreactor system, and 50% (w/v) glucose was added according to the glucose levels in the media. The time profiles of these three fed-batch cultures are shown in Fig. 6 (indicated as Act, ORF26, and CaiC, respectively). Growth of the Act, ORF26 and CaiC strains entered the stationary phase at 24 hours. Glucose feeding started immediately once there was less than 1 g/L glucose in the medium, and the cells continued to grow to an $OD_{600}$ of 211 (Act), 157 (ORF26), and 190 (CaiC) at 96 hours (Fig. 6). The valerolactam titers of these mutants reached 12.33 g/L (Act), 11.88 g/L (ORF26), and 12.15 g/L (CaiC) at the end of fed-batch fermentation (Fig. 6, Table 2), which are the highest levels reported thus far. In particular, the valerolactam titer of the Act mutants was 10-fold higher than that in previous research (1.18 g/L), which used a valerolactam biosynthetic pathway in *E. coli* with a constitutive promoter that drove the same enzymes used here (DavA, DavB, Act) (Chae et al., 2017). 5-AVA accumulated in these three cultures, indicating that the titer of valerolactam can be further increased by engineering the enzyme activity of Act/ORF26/CaiC (Fig. 6, Table 2).

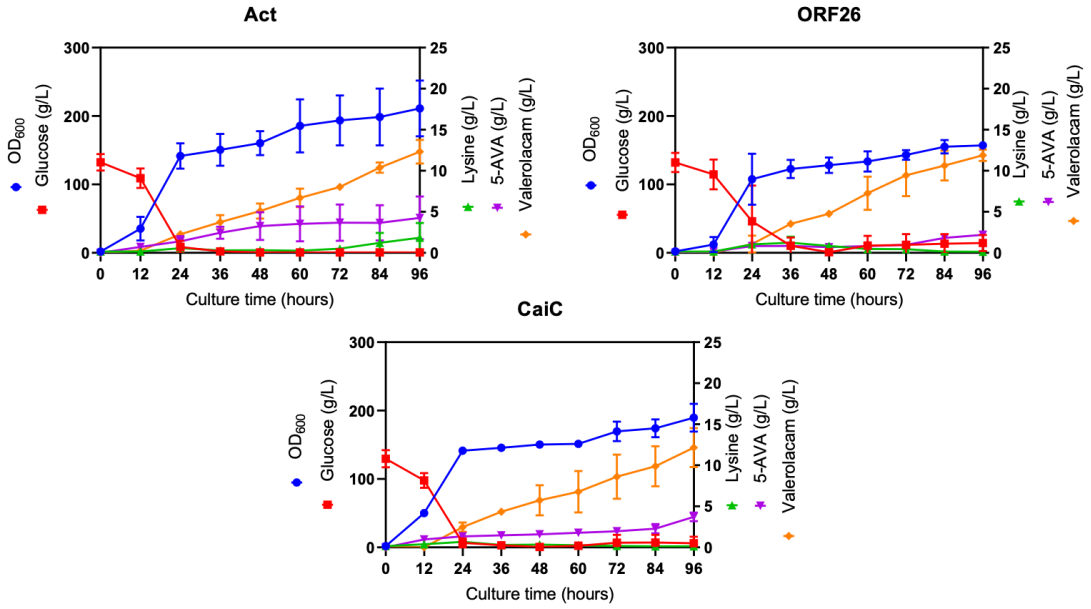


721

722 **Figure 6.** Fed-batch fermentation of valerolactam production in *C. glutamicum*

723 Val-9 (Act), *C. glutamicum* Val-11 (ORF26) and *C. glutamicum* Val-13 (CaiC).

724 (There are two replicates for *C. glutamicum* Val-11, and three replicates for *C.*

725 *glutamicum* Val-9 and *C. glutamicum* Val-13)

726

727 **Table 2.** Fermentation results summary of the *C. glutamicum* XT1 with different

728 valerolactam biosynthetic pathway.

| Strains | Valerolactam titer (g/L) | 5-aminovaleric acid titer (g/L) |
|---|---|---|
| *C. glutamicum* Val-9 (Act) | 12.33±1.44 | 4.26±2.61 |
| *C. glutamicum* Val-11 (ORF26) | 11.88±0.70 | 2.19±0.24 |
| *C. glutamicum* Val-13 (CaiC) | 12.15±2.37 | 3.71±0.52 |

## 4. Discussion

The complete biosynthesis of valerolactam has been studied in *E. coli*, and the major rate-limiting step in its production is the cyclization of 5-AVA to valerolactam (Gordillo Sierra and Alper, 2020)(Zhang et al., 2017b). In this study, we found that the Act-catalyzed activation of 5-AVA followed by the spontaneous cyclization to valerolactam was also a limiting step in our system (Fig. S2). A valerolactam biosensor-based dynamic upregulation system (positive feedback loop) was designed to enhance production of this rate-limiting enzyme (Fig. 2A), and the final titer of valerolactam from this pathway with dynamic upregulation of Act increased to 12.33 g/L in fed-batch culture. This dynamic upregulation system was also used to overexpress ORF26 and CaiC, which have been reported to be important for the cyclization of 5-AVA to valerolactam, and the valerolactam titers of these two strains reached 11.88 g/L and 12.15 g/L, respectively, in a glucose fed-batch fermentation, the titer of valerolactam with dynamic upregulation system in this research is also much higher than Cheng et al., reported 6.88 g/L valerolactam which was synthesized from L-lysine by a combination of enzymatic catalysis and pH optimization (Cheng et al., 2021).

To increase the titer of valerolactam, traditional metabolic engineering methods, such as optimizing the promoter activity and increasing the plasmid copy number, have been tested, and the results showed that these methods

751 contribute little to increasing the titer of valerolactam but instead to conversion
752 of L-lysine to 5-AVA (Fig. 2 and Fig. S2), the precursor to valerolactam. Thus,
753 we speculated that the cyclization of 5-AVA to valerolactam by Act limits the
754 production of valerolactam, and we therefore need to increase the expression
755 of Act to solve this bottleneck. A genetic signal amplifier was designed based
756 on a LuxR positive feedback loop and showed a great ability to increase the
757 expression of the regulated gene (Nistala et al., 2010). We developed the
758 ChnR/Pb system as a valerolactam biosensor. Thus, we first constructed a
759 gene amplifier in a positive feedback loop with the valerolactam biosensor
760 ChnR/Pb system to regulate the expression of Act (Fig. 2). However, the results
761 from flask culture indicated that the Act overexpressed by dynamic upregulation
762 (ChnR/Pb system) was not sufficient to improve the titer of valerolactam. We
763 found that the sensitivity and dynamic output range of the biosensor pBbS-
764 sfGFP (ChnR/Pb system) for valerolactam may limit the maximum expression
765 level of Act under the control of dynamic upregulation. Based on a previous
766 transcription factor engineering method (Snoek et al., 2020), a valerolactam
767 biosensor mutant with higher sensitivity and a larger dynamic output range was
768 obtained (pBbS-E1B1 in Fig. 3). After testing with different combinations of
769 promoter-regulator systems, compared with the strong constitutive control in *C.*
770 *glutamicum* Val-3, the titer of valerolactam was increased by 103% in *C.*
771 *glutamicum* Val-9 (ChnR-B1/Pb-E1 system) under the same culture conditions
772 (Fig. 4B). The flask culture results indicated that the dynamic upregulation

773 system with the ChnR-B1 mutation can significantly increase valerolactam
774 production, while the dynamic upregulation system designed based on wild-
775 type ChnR showed no effect on valerolactam biosynthesis (Fig. 2B and Fig. 4B).
776 In addition, we noticed that the titer of valerolactam from *C. glutamicum* Val-7
777 (ChnR/Pb-E1 system) was similar to that from *C. glutamicum* Val-5 (ChnR/Pb
778 system); however, the dynamic output range of biosensor pBbS-E1 (ChnR/Pb-
779 E1 system) with valerolactam was much higher than that of pBbS-sfGFP
780 (ChnR/Pb system). We suspect that the performance of our designed dynamic
781 upregulation system, a positive feedback amplifier for regulating the expression
782 of the rate-limiting enzymes, is mainly affected by the properties of the
783 transcription factor ChnR-B1. Furthermore, our dynamic upregulation system
784 was used to amplify the expression of ORF26 and CaiC for valerolactam
785 biosynthesis, and the titer of valerolactam increased by approximately 31% and
786 64%, respectively, compared with that of the strong promoter H1 control under
787 flask culture conditions (Fig. 5B). From the flask culture and fed-batch
788 fermentation results, 5-AVA accumulated as a byproduct (Fig. 5B, Table 2), and
789 the lower catalytic activity of these enzymes to activate 5-AVA for its cyclization
790 into valerolactam may be the main reason. Previous research from our lab
791 showed that ORF26 is insoluble, which may affect the growth of *C. glutamicum*
792 Val-11 in the fed-batch fermentation (Fig. 6), has an optimal pH of 8.0 and
793 catalyzes significant ATP and ADP hydrolysis (Zhang et al., 2017b), while *C.*
794 *glutamicum* growth should occur at pH 7.0. Thus, engineering an ORF26

mutant with reduced ATP and ADP hydrolysis, an optimal pH of 7.0 and increased solubility may further increase the titer of valerolactam from *C. glutamicum*. In addition, our engineered valerolactam biosensor pBbS-E1B1 showed a higher dynamic output range for caprolactam than valerolactam (Fig. S4), and there was no effect of caprolactam on the growth *C. glutamicum* (Fig. S5); thus, we suppose that our dynamic upregulation system (ChnR-B1/Pb-E1) can also be used to design a method for caprolactam biosynthesis in *C. glutamicum*.

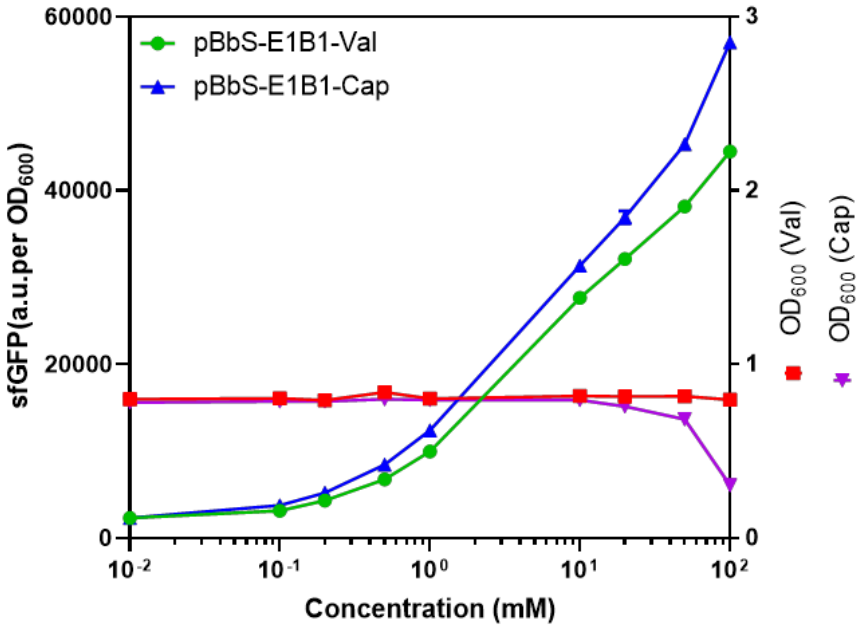


**Figure S4.** Biosensor characterization of pBbS-E1B1 sensitivity to valerolactam (Val) and caprolactam (Cap) in *E. coli*.

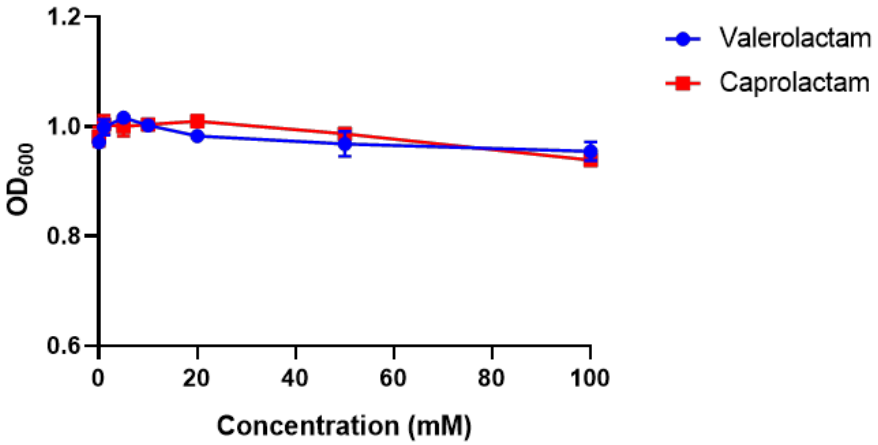


**Figure S5.** The effect of valerolactam and caprolactam on growth. of *C. glutamicum* XT1.

## 5. References

Becker, J., Zelder, O., Häfner, S., Schröder, H., Wittmann, C., 2011. From zero to hero-Design-based systems metabolic engineering of *Corynebacterium glutamicum* for l-lysine production. Metab Eng. 13, 159–168. https://doi.org/10.1002/ccd.27579

Brockman, I.M., Prather, K.L.J., 2015. Dynamic metabolic engineering: New strategies for developing responsive cell factories. Biotechnol J. 10, 1360. https://doi.org/10.1002/BIOT.201400422

Chae, T.U., Ko, Y.S., Hwang, K.S., Lee, S.Y., 2017. Metabolic engineering of *Escherichia coli* for the production of four-, five- and six-carbon lactams. Metab Eng. 41, 82–91. https://doi.org/10.1016/j.ymben.2017.04.001

Cheng, J., Tu, W., Luo, Z., Liang, L., Gou, X., Wang, X., Liu, C., Zhang, G., 2021. Coproduction of 5-aminovalerate and δ-valerolactam for the

synthesis of nylon 5 from L-lysine in *Escherichia coli*. Front Bioeng Biotechnol. 9, 1–9. https://doi.org/10.3389/fbioe.2021.726126

Cheng, Q., Thomas, S.M., Kostichka, K., Valentine, J.R., Nagarajan, V., 2000. Genetic analysis of a gene cluster for cyclohexanol oxidation in *Acinetobacter* sp. Strain SE19 by in vitro transposition. J Bacteriol. 182, 4744–4751.

Choi, J.W., Yim, S.S., Jeong, K.J., 2018. Development of a high-copy-number plasmid via adaptive laboratory evolution of *Corynebacterium glutamicum*. Appl Microbiol Biotechnol. 102, 873–883. https://doi.org/10.1007/s00253-017-8653-2

Dahl, R.H., Zhang, F., Alonso-Gutierrez, J., Baidoo, E., Batth, T.S., Redding-Johanson, A.M., Petzold, C.J., Mukhopadhyay, A., Lee, T.S., Adams, P.D., Keasling, J.D., 2013. Engineering dynamic pathway regulation using stress-response promoters. Nat Biotechnol. 31, 1039–1046. https://doi.org/10.1038/nbt.2689

Gordillo Sierra, A.R., Alper, H.S., 2020. Progress in the metabolic engineering of bio-based lactams and their ω-amino acids precursors. Biotechnol Adv. 43, 107587. https://doi.org/10.1016/J.BIOTECHADV.2020.107587

Green, M.R., Sambrook, J., 2012. Molecular cloning: a laboratory manual, Fourth edition, Cold Spring Harbor Laboratory Press, Cold Spring Harbor, New York (2012).

Jones, J.A., Toparlak, T.D., Koffas, M.A.G., 2015. Metabolic pathway balancing

847 and its role in the production of biofuels and chemicals. Curr Opin
848 Biotechnol. 33, 52–59. https://doi.org/10.1016/J.COPBIO.2014.11.013
849 Mannan, A.A., Liu, D., Zhang, F., Oyarzún, D.A., 2017. Fundamental design
850 principles for transcription-factor-based metabolite biosensors. ACS Synth
851 Biol. 6, 1851–1859. https://doi.org/10.1021/acssynbio.7b00172
852 Matsu-Ura, T., Dovzhenok, A.A., Coradetti, S.T., Subramanian, K.R., Meyer,
853 D.R., Kwon, J.J., Kim, C., Salomonis, N., Glass, N.L., Lim, S., Hong, C.I.,
854 2018. Synthetic gene network with positive feedback loop amplifies
855 cellulase gene expression in *Neurospora crassa*. ACS Synth Biol. 7, 1395–
856 1405. https://doi.org/10.1021/acssynbio.8b00011
857 Nistala, G.J., Wu, K., Rao, C. V., Bhalerao, K.D., 2010. A modular positive
858 feedback-based gene amplifier. J Biol Eng. 4, 1–8.
859 https://doi.org/10.1186/1754-1611-4-4
860 Ohnishi, J., Mitsuhashi, S., Hayashi, M., Ando, S., Yokoi, H., Ochiai, K., Ikeda,
861 M., 2002. A novel methodology employing *Corynebacterium glutamicum*
862 genome information to generate a new L-lysine-producing mutant. Appl
863 Microbiol Biotechnol. 58, 217–223. https://doi.org/10.1007/S00253-001-
864 0883-6
865 Park, J.U., Jo, J.H., Kim, Y.J., Chung, S.S., Lee, J.H., Lee, H.H., 2008.
866 Construction of heat-inducible expression vector of *Corynebacterium*
867 *glutamicum* and *C. ammoniagenes*: fusion of lambda operator with
868 promoters isolated from *C. ammoniagenes*. J Microbiol Biotechnol. 18,

639–647.

Park, S.J., Oh, Y.H., Noh, W., Kim, H.Y., Shin, J.H., Lee, E.G., Lee, S., David, Y., Baylon, M.G., Song, B.K., Jegal, J., Lee, S.Y., Lee, S.H., 2014. High-level conversion of L-lysine into 5-aminovalerate that can be used for nylon 6,5 synthesis. Biotechnol J. 9, 1322–1328. https://doi.org/10.1002/biot.201400156

Rohles, C., Pauli, S., Gießelmann, G., Kohlstedt, M., Becker, J., Wittmann, C., 2022. Systems metabolic engineering of *Corynebacterium glutamicum* eliminates all by-products for selective and high-yield production of the platform chemical 5-aminovalerate. Metab Eng. 73, 168–181. https://doi.org/10.1016/J.YMBEN.2022.07.005

Rohles, C.M., Gießelmann, G., Kohlstedt, M., Wittmann, C., Becker, J., 2016. Systems metabolic engineering of *Corynebacterium glutamicum* for the production of the carbon-5 platform chemicals 5-aminovalerate and glutarate. Microb Cell Fact. 15, 1–13. https://doi.org/10.1186/s12934-016-0553-0

Ruan, Y., Zhu, L., Li, Q., 2015. Improving the electro-transformation efficiency of *Corynebacterium glutamicum* by weakening its cell wall and increasing the cytoplasmic membrane fluidity. Biotechnol Lett. 37, 2445–2452. https://doi.org/10.1007/s10529-015-1934-x

Schäfer, A., Tauch, A., Jäger, W., Kalinowski, J., Thierbach, G., Pühler, A., 1994. Small mobilizable multi-purpose cloning vectors derived from the

*Escherichia coli* plasmids pK18 and pK19: selection of defined deletions in the chromosome of *Corynebacterium glutamicum*. Gene. 145, 69–73. https://doi.org/10.1016/0378-1119(94)90324-7

Shin, J.H., Park, S.H., Oh, Y.H., Choi, J.W., Lee, M.H., Cho, J.S., Jeong, K.J., Joo, J.C., Yu, J., Park, S.J., Lee, S.Y., 2016. Metabolic engineering of *Corynebacterium glutamicum* for enhanced production of 5-aminovaleric acid. Microb Cell Fact. 15, 1–13. https://doi.org/10.1186/s12934-016-0566-8

Snoek, T., Chaberski, E.K., Ambri, F., Kol, S., Bjørn, S.P., Pang, B., Barajas, J.F., Welner, D.H., Jensen, M.K., Keasling, J.D., 2020. Evolution-guided engineering of small-molecule biosensors. Nucleic Acids Res. 48, 1–14. https://doi.org/10.1093/nar/gkz954

Wei, L., Xu, N., Wang, Y., Zhou, W., Han, G., Ma, Y., Liu, J., 2018. Promoter library-based module combination (PLMC) technology for optimization of threonine biosynthesis in *Corynebacterium glutamicum*. Appl Microbiol Biotechnol. 102, 4117–4130. https://doi.org/10.1007/s00253-018-8911-y

Yang, Y., Lin, Y., Wang, Jian, Wu, Y., Zhang, R., Cheng, M., Shen, X., Wang, Jia, Chen, Z., Li, C., Yuan, Q., Yan, Y., 2018. Sensor-regulator and RNAi based bifunctional dynamic control network for engineered microbial synthesis. Nat Commun. 9, 1–10. https://doi.org/10.1038/s41467-018-05466-0

Yeom, S.-J., Kim, M., Kwon, K.K., Fu, Y., Rha, E., Park, S.-H., Lee, H., Kim, H.,

Lee, D.-H., Kim, D.-M., Lee, S.-G., 2018. A synthetic microbial biosensor for high-throughput screening of lactam biocatalysts. Nat Commun. 9, 5053. https://doi.org/10.1038/s41467-018-07488-0

Zhang, F., Carothers, J.M., Keasling, J.D., 2012. Design of a dynamic sensor-regulator system for production of chemicals and fuels derived from fatty acids. Nat Biotechnol. 30, 354–359. https://doi.org/10.1038/nbt.2149

Zhang, J., Barajas, J.F., Burdu, M., Ruegg, T.L., Dias, B., Keasling, J.D., 2017a. Development of a transcription factor-based lactam biosensor. ACS Synth Biol. 6, 439–445. https://doi.org/10.1021/acssynbio.6b00136

Zhang, J., Barajas, J.F., Burdu, M., Wang, G., Baidoo, E.E., Keasling, J.D., 2017b. Application of an acyl-CoA ligase from *Streptomyces aizunensis* for lactam biosynthesis. ACS Synth Biol. 6, 884–890. https://doi.org/10.1021/acssynbio.6b00372

**Author contributions**

Xixi Zhao: Conceptualization, Methodology, Validation, Formal analysis, Investigation, Writing-original Draft, Visualization. Yanling Wu: Methodology, Validation, Investigation. Tingye Feng: Validation, Investigation. Junfeng Shen: Resources. Huan Lu: Validation. Yunfeng Zhang: Validation. Howard C. Chou: Conceptualization, Writing-review & editing. Xiaozhou Luo: Conceptualization, Writing-review & editing, Supervision, Project administration, Funding acquisition. Jay D. Keasling: Conceptualization, Writing-review & editing,

Supervision, Funding acquisition.

**Acknowledgement**

This work is supported by the National Key R&D Program of China (2020YFA0907700), National Natural Science Foundation of China (32101201), Guangdong Basic and Applied Basic Research Foundation (2021B1515020049 and 2019A1515110549), Shenzhen Institute of Synthetic Biology Scientific Research Program (JCHZ20200004), China Postdoctoral Science Foundation (2019M653121) and Shenzhen Science and Technology Program (ZDSYS20210623091810032 and CYJ20190807154003687). We thank Prof. Sang Yup Lee of the Korea Advanced Institutes of Science and Technology for providing the pCES208 plasmid. We thank Dr. Haibing He for helpful discussion and Miss Zhenqin Wei for helping organization the meeting about this project.

**Conflict of Interest**

X.L. has a financial interest in Demetrix and Synceres. J.D.K. has a financial interest in Amyris, Lygos, Demetrix, Maple Bio, Napigen, Apertor Pharma, Ansa Biotechnologies, Berkeley Yeast, and Zero Acre Farms.

954 **Supplementary Material**

955 **Table S1.** Plasmids used in this study

| Plasmids | Description | Source |
|---|---|---|
| pK18mobsacB | Kana$^r$, *sacB* from *B.subtilis* | Schäfer et al., 1994 |
| pK18-lysC | pK18mobsacB derivate, harboring *lysC* gene with point mutation at C932T and 588 bp *lysC* downstream fragment from the *C. glutamicum* ATCC13032 genome | This study |
| pEC-XK99E | *E. coli* and *C. glutamicum* shuttle vector, Kana$^r$ | Lab Stock |
| pH1-mCherry | pEC-XK99E derivate, H1-mCherry | This study |
| pH2-mCherry | pEC-XK99E derivate, H2-mCherry | This study |
| pH9-mCherry | pEC-XK99E derivate, H9-mCherry | This study |
| pH10-mCherry | pEC-XK99E derivate, H10-mCherry | This study |
| pCES208 | Shuttle vector between *E. coli* and *C. glutamicum*, Kana$^r$ | Park et al., 2008 |
| pCES208- | pCES208 derivate, H1, codon-optimized | This |

| | | |
|---|---|---|
| H1davAB | *davA*, *davB* | study |
| pCES208-H1davAB-act | pCES208 derivate, H1, codon-optimized *davA*, *davB* and *act* | This study |
| pHCP | pCES208 derivate, *parB* nonsense mutation, Kana$^r$ | This study |
| pHCP-H1davAB-act | pHCP derivate, H1, codon-optimized *davA*, *davB* and *act* | This study |
| pHCP-H1davAB-H1act | pHCP derivate, H1, codon-optimized *davA*, *davB* and H1-*act* | This study |
| pHCP-H1davAB-Pb-act-chnR | pHCP derivate, H1, codon-optimized *davA*, *davB* and Pb-*act*-chnR | This study |
| pBbSlactam | Lactam biosensor, harboring the *chnR* from *Acinetobacter sp.* and mCherry under control of Pb (the promoter of *chnB* from *Acinetobacter sp.*), Cm$^R$ | Zhang et al., 2017a |
| pBbS-sfGFP | pBbSlactam derivate, mCherry was replaced with sfGFP | This study |
| pBbS-E1 | pBbS-sfGFP derivate, with mutation in the Pb of ChnR binding site, and sfGFP under control of the Pb mutant (Pb-E1) | This study |
| pBbS-E1B1 | pBb-E1 derivate, with a *chnR* mutant (ChnR-M-B1) | This study |
| pBbS-E1E5 | pBb-E1 derivate, with a *chnR* mutant (ChnR-M-E5) | This study |
| pBbS-E1A4 | pBb-E1 derivate, with a *chnR* mutant (ChnR- | This |

| | | |
|---|---|---|
| | M-A4) | study |
| pHCP-H1davAB-E1-act | pHCP derivate, H1, codon-optimized *davA*, *davB* and Pb-E1-*act* | This study |
| pHCP-H1davAB-E1-act-chnR | pHCP derivate, H1, codon-optimized *davA*, *davB* and Pb-E1-*act*-chnR | This study |
| pHCP-H1davAB-Pb-act-B1 | pHCP derivate, H1, codon-optimized *davA*, *davB* and Pb-*act*-ChnR-B1 | This study |
| pHCP-H1davAB-E1-act-B1 | pHCP derivate, H1, codon-optimized *davA*, *davB* and Pb-E1-*act*-ChnR-B1 | This study |
| pHCP-H1davAB-orf26 | pHCP derivate, H1, codon-optimized *davA*, *davB* and *orf26* | This study |
| pHCP-H1davAB-E1-orf26-B1 | pHCP derivate, H1, codon-optimized *davA*, *davB* and Pb-E1-*orf26*-ChnR-B1 | This study |
| pHCP-H1davAB-caiC | pHCP derivate, H1, codon-optimized *davA*, *davB* and *caiC* | This study |
| pHCP-H1davAB-E1-caiC-B1 | pHCP derivate, H1, codon-optimized *davA*, *davB* and Pb-E1-*caiC*-ChnR-B1 | This study |

**Table S2.** Primers used in this study

| Primer | Sequence (5' to 3') |
|---|---|
| P1 | cgtaatcatggtcatagctg |
| P2 | agtcgacctgcaggcatg |
| P3 | atgcctgcaggtcgactATGGCCCTGGTCGTACAG |

| | |
|---|---|
| P4 | CGAGGGCAGGTGAAGATGATGTCGGTGGTGC |
| P5 | ATCTTCACCTGCCCTCGTTC |
| P6 | ctatgaccatgattacgCATCATGGACGAACTCAACG |
| P7 | GCTATATATGCTTATACTGGGCTAAATTAGAGCCTTAGCGAAAGGATGG GCatgcgtaaaggagaagaag |
| P8 | cgactctagtttgtatagttcatccatg |
| P9 | actatacaaactagagtcgacctgcagg |
| P10 | TATAAGCATATATAGCCGGCGCAAGCAAGTACGAGACTCAAGAGCGAG Cattcaccaccctgaattgac |
| P11 | GTCGAGGAATACTGTATACTATTTAAAATTCATTGGATAGCAAAGGACG GATatgcgtaaaggagaag |
| P12 | TATACAGTATTCCTCGACAGAATACCAGGCACAGTAAGTCGAGACAGA GCattcaccaccctgaattgac |
| P13 | CATTCTGGTAAGGTACGATCCTAGAGTCTTAAGAGAACGGAAAGGAATT GCatgcgtaaaggagaagaag |
| P14 | GTACCTTACCAGAATGTCGCCCTGAAAACTAATATGTATACCATGGGAG Cattcaccaccctgaattgac |
| P15 | GCGTATGGTAAGCTCTGTTATGTATAGTCCGAGCACGGCGAAAGGATA CTCatgcgtaaaggagaagaag |
| P16 | AGAGCTTACCATACGCCGCCGGCTTAGAGCCGACCGGTAAGGGTTGA GCattcaccaccctgaattgac |
| P17 | ccaccgCAGTAGGCtCAACTGATTCG |
| P18 | ttgAgcctactgcggtggcctgattc |
| P19 | GCTATATATGCTTATACTGGGCTAAATTAGAGCCTTAGCGAAAGGATGG GCATGCATCACCATCACCATCATC |

| | |
|---|---|
| P20 | ATTTTCCTCCTTTttagcctttacgcaggtgc |
| P21 | taaaggctaaAAAGGAGGAAAATCatgaac |
| P22 | TGTATGTCCTCCTGGACTTCttaatctgccagggcgatc |
| P23 | AAGTCCAGGAGGACATACAATGAAGCGCCCTCTCGAAGG |
| P24 | tactgccgccaggcagcggccgcTTAGATGACGTTCTTCTCC |
| P25 | cgctgcctggcggcagtag |
| P26 | TATAAGCATATATAGCCGGCGCAAGCAAGTACGAGACTCAAGAGCGAG Ccagcttttgttccctttagtg |
| P27 | tactgccgccaggcagcggccgcttaatctgccagggcgatcg |
| P28 | AGTATAAGCATATATAGCCGGCGCAAGCAAGTACGAGACTCAAGAGCG AGCttaatctgccagggcgatcg |
| P29 | gtgatatcccgcggccattaatctgccagggcgatcg |
| P30 | tggccgcgggatatcactag |
| P31 | tATGTCCTCCTGGACTTCtgaatttattcaaaatctgc |
| P32 | AAGTCCAGGAGGACATACAATGCATCACCATCACCATCATCATAAGCGC CCTCTCGAAG |
| P33 | gtctgtgctcatATTCATCCTTTTTAGATGACGTTCTTCTCC |
| P34 | AAAGGATGAATatgagcacagacaaagc |
| P35 | actgccgccaggcagcggccgctcaaaaaacaatagaggag |
| P36 | AAGTCCAGGAGGACATACAATGCATCACCATCACCATCATCATACCGCA AAAATCTTTGCCG |
| P37 | actgccgccaggcagcggccgcTTATTCGGCTGCCATGCGGG |
| P38 | gctcatATTCATCCTTTTTATTCGGCTGCCATGCG |
| P39 | gattaaGAAGTCCAGGAGGACATACAATGGACATTATCGGTGGC |
| P40 | actgccgccaggcagcggccgcTTACTTGAGGTTCTTGC |

| | |
|---|---|
| P41 | gtctgtgctcatATTCATCCTTTTTACTTGAGGTTCTTGCGG |
| P42 | tttgtacagttcatccatac |
| P43 | atgcgtaaaggcgaagagc |
| P44 | tggatgaactgtacaaatgaggatccaaactcgagtaagg |
| P45 | tcttcgcctttacgcatggtaccctccattacgac |
| P46 | tctcttttagttgcaagcttc |
| P47 | gcagatgaagaagcttgcaactaaaagagaNNNNNNNNNNNagttacccaaaatcgttg |
| P48 | agagtcaattcagggtggtg |
| P49 | gagattggtgtgttcctgtc |
| P50 | aggaacacaccaatctcgtgtctg |
| P51 | caccctgaattgactctcttc |

**Table S3.** Sequence of codon optimized *davA* and *davB* genes from *P. putida*, *act* gene from *C. propionicum*, *orf26* gene from *S. aizunensis*, *caiC* gene from *E. coli*.

| Gene | Codon optimized sequence |
|---|---|
| *davA* | atgcgcatcgcactgtaccaaggcgcacccaagccactagacgttcctggtaaccttcaacggctgcg<br>ccaccaggcgcagctggcagctgaacgcggagctcagttgctggtgtgcccagagatgttcctcaccg<br>gctacaacattggcctggcccaagtcgaacgtctcgccgaagccgcagatggcccagcagcaatga<br>ccgtggtcgaaatcgctcaggctcaccgcatcgcaattgtttacggttacccggagcgcggtgatgacg<br>gagctatctacaactccgttcagttgatcgatgcgcatggacgatctctgtcaaattatcgcaagacgca<br>cttgttcggtgaactcgatcgctcgatgttctcccctggtgcggaccacttcccagtcgtggaactggaag<br>gctggaaggttggacttcttatctgttacgacatcgagttcccagagaacgcccgtcgactagcgttggat |

| | |
|---|---|
| | ggagccgagcttatccttgtgcccaccgctaacatgactccgtacgattttacctgccaagtgactgtccg<br>tgcgagggcacaggaaaatcagtgctacctcgtatatgcaaactactgcggtgctgaagacgagattg<br>aatattgtgggcaatctagcattattggaccggatggctccttgctcgctatggccggtcgcgatgaatgc<br>cagttgcttgcagagcttgagcatgagcgggtcgttcaggggcgtacagcttttccttatttaaccgacctc<br>cgtcaggagctgcacctgcgtaaaggctaa |
| *davB* | atgaacaagaagaatcgacaccccgccgacggcaagaagccgattaccattttcggaccagatttcc<br>cttttgctttcgatgattggctagaacacccagcaggcctgggaagcattccagctgagcgccatggag<br>aagaggtggctatcgtcggagctggtatcgctggcctcgtagcggcatacgagctgatgaagctgggc<br>ctcaagcctgtggtgtatgaggcttccaagctcggcggccggctccgctcccaagccttcaatggaact<br>gacgggatcgttgccgagctgggtggcatgcgcttcccagtgtcttccactgccttctaccactacgtcga<br>caaattgggcctggaaacgaaacccttccccaatcctttgaccccagcttccggaagtacggttattgat<br>cttgaaggacagacctattacgccgagaaacctacagaccttccacaactgtttcatgaggttgccgac<br>gcatgggctgatgctctggagtcgggtgcgcagttcgccgatatccagcaggcaatccgcgatcgtgat<br>gtaccacgccttaaggaattatggaacaagttggttccactgtgggacgaccgtaccttctacgacttcgt<br>cgctacctctcgctcctttgctaaactgagctttcaacacagagaagtgtttggccaggtcggtttcggcac<br>cggcggttgggattcggacttccctaacagtatgttggaaatcttccgcgtggttatgaccaactgcgacg<br>accaccagcacctggttgttgggggtgtggaacaagtcccacaaggaatctggcgccacgtgccgga<br>acgttgtgtgcattggccagaagggactagcctgagcacgctgcatggtggcgcaccgcgtaccggtg<br>tcaagcgcattgcccgcgcatccgatggccgcttggcagtcacggacaactggggtgatacccgcca<br>ctattccgcagtactagctacctgtcagacatggttgcttaccactcaaatcgactgcgaagaatctctgtt<br>ctcgcaaaagatgtggatggcactggaccggacccgctacatgcagtcgtctaaaacctttgtcatggt<br>cgacaggccgttctggaaggataaggaccctgagaccggtcgtgacctgctgagcatgaccctcact<br>gatcgtctcactcgcggcacttatctttttgataacggtaacgataaacccggggtgatctgcctgtcatac<br>tcatggatgtctgatgcgctgaagatgctgccacacccggtggagaagcgcgtacagcttgccctggat<br>gcgctcaagaagatttatccgaaaaccgatatcgcaggccatatcatcggcgatccaatcacggtttcc |

| | |
|---|---|
| | tgggaggccgacccctactttctcggcgcgttcaaaggcgcgttaccgggtcattaccgctacaaccag<br>cgaatgtacgcgcacttcatgcagcaggatatgccggcagagcagcgcggtatttttattgctggtgatg<br>acgtgtcatggacccctgcctgggttgaaggcgcggtccagacatctctgaacgcagtgtggggtatca<br>tgaatcactttggtgggcacacccacccagacaatccaggcccgggagatgtgttcaacgagatcgg<br>cccgatcgccctggcagattaa |
| *act* | atgaagcgccctctcgaaggcatccgtgtgctggacctcacccaagcttactccggcccattctgcacta<br>tgaacctcgcagatcatggcgccgaggtcatcaagatcgaacgccccggttccggtgatcagacccg<br>cggctggggtcctatggaaaacgactactccggctactacgcatacatcaaccgcaacaagaagggt<br>atcactttaaatctcgcatccgaagagggcaagaaggtgttcgcagagctggtcaagtccgccgacgt<br>catttgcgagaactacaaggtgggcgtgctggaaaagctgggcttctcctacgaggttttaaaggagct<br>caatccacgtatcatctacggctccatctccggcttcggtttaactggcgaactgtcctctcgcccttgctac<br>gatatcgtggcacaagctatgtccggcatgatgtccgtgaccggcttcgcagatggtcctccttgcaaga<br>tcggtccttccgtgggcgactcctataccggtgcatacctctgcatgggcgtgctcatggctttatacgagc<br>gcgagaagactggcgtgggtcgtcgcattgacgtcggcatggtcgacactttattctccactatggagaa<br>cttcgtggtggagtacaccatcgctggtaagcacccacaccgcgctggtaaccaagatccatccatcg<br>ccccttttcgactccttccgtgccaaggactccgacttcgtcatgggctgcggcaccaacaaaatgttcgc<br>cggtctgtgcaaggccatgggccgcgaggatttaatcgacgatccacgcttcaacaccaatttaaacc<br>gctgcgacaactatttaaacgatttaaagccaatcattgaggagtggacccagaccaagaccgtggca<br>gagctggaggaaatcatctgcggtttatccatcccattcggccctattttaactatcccagagatttccgag<br>cactctctgaccaaggagcgcaatatgctctgggaagtgtaccaacccggtatggatcgcaccatccg<br>cattcccggttcccctatcaagattcacggtgaggaggacaaggcacagaaaggcgccccaattttag<br>gcgaagacaacttcgcagtgtacgcagagatcctcggtctgtccgtcgaagagatcaagtctttagagg<br>agaagaacgtcatctaa |
| *orf26* | atgaccgcaaaaatctttgccgtggactccgtccgcccaatcgacgagttcgaacaagatgcactgcg<br>cgtcgccgacgtgattcgcgaacgtggcgtgtgtttaggcgatcgcgtgatgctcaaggctggtaactcc |

| | |
|---|---|
| | gcatcttacgtgtgcgtgctgtacgcactcatgcacattggtgcctccatcgtgctggtggaccagcaag<br>aacataaggaagagacccgccgcattgcactgcgcaccggtgtgaaggtgaccttcgtggacgatga<br>gaccccaatcgatcaagacgccgatcctatccatttatacgagctcatggtggcaacccagaaccgtc<br>cacctatggactccgctttatccttcgatgcttggggcgaactgtccgacggtttaattatgtggacctccg<br>gctccaccggttctccaaagggcgtcgtgaagtccggcggtaaatttctggcaaatttacgtcgcaacg<br>cacaccaagtgggccaccgcccagacgatgttttaatgccactgctcccattcgcccatcagtatggttt<br>atccatggtgctgattgcttggctgacccgctgctctctcgtgatcgccccataccgtcgtttagatcgcgct<br>ttacgtatggcacgcgattccggcaccaccgtgatcgacgcaaccccatcctcctaccgctctatcctcg<br>gtttagtcacccgcaaaccagctttacgtgcacatttagctggtacccgtatgttctgcgtgggcgcagca<br>ccactcgacgcaccactggtggaatcctacgtgcaagaattcggtctgccattattagattcttacggctc<br>caccgaactgaacaacatcgcctttgccactctggataacccagtgtcttgtggccgcgcaatggaggg<br>tatcggtttacgtatcgtggatgaggatggccgcgaagtcgcagctggtcagcccggtgaaattgaagt<br>ggacacccccgatgcactggagggtcagatcgccgaagatggctccatcatcccagcaccaactgg<br>ctggcaacgcaccggcgatttaggtcacctcgatgcagacggcaacctctacgttttaggccgcaagttt<br>gccgtgcaccgcatgggttacactttatacccagagctgatcgaacgcaaagtggccgcagagggct<br>gtcctacccgcatcgtgccactcccagatgagctgcgcggttcccagctcgtgttcttcgtggaggatgat<br>gagcagcgcgatgccggttactggcgtgaacgtctgtgtggcttattaccagcattcgaacagccaaac<br>aaggtggtggttttagagcaattccctctcaaccgcaacggcaagccagataagaaggaactgaccc<br>gcatggcagccgaataa |
| *caiC* | atggacattatcggtggccagcatttacgccaaatgtgggacgacctcgcagatgtctacggtcacaag<br>accgctttaatttgcgaatcctccggtggcgtcgtgaatcgttactcctacctcgagctcaaccaagaaat<br>caatcgcaccgccaatctgttctacactttaggcatccgcaagggcgacaaggtggcactgcatttaga<br>caactgccccgaattcatcttctgctggttcggtttagcaaaaatcggcgcaatcatggtgcctatcaatg<br>cccgtttactgtgtgaggaatccgcatggattttacagaactcccaagcttgtttactggtgacctctgccc<br>agttttacccaatgtaccagcagatccaacaagaagacgcaacccagctgcgccacatctgtctcacc |

| | |
|---|---|
| | gatgtggcactccccgctgacgatggtgtctcctcctttacccagctgaaaaaccagcaacccgctacc<br>ctctgctacgcaccaccactgtccaccgacgataccgcagaaattttatttacttctggcaccacctctcg<br>ccctaagggcgtcgtgattacccactataatttacgcttcgctggttactactccgcttggcaatgcgccct<br>ccgcgacgatgacgtgtacctcaccgtgatgccagccttccacatcgactgtcaatgcactgcagcaat<br>ggcagcattctctgccggcgccaccttcgtgctcgtggagaaatactccgcacgcgccttttggggcca<br>agtgcagaagtatcgcgccaccgtcaccgagtgtattccaatgatgatccgtactttaatggtgcagcca<br>ccttccgccaacgatcagcagcatcgcctccgcgaagtgatgttttatttaaatttatccgagcaagaaa<br>aggacgcattctgcgagcgcttcggcgtgcgtttactgacctcctatggcatgaccgagaccatcgtgg<br>gtatcattggcgatcgccccggtgataagcgccgttggccttctatcggtcgcgtgggcttctgctacgaa<br>gccgaaattcgcgacgatcacaaccgccctctccccgctggtgaaatcggcgaaatctgcatcaagg<br>gcattcccggtaagaccattttcaaggaatactttctgaacccacaagctactgccaaggtgctggagg<br>ccgatggctggctgcataccggtgataccggctatcgcgacgaggaagatttcttctacttcgtggaccg<br>ccgctgcaacatgatcaagcgtggcggcgagaacgtgtcttgcgtcgagctggagaacatcatcgca<br>gcccatccaaagatccaagatatcgtggtggtgggcatcaaagactccatccgcgatgaagccatca<br>aggcattcgtcgtgctcaacgagggtgagactctgtccgaggaggagttcttccgcttctgcgagcaaa<br>acatggccaagttcaaggtcccttcctatttagaaatccgcaaggatttaccacgcaactgctccggcaa<br>gatcatccgcaagaacctcaagtaa |

963